Introduction to Climate

Ryo Mizuta

Climate Research Department

Meteorological Research Institute (MRI), JMA

Outline of the lecture

1. Climate System (60 min. + α)
   1.1 Introduction
   1.2 Radiative Balance
   1.3 Horizontal Radiative Imbalance and Circulations
   1.4 Seasonal Change
   1.5 Role of Orography on Climate
2. Climate Variability (90 min. + α)
   2.1 Introduction
   2.2 Intraseasonal Variability: Quasi-stationary Rossby wave, MJO and equatorial waves
   2.3 Interannual Variability: ENSO, El Nino Modoki, IOD
   2.4 Decadal Variability: PDO, ENSO-Monsoon relation
3. Climate change due to anthropogenic forcing (30 min. + α)

Outline of the lecture

1. Climate System (60 min. + α)

    1.1 Introduction

    1.2 Radiative Balance

    1.3 Horizontal Radiative Imbalance and Circulations

    1.4 Seasonal Change

    1.5 Role of Orography on Climate

2. Climate Variability (90 min. + α)

    2.1 Introduction

    2.2 Intraseasonal Variability: Quasi-stationary Rossby wave, MJO and equatorial waves

    2.3 Interannual Variability: ENSO, El Nino Modoki, IOD

    2.4 Decadal Variability: PDO, ENSO-Monsoon relation

3. Climate change due to anthropogenic forcing (30 min. + α)

1.1 Introduction

Climate and Climate System

From WMO HP

What is Climate?

Climate, sometimes understood as the "average weather," is defined as the measurement of the mean and variability of relevant quantities of certain variables (such as temperature, precipitation or wind) over a period of time, ranging from months to thousands or millions of years.

Climate in a wider sense is the state, including a statistical description, of the climate system.

What is the Climate System?

The climate system consists of five major components: the atmosphere the hydrosphere, the cryosphere, land surface, and the biosphere.

The climate system is continually changing due to the interactions between the components as well as external factors such as volcanic eruptions or solar variations and human-induced factors such as changes to the atmosphere and changes in land use.

The climate system is complicated!

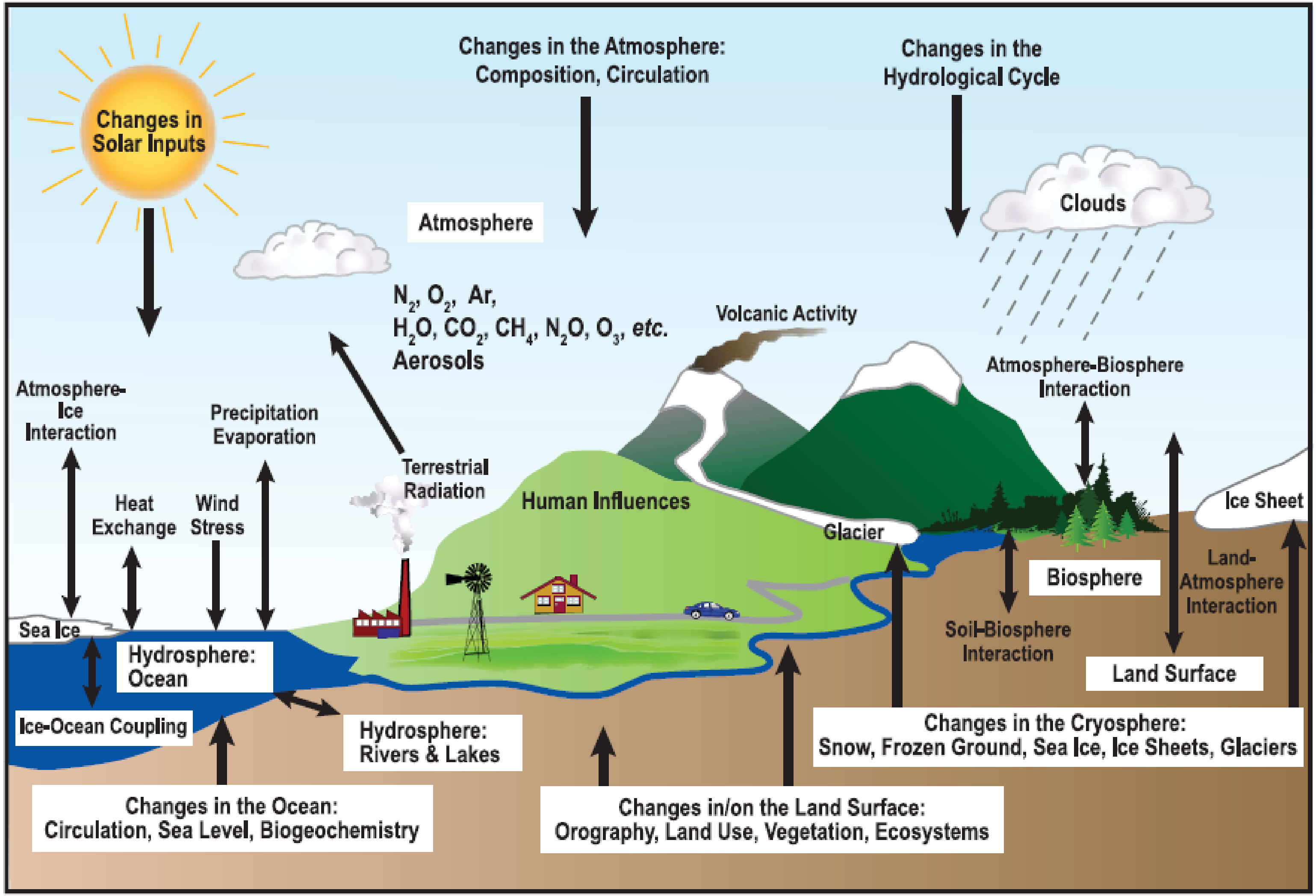

FAQ 1.2, Figure 1. *Schematic view of the components of the climate system, their processes and interactions.*

(IPCC AR4)

1.2 Radiative Balance

Terrestrial Radiation

Earth

Solar radiation

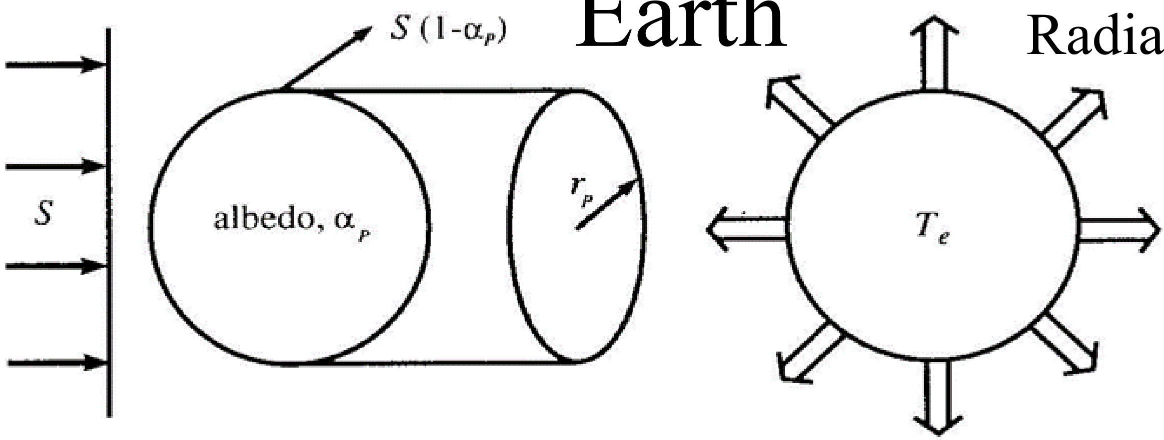

Absorbed $= S\,(1-\alpha_p)\,\pi r_p^2$ = Lost $= \sigma T_e^4 4\pi r_p^2$

Absorption = Emission

$>$ Warming of Climate System

$<$ Cooling of Climate System

Radiative Balance between Earth and Space

Solar Radiation

- **Solar constant :** $S \approx 1370\, Wm^{-2}$
- **insolation :** $\frac{S}{4} \approx 342 Wm^{-2}$
- **planetary albedo :** $\alpha_P \approx 0.31$
- **absorption :** $\frac{S}{4}(1-\alpha_P) \approx 235 Wm^{-2}$

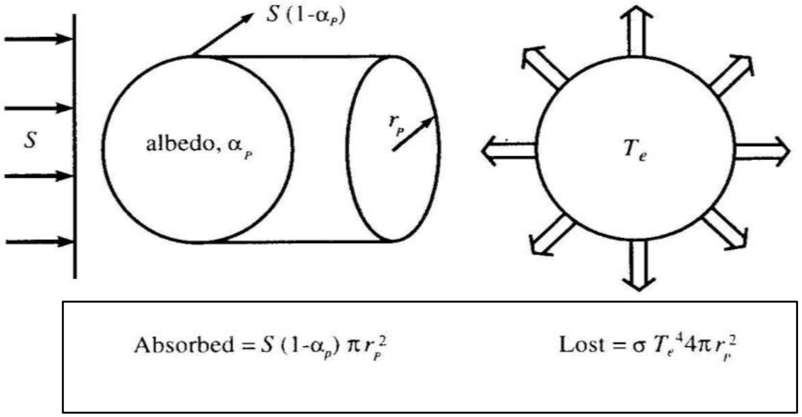

Terrestrial Radiation

- **equilibrium radiative temperature :** T_e^*
- **emission :** σT_e^{*4}

Radiation Balance

- **Balance between absorbed solar radiation and terresitrial emission**

$$T_e^* = \sqrt[4]{\frac{S(1-\alpha_P)}{4\sigma}} \approx 254K \approx -19°C$$

Earth's temperature observed from the cosmic space

Surface Temperature = 15° C

Absorption of Radiation from 6000K (Sun) and 255K (Earth) Blackbodies

Solar radiation

"Short Wave"

Terrestrial radiation

"Long Wave"

Percentage of atmospheric absorption

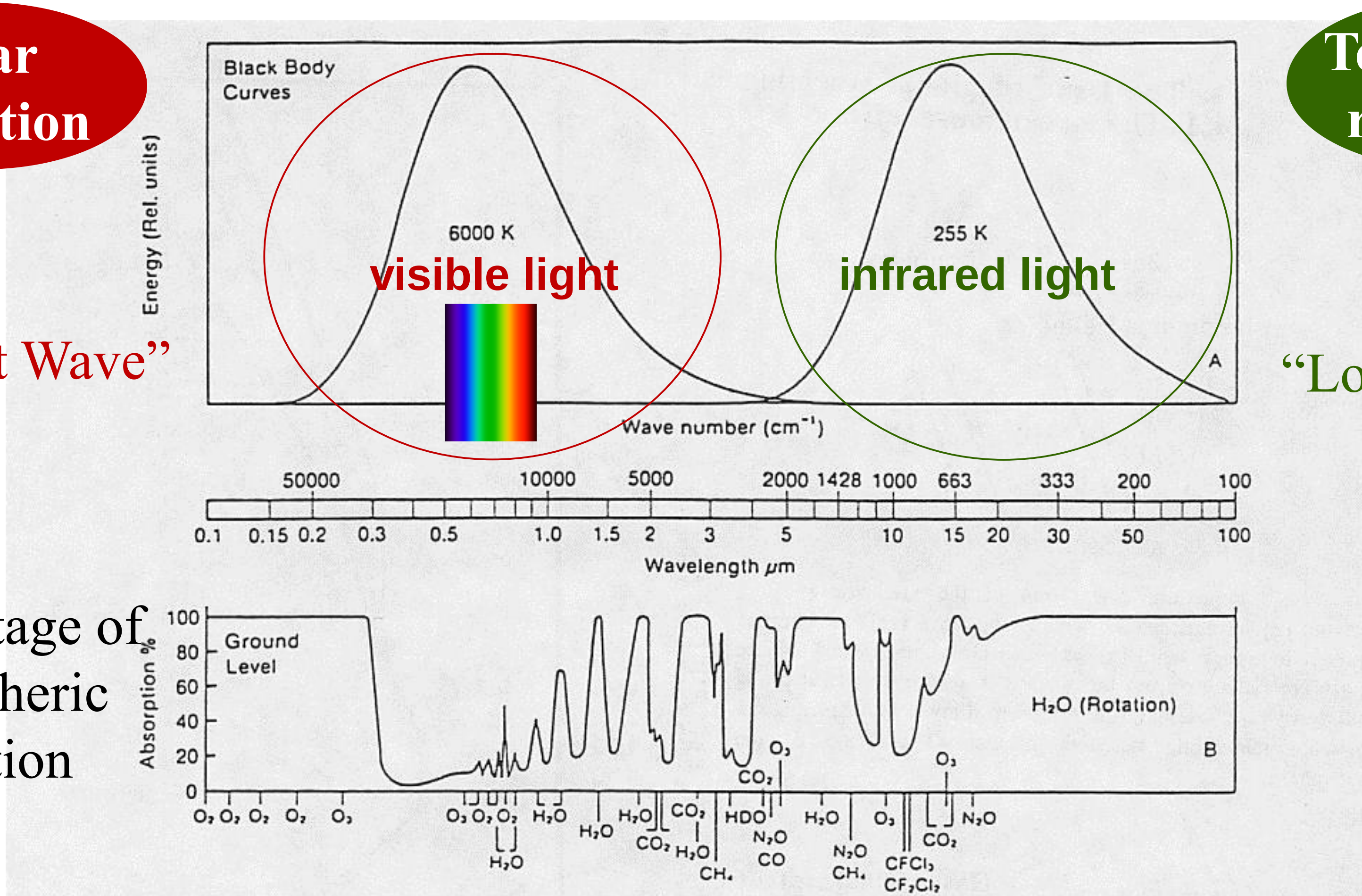

(*a*) Spectral distribution of long-wave emission from blackbodies at 6000 K and 255 K, corresponding to the mean emitting temperatures of the Sun and Earth, respectively, and (*b*) percentage of atmospheric absorption for radiation passing from the top of the atmosphere to the surface. Notice the comparatively weak absorption of the solar spectrum and the region of weak absorption from 8 to 12 μm in the long-wave spectrum [from *MacCracken and Luther*, 1985].

Pictures are from NASA web-sites

The simplest greenhouse model

1-layer atmosphere is placed between space and surface

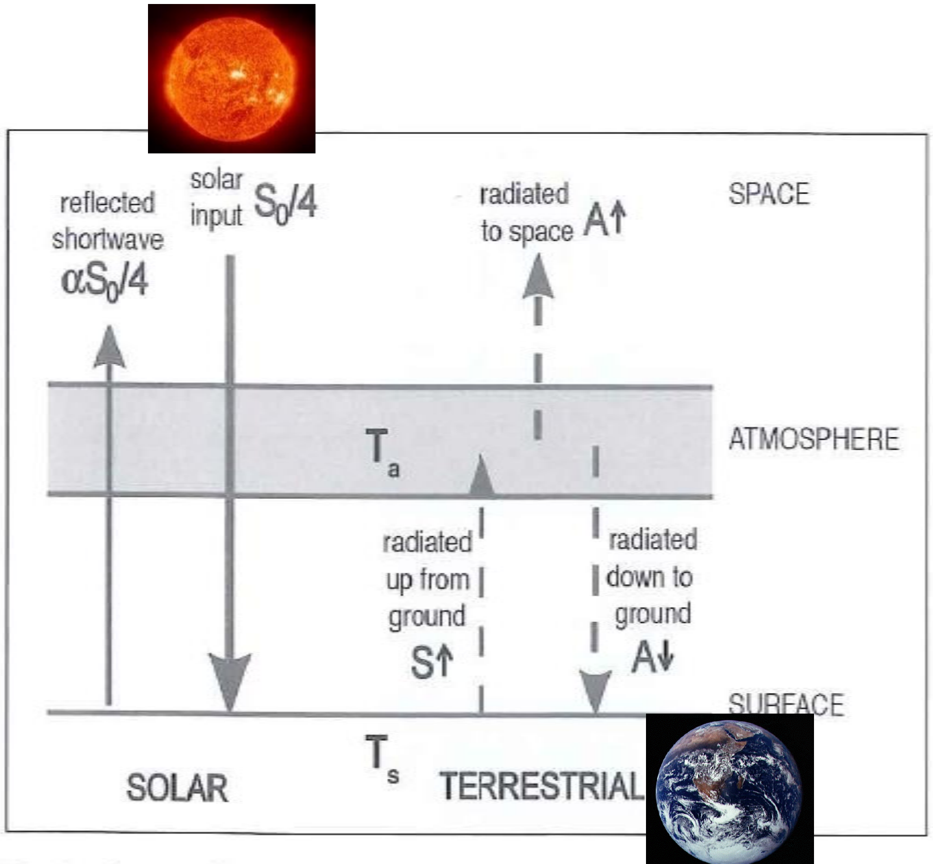

FIGURE 2.7. The simplest greenhouse model, comprising a surface at temperature T_s, and an atmospheric layer at temperature T_a, subject to incoming solar radiation $S_o/4$. The terrestrial radiation upwelling from the ground is assumed to be completely absorbed by the atmospheric layer.

$$S\uparrow=(1-\alpha)S_0/4+A\downarrow$$
$$=2A\downarrow$$

$$S\uparrow \propto Ts^4$$

$$A\uparrow \propto Ta^4$$

$$Ts=2^{1/4}Ta > Ta$$

$$Ts=2^{1/4}x255K$$
$$=303K\ ??$$

From Marshall J., and R. A. Plumb, 2008: Atmosphere, Ocean, and Climate Dynamics, Academic Press, 319pp.

Pictures are from NASA web-sites

Atmosphere at Various Planets

- Venus
  - Solar constant : 2600 W/m2
  - planetary albedo : 0.77
  - Equilibrium radiative temperature : - 46° C
- Earth
  - Solar constant : $S \approx 1370\, Wm^{-2}$
  - planetary albedo : $\alpha_P \approx 0.31$
  - Equilibrium radiative temperature

$$T_e^* = \sqrt[4]{\frac{S(1-\alpha_P)}{4\sigma}} \approx 254K \approx -19°C$$

- Mars
  - Solar constant : 590 W/m2
  - planetary albedo : 0.15
  - Equilibrium radiative temperature : -56° C

Surface Temperature

457° C

Surface Pressure

90,000hPa

Surface Temperature

15° C

Surface Pressure

1,000hPa

Surface Temperature

-55° C

Surface Pressure

10hPa

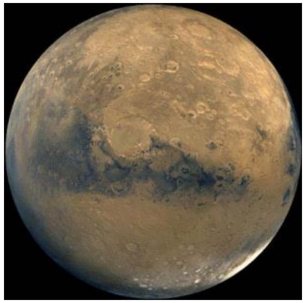

Pictures are from NASA web-sites

Radiative Equilibrium and Radiative-Convective Equilibrium

Radiative heating tends to create vertical instability between heated ground and cooled atmosphere

One-Dimensional Vertical Profile Model

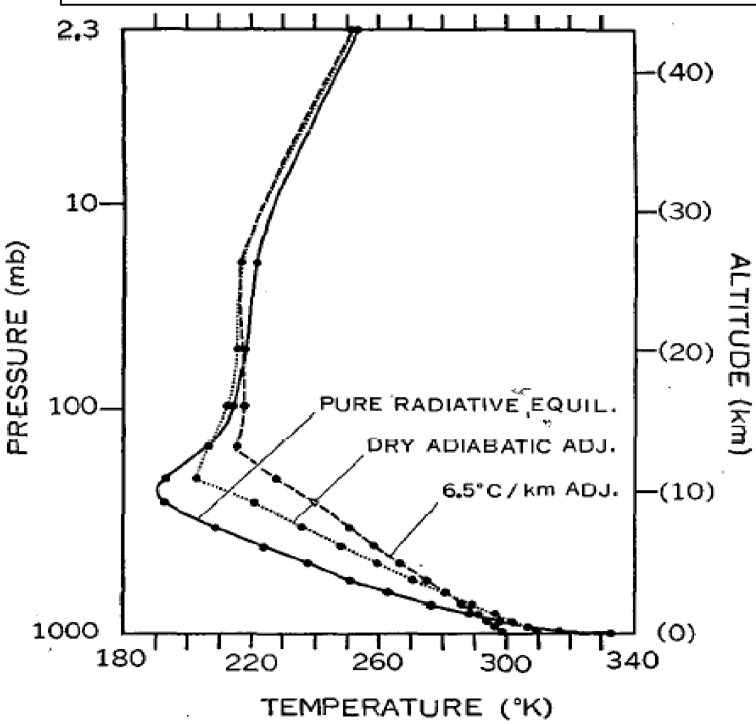

FIG. 4. The dashed, dotted, and solid lines show the thermal equilibrium with a critical lapse rate of 6.5 deg km^{-1}, a dry-adiabatic critical lapse rate (10 deg km^{-1}), and pure radiative equilibrium.

Thermal Equilibrium of the Atmosphere with a Convective Adjustment

SYUKURO MANABE AND ROBERT F. STRICKLER

General Circulation Research Laboratory, U. S. Weather Bureau, Washington, D. C.

(Manuscript received 19 December 1963, in revised form 13 April 1964)

Typical condition at 35N in April

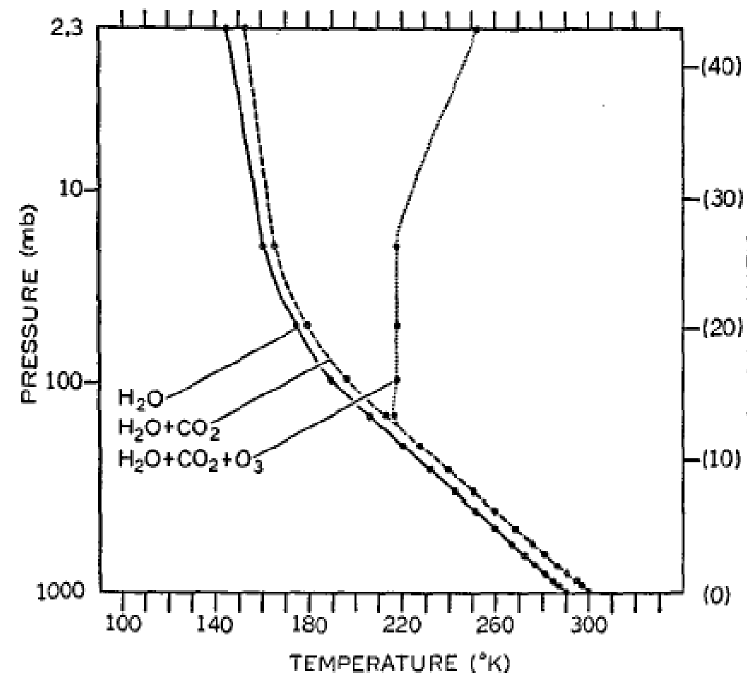

FIG. 6c. Thermal equilibrium of various atmospheres which have a critical lapse rate of 6.5 deg km^{-1}. Vertical distributions of gaseous absorbers at 35N, April, were used. $S_c = 2$ ly min^{-1}, $\cos\bar{\zeta} = 0.5$, $r = 0.5$, no clouds.

Energy Budget

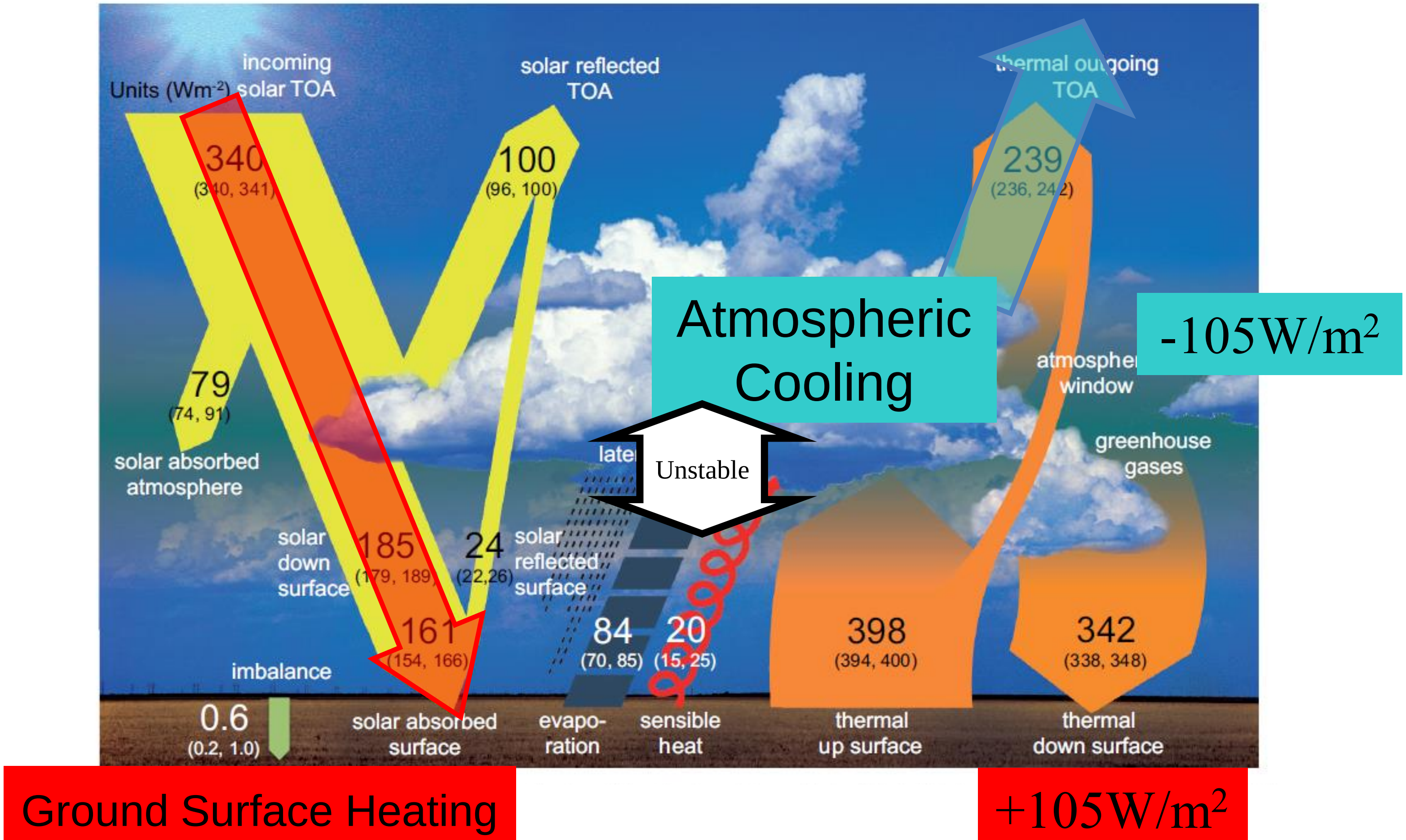

Fig. 2 Schematic diagram of the global mean energy balance of the Earth. Numbers indicate best estimates for the magnitudes of the globally averaged energy balance components together with their uncertainty ranges, representing present day climate conditions at the beginning of the twenty first century. Units Wm-2. Source: Wild et al.(2013.)

1-D model is not perfect

What process is lacked in 1-D model?

Thermal Equilibrium of the Atmosphere with a Convective Adjustment

SYUKURO MANABE AND ROBERT F. STRICKLER

General Circulation Research Laboratory, U. S. Weather Bureau, Washington, D. C.

(Manuscript received 19 December 1963, in revised form 13 April 1964)

Observed Temperature

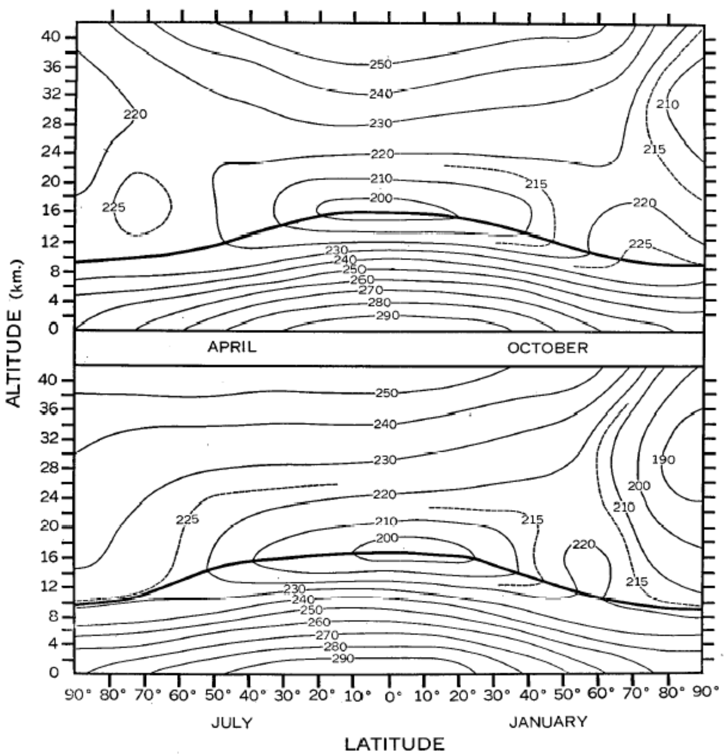

FIG. 12. Distribution of the observed temperature (deg k) in the northern hemisphere for different seasons. From J. London (1956).

One-Dimensional Vertical Profile Model

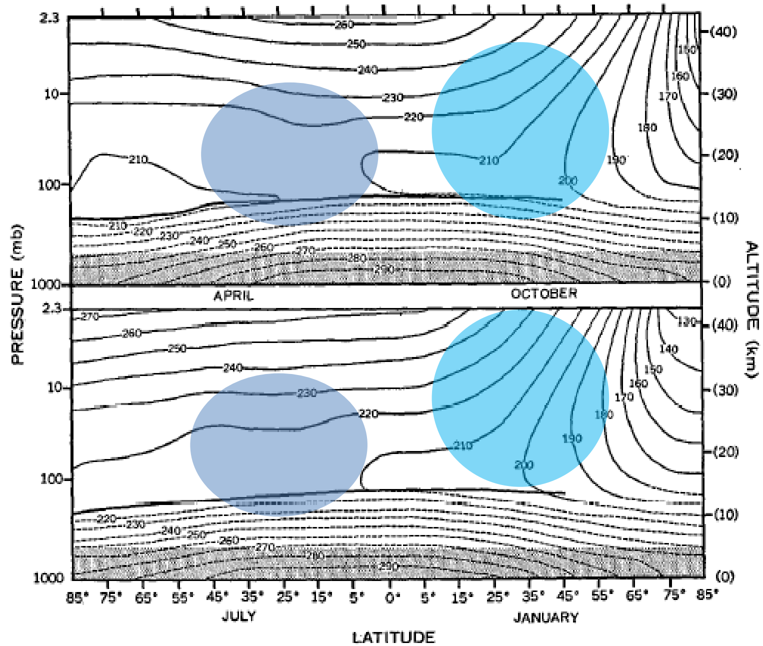

FIG. 13. The local radiative equilibrium temperature of the stratosphere. The shaded area is the region where the temperature was fixed at the observed value. Above the shaded area the state of the convective equilibrium, whose critical lapse rate for convective adjustment is deg km^{-1}, is shown. The region covered by solid lines is in local radiative equilibrium.

- 1.3 Horizontal Radiative Imbalance and Circulations

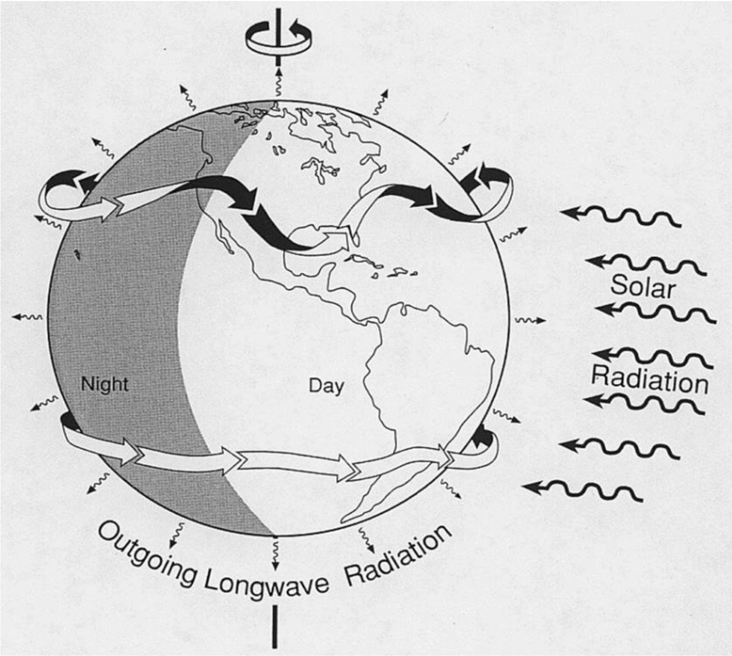

Meridional distribution of Annual mean radiation balance

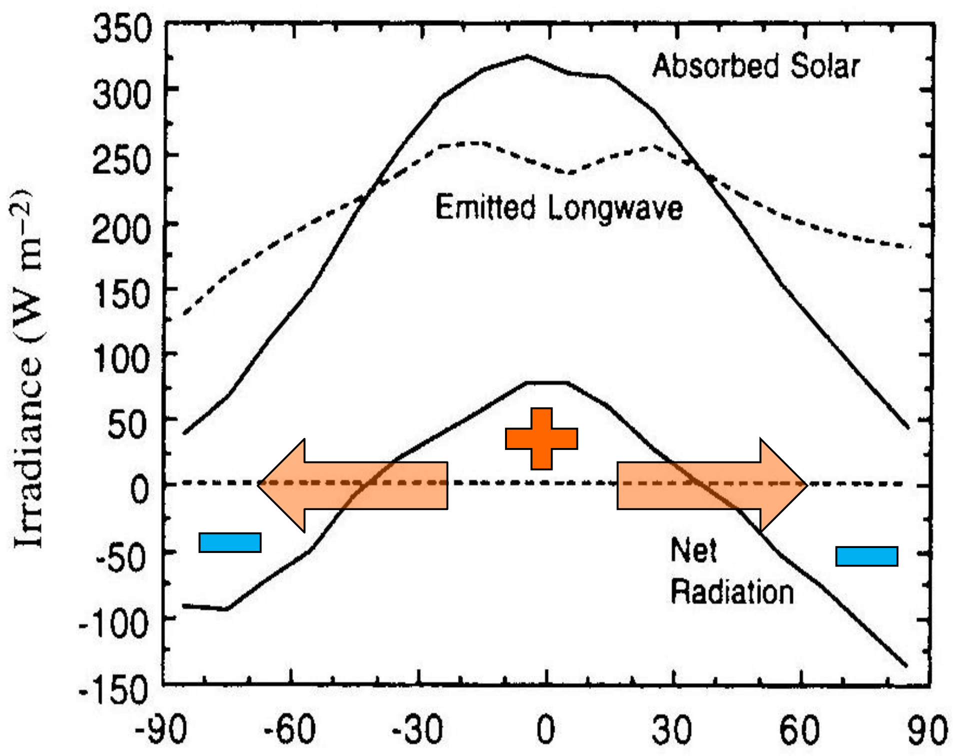

Hartmann (1994)

- Solar radiation
  - Global mean : 235 Wm^{-2}
  - Low latitude : over 300 Wm^{-2}
  - Poles : about 50 Wm^{-2}
- Terrestrial radiation
  - Global mean : 235 Wm^{-2}
  - Less gradient between low latitudes and poles compared to that in solar radiation
- Net radiation
  - Global mean : 0 Wm^{-2}
  - Positive in low latitudes, negative in high latitudes
- **Poleward heat transport by the atmosphere and ocean balances this meridional heat imbalance**

Energy transport by the atmosphere and ocean

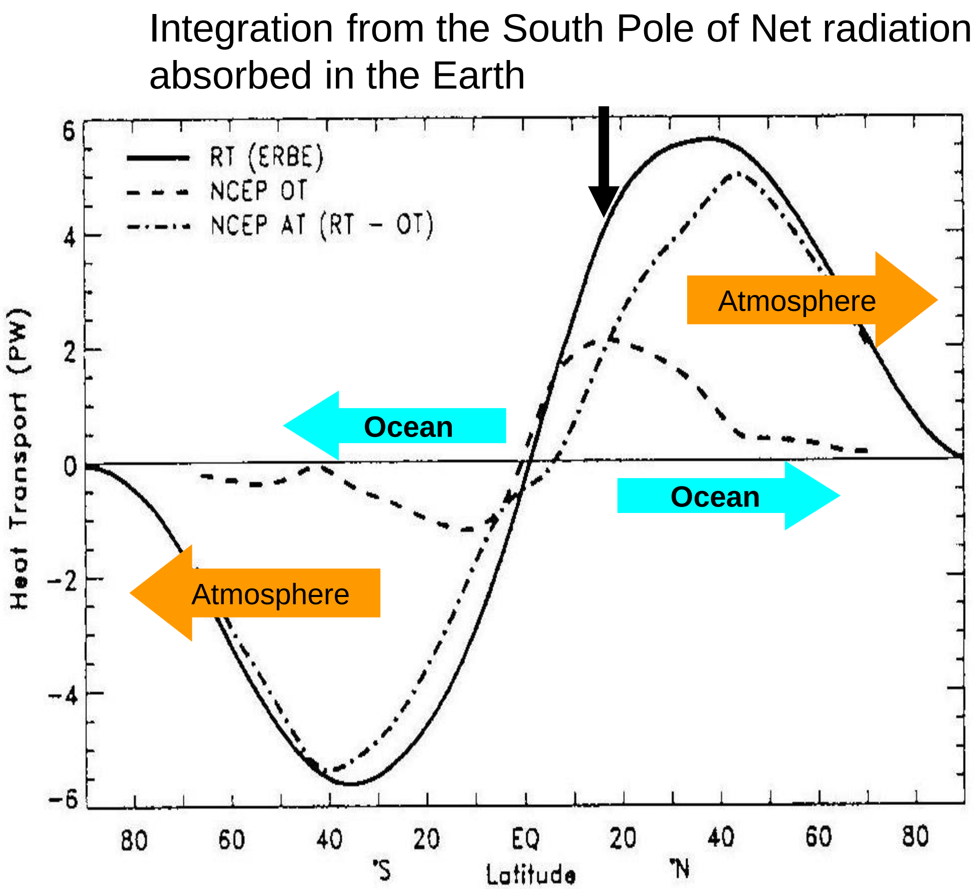

Trenberth and Caron (2001)

- **Both the atmosphere and ocean are responsible for energy transport**
- Atmospheric transport is larger, particularly in the mid and high latitudes
- Oceanic transport is large in low-latitudes

General atmospheric circulation from a state of rest in a climate model

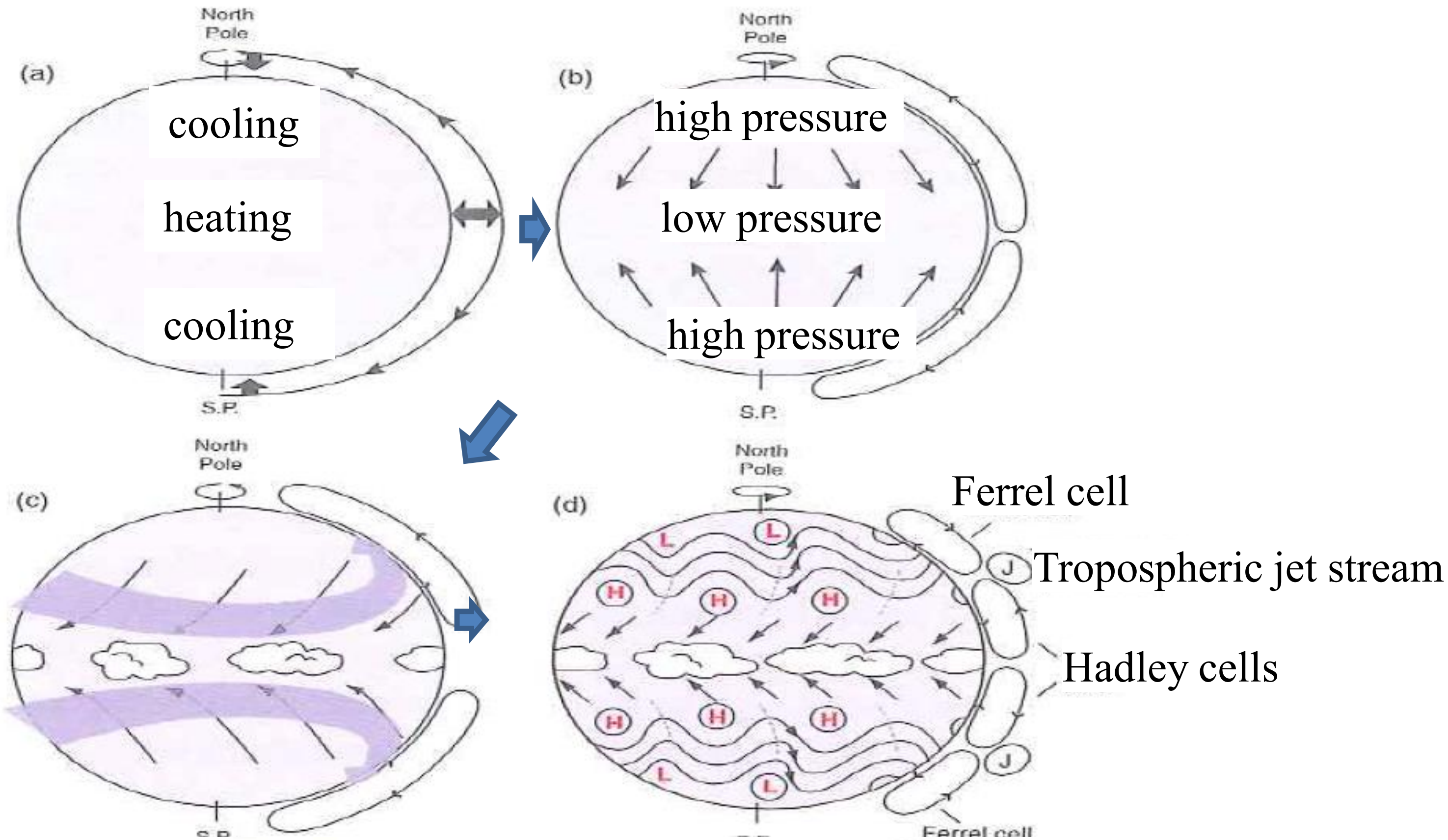

Fig. 7.21 Schematic depiction of the general circulation as it develops from a state of rest in a climate model for equinox conditions in the absence of land–sea contrasts. See text for further explanation.

From Wallace, J.M. and P. V. Hobbs, 2006: Atmospheric Science. Academic Press, 483pp.

Observed atmospheric general circulation

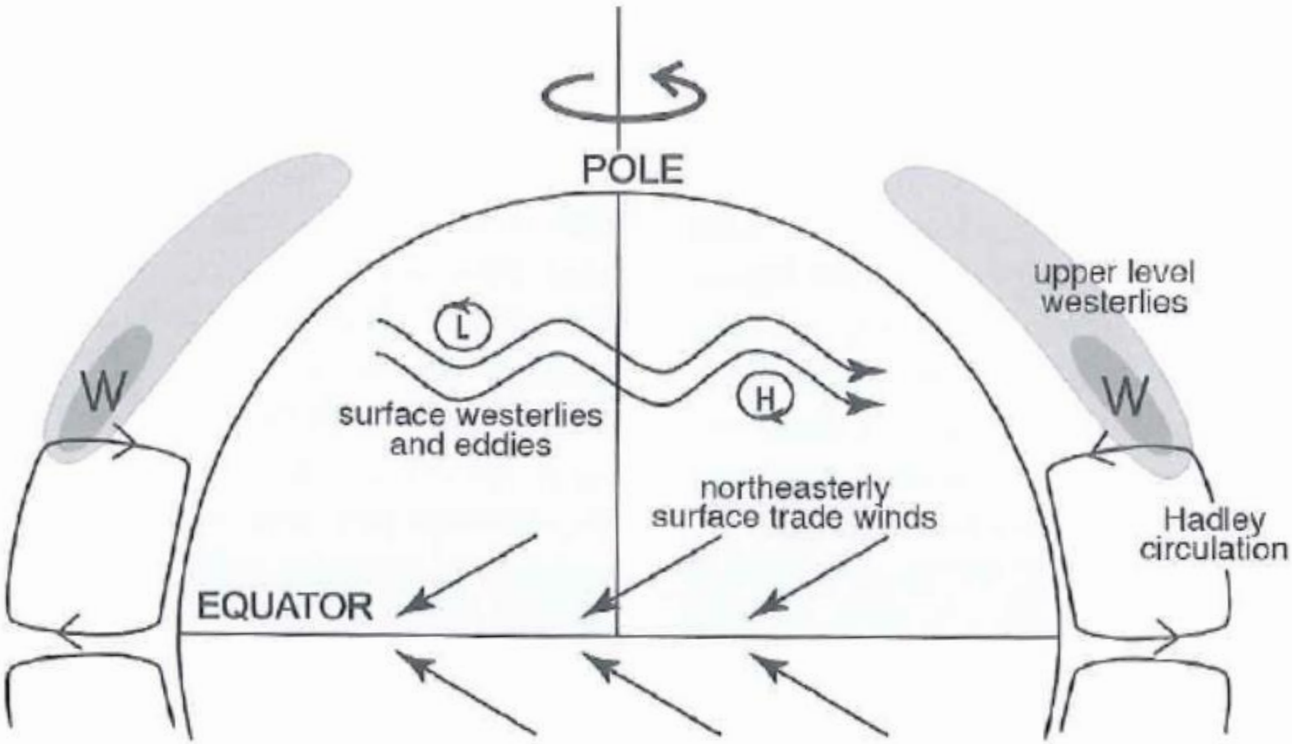

FIGURE 8.2. Schematic of the observed atmospheric general circulation for annual-averaged conditions. The upper level westerlies are shaded to reveal the core of the subtropical jet stream on the poleward flank of the Hadley circulation. The surface westerlies and surface trade winds are also marked, as are the highs and lows of middle latitudes. Only the northern hemisphere is shown. The vertical scale is greatly exaggerated.

From Marshall J., and R. A. Plumb, 2008: Atmosphere, Ocean, and Climate Dynamics, Academic Press, 319pp.

Energy Transport by Atmospheric Circulation in the tropics

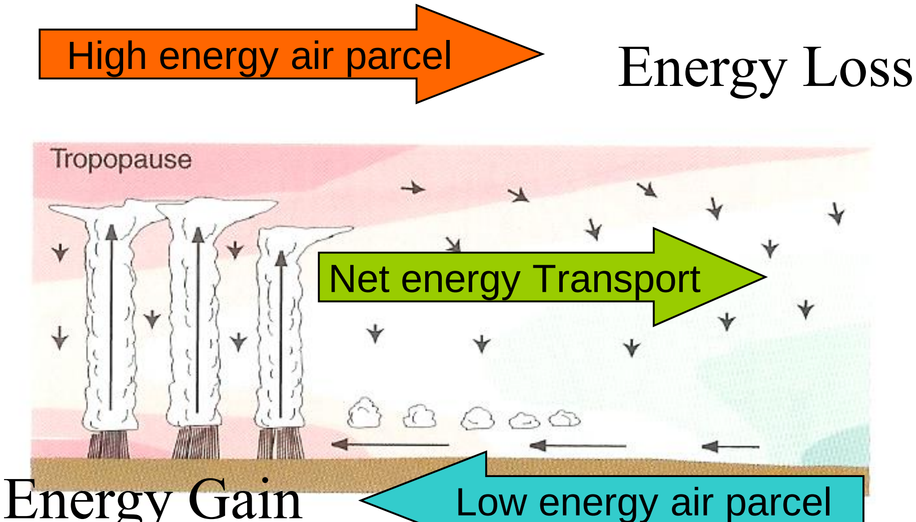

Fig. 10.3 Schematic of air parcels circulating in the atmosphere. The Colored shading represents potential temperature or moist static energy, with pink indicating higher values and blue lower values. Air parcels acquire latent and sensible heat during the time that they reside within the boundary layer, raising their moist static energy. They conserve moist static energy as they ascend rapidly in updrafts in clouds, and they cool by radiative transfer as they descend much more slowly in clear air.

- Moist Static Energy

  $H = C_pT + gZ + Lq$

  T: Temperature

  Z: Height

  q: Specific Humidity

H of air parcels is conserved even through adiabatic process and/or condensation process,

but, not conserved through the processes of radiation, heat and moisture supply from ground surface.

From Wallace, J.M. and P. V. Hobbs, 2006: Atmospheric Science. Academic Press, 483pp.

Energy transport by atmospheric general circulation

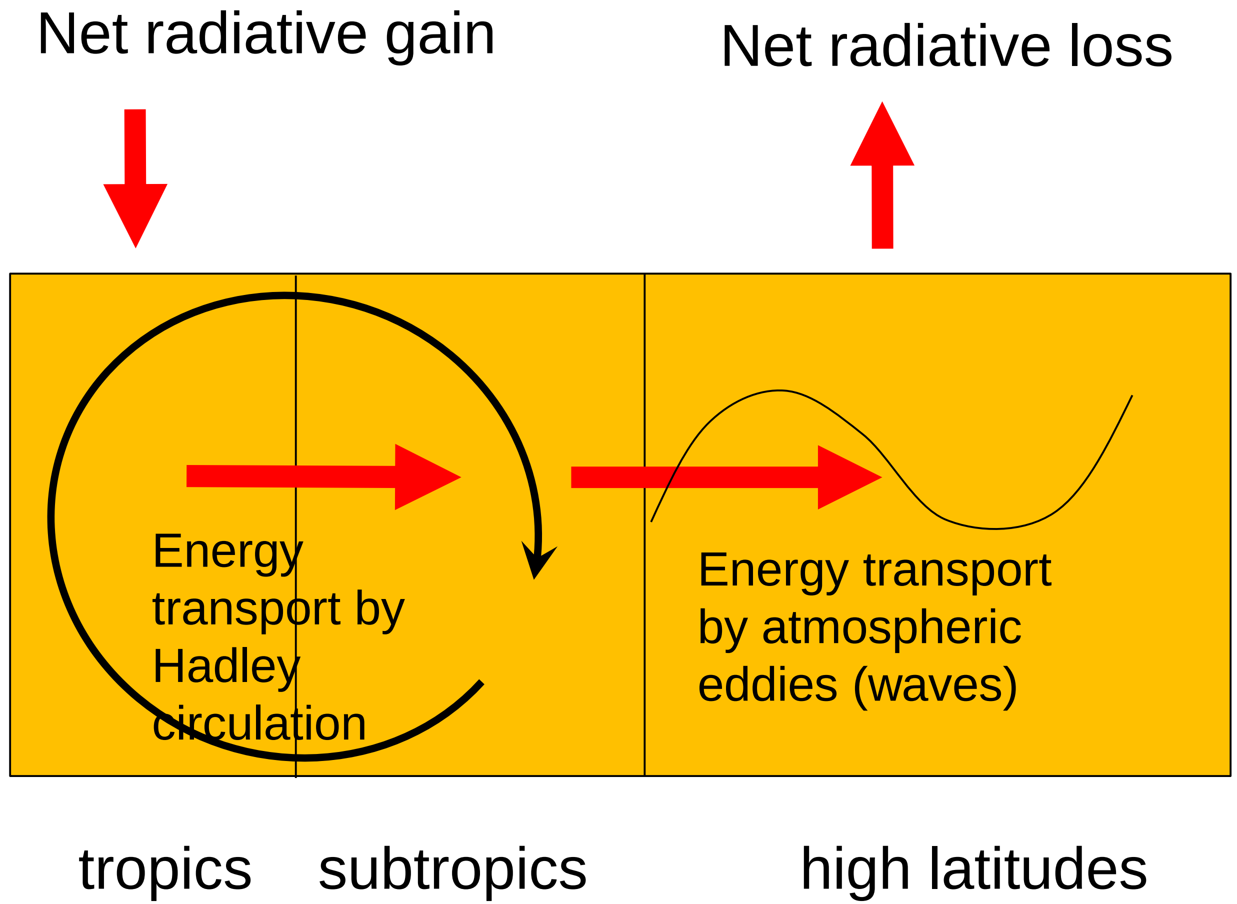

Momentum transport by atmospheric general circulation

tropics middle latitudes

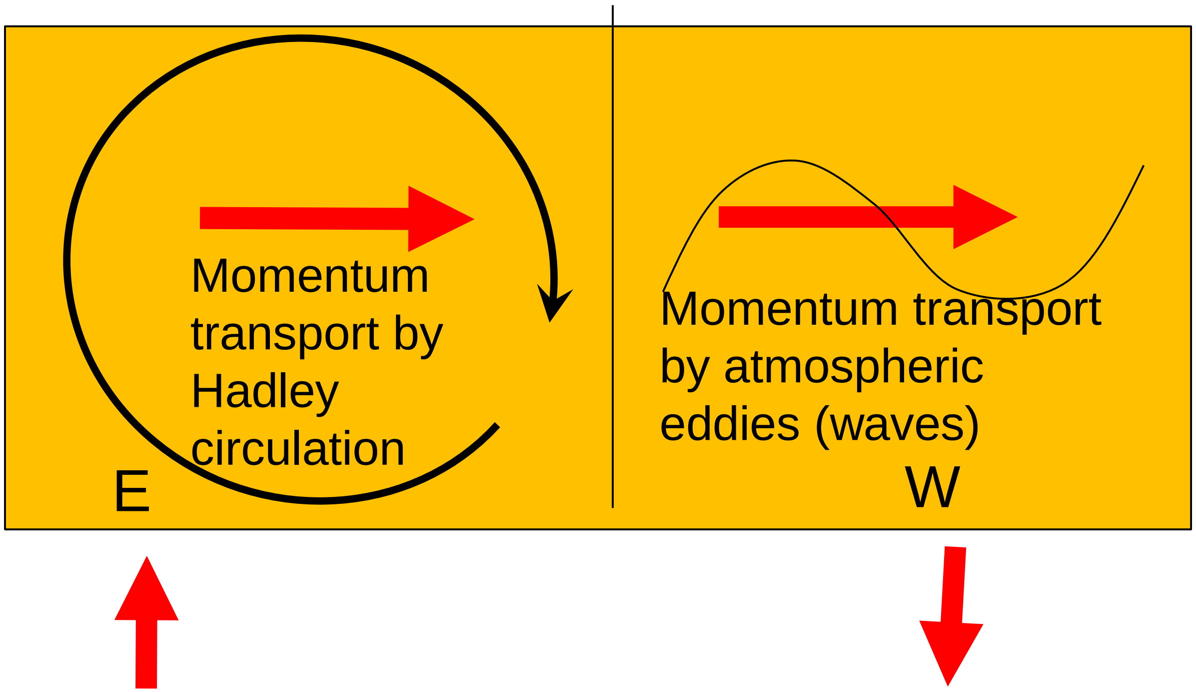

momentum gain momentum loss

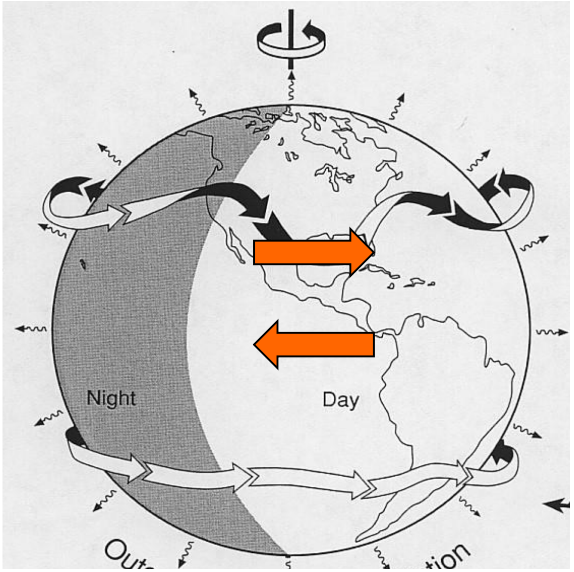

1.4 Seasonal Change

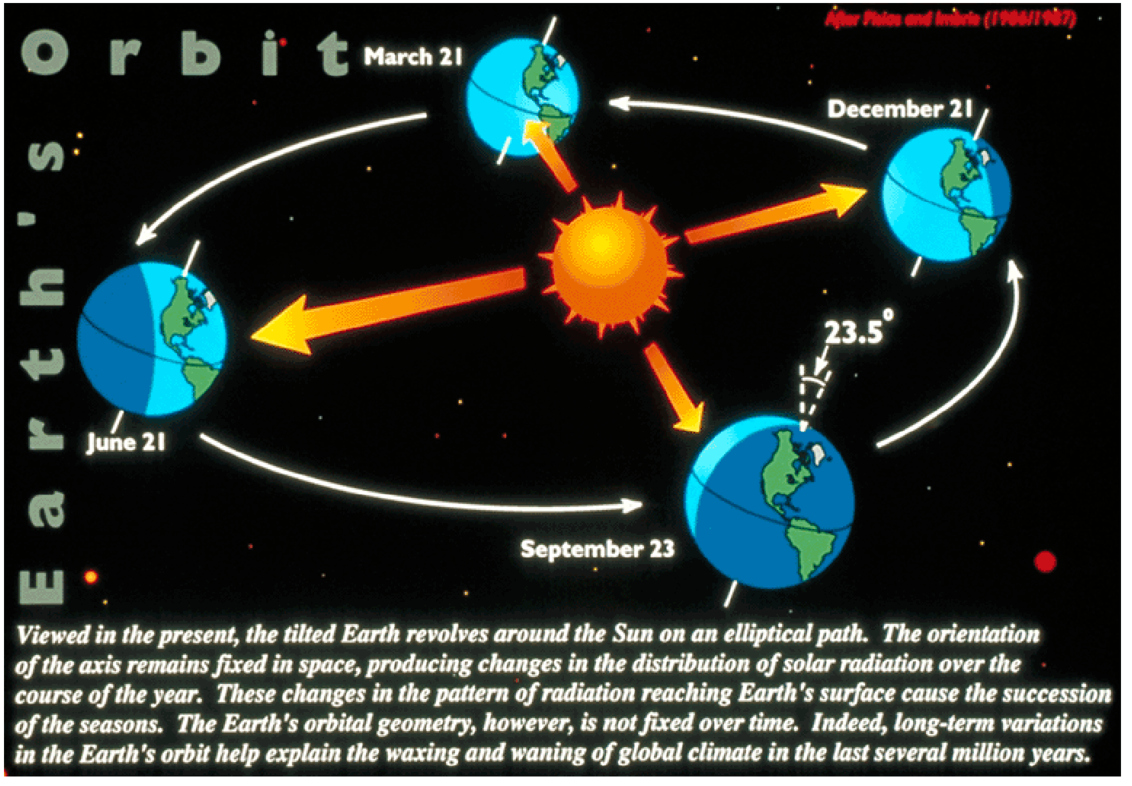

Seasonal Change of Solar Insolation and Temperature

Solar Insolation W/m2

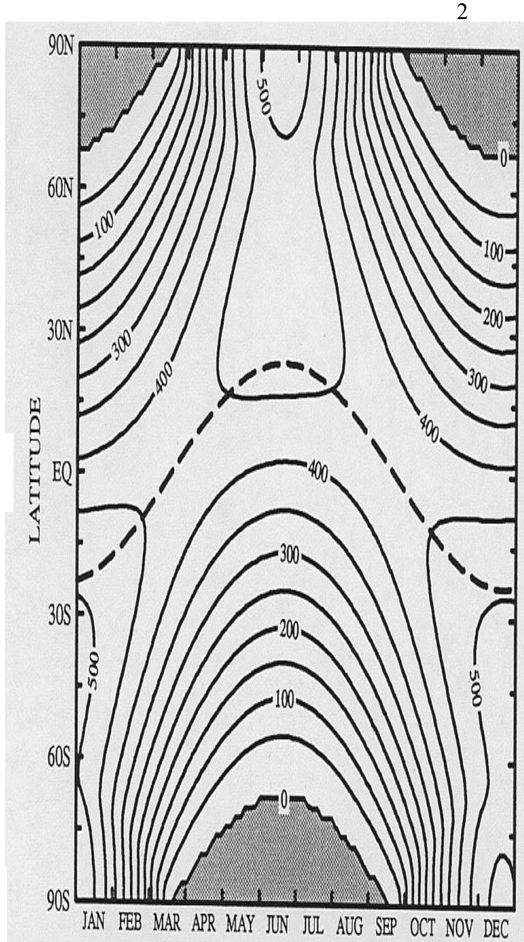

Temperature in the stratosphere (50hPa) ℃

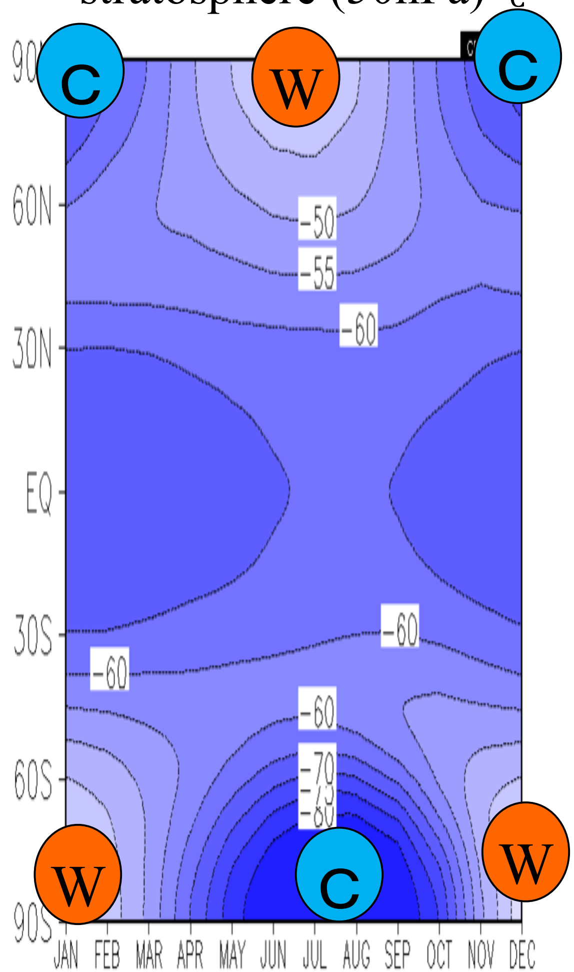

Temperature in the troposphere (850hPa) ℃

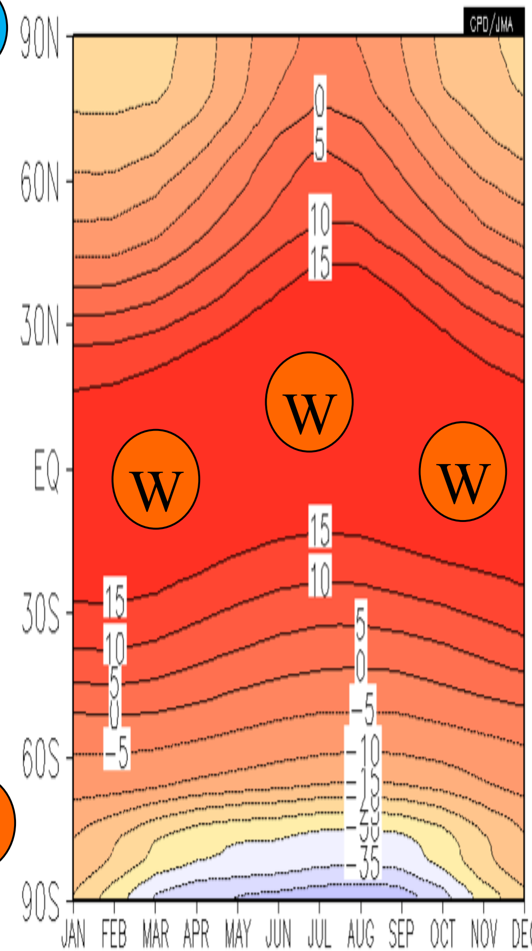

90N

EQ.

90S

JAN JUL DEC JAN JUL DEC

Month of maximum monthly mean temperature

Solar max/min = Dec/Jun **Temperature max/min = Jan,Feb/Jun,Jul**

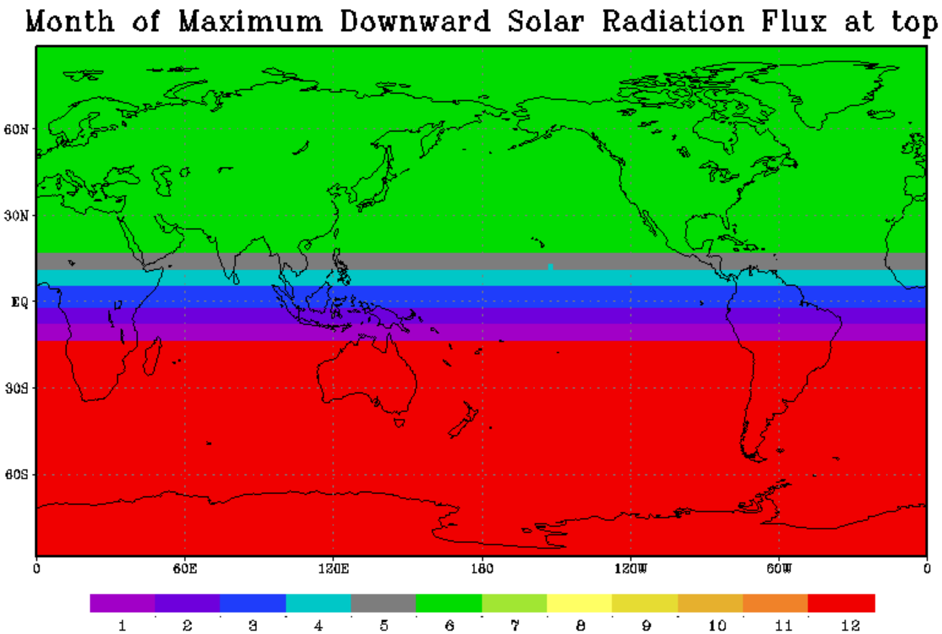

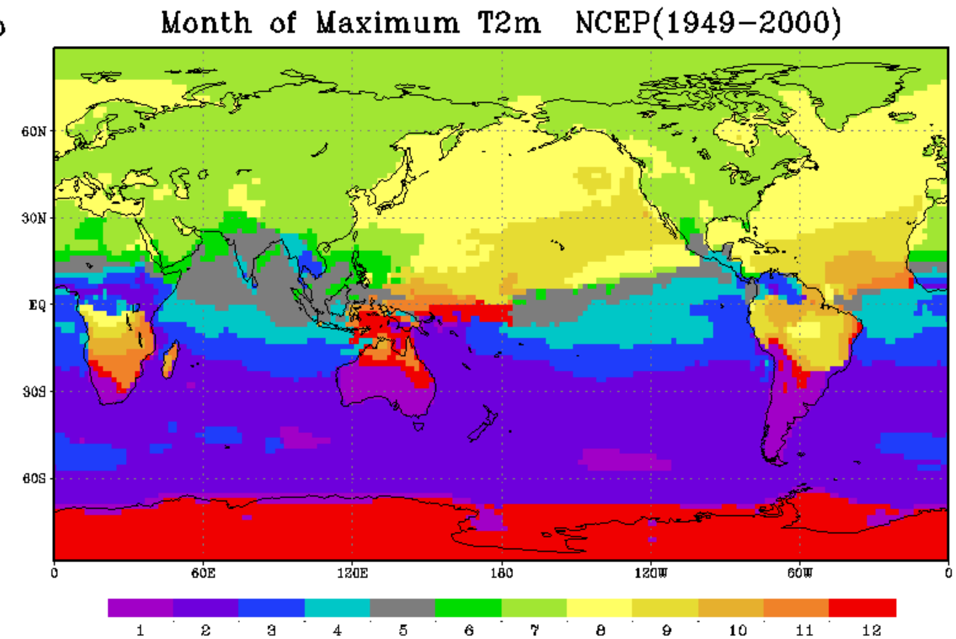

(Left) Downward solar radiation at the top of the atmosphere is maximum in June (December) poleward of about 15° latitude in the NH (SH). In the tropics, it is January, February, March, April and May at 10° S, 4° S, 2° N, 8° N and 14° N, respectively.

(Right) Actual month of maximum monthly mean temperature is quite different due to inertia of atmosphere, land and ocean. It is July over the continents and August over the oceans in the NH, but its distribution is not simple.

Seasonal Change of Sea Surface Temperature (SST)

Solar Insolation

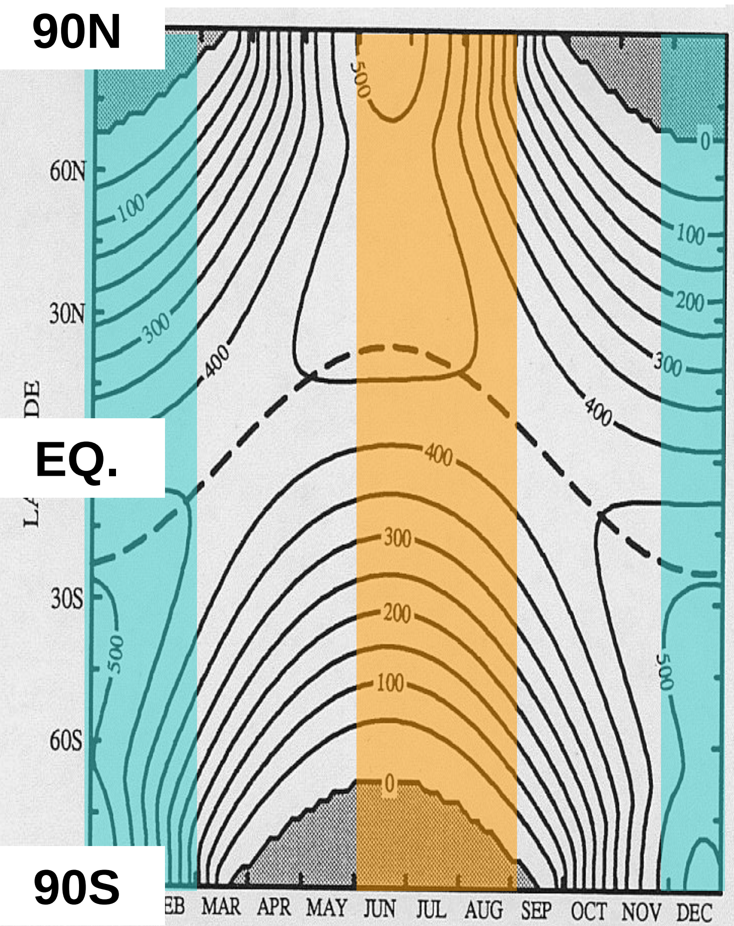

Dec.-Jan.-Feb.

Jun-July-August

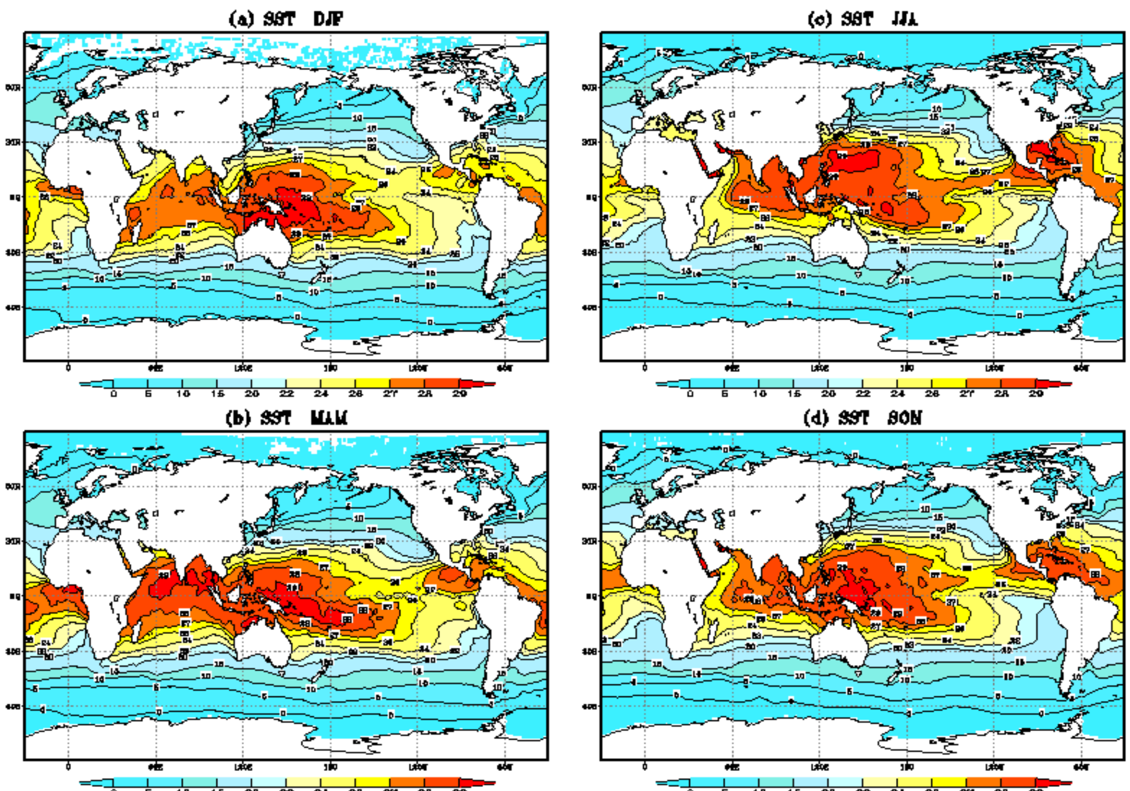

Mar.-Apr.-May

Sep.-Oct.-Nov.

Heat Capacity of atmosphere and ocean

	Atmosphere	Ocean
Density	1.2-1.3kgm^{-3}	$10^3 kgm^{-3}$ ：atom. X 800
Mass(per 1 m^2)	（Top ～ Surface） $10^4 kgm^{-2}$	（Surface ～10m depth） $10^4 kgm^{-2}$ ：Mass of the atmosphere is the same as that of ocean with 10m depth
Specific heat	$10^3 Jkg^{-1}K^{-1}$	$4 \times 10^3 Jkg^{-1}K^{-1}$ ：atom. X 4
Heat capacity (per 1 m^2)	（Top ～ Surface） $10^7 JK^{-1}m^{-2}$	（Surface ～2.5m depth） $10^7 JK^{-1}m^{-2}$ ：Heat capacity of the atmosphere is the same as that of ocean with 2.5m depth

"1K in 250m depth ocean" is near equal to "100K in the atmosphere"

＊from Gill 1982

Jan-Jul contrast of surface temperature (℃)

January

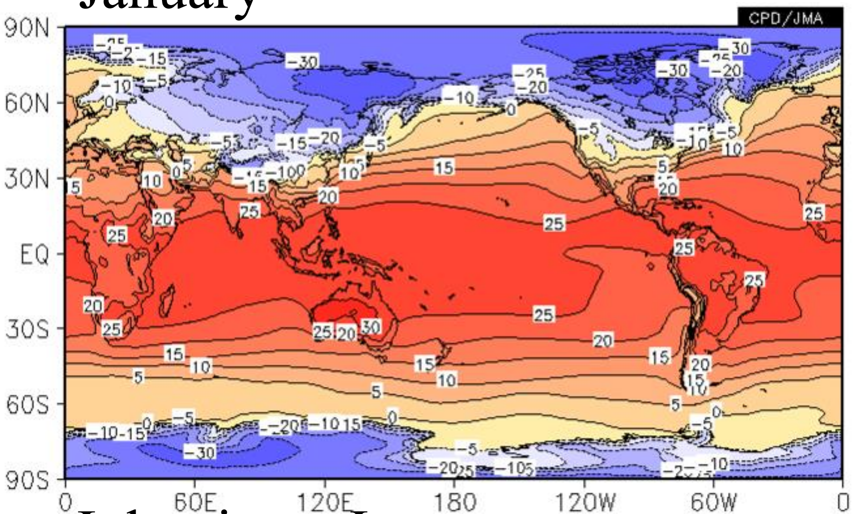

July

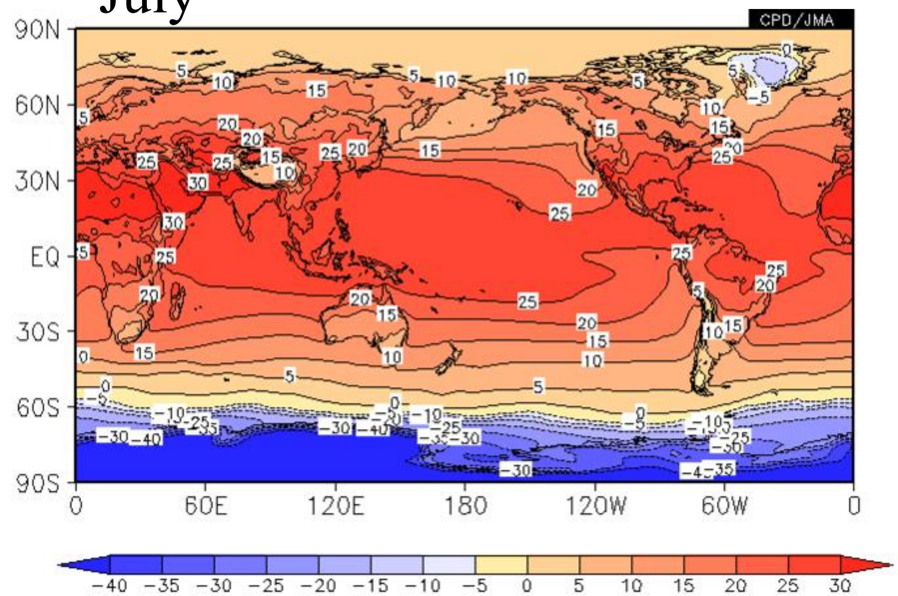

Jul. minus Jan.

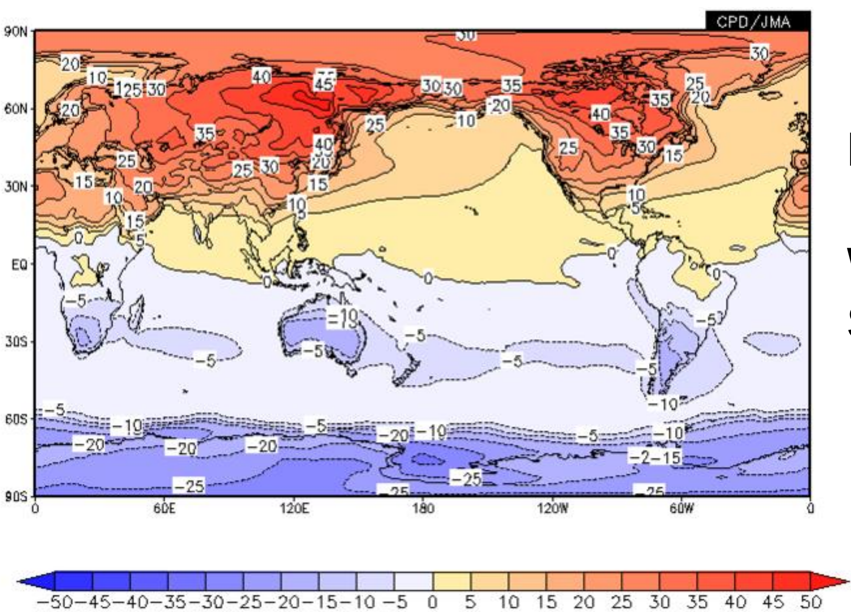

Larger temperature contrast over lands

Winter: land temp. < ocean temp.
Summer: land temp. > ocean temp.

Monsoon circulation

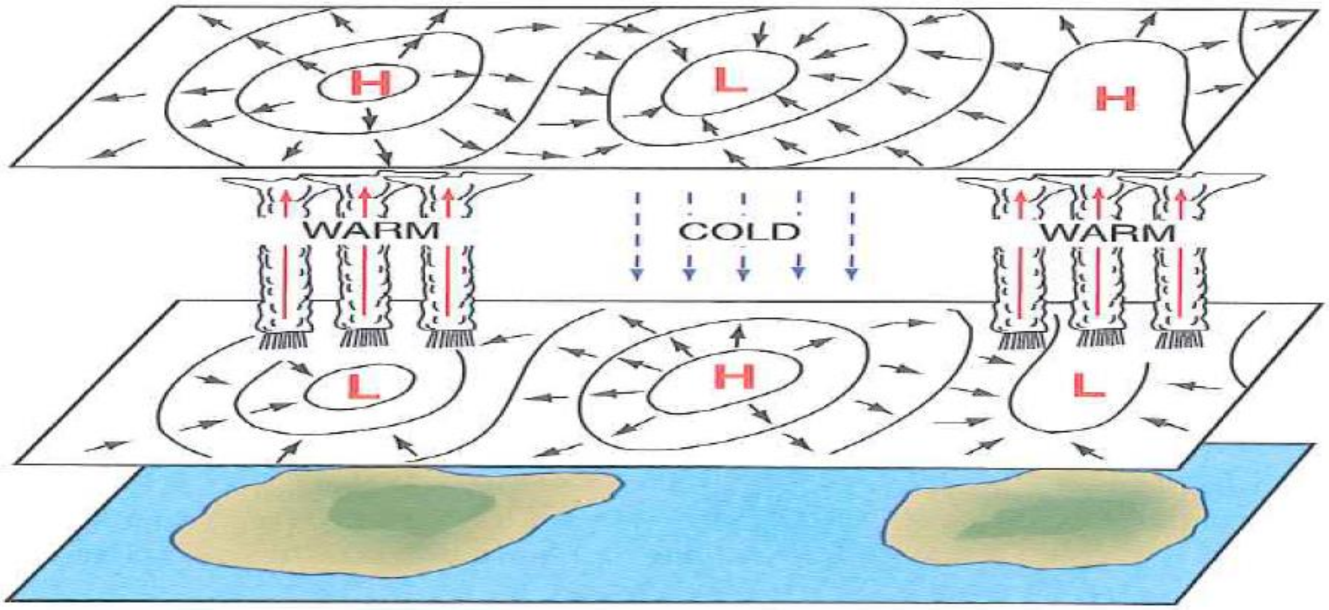

Fig. 10.9 Idealized representation of the monsoon circulations. The islands represent the subtropical continents in the summer hemisphere. Solid lines represent isobars or height contours near sea level (lower plane) and near 14 km or 150 hPa (upper plane). Short solid arrows indicate the sense of the cross-isobar flow. Vertical arrows indicate the sense of the vertical motions in the middle troposphere. Regions that experience of summer monsoon rainfall are also indicated.

From Wallace, J.M. and P. V. Hobbs, 2006: Atmospheric Science. Academic Press, 483pp.

Northern Summer Monsoon

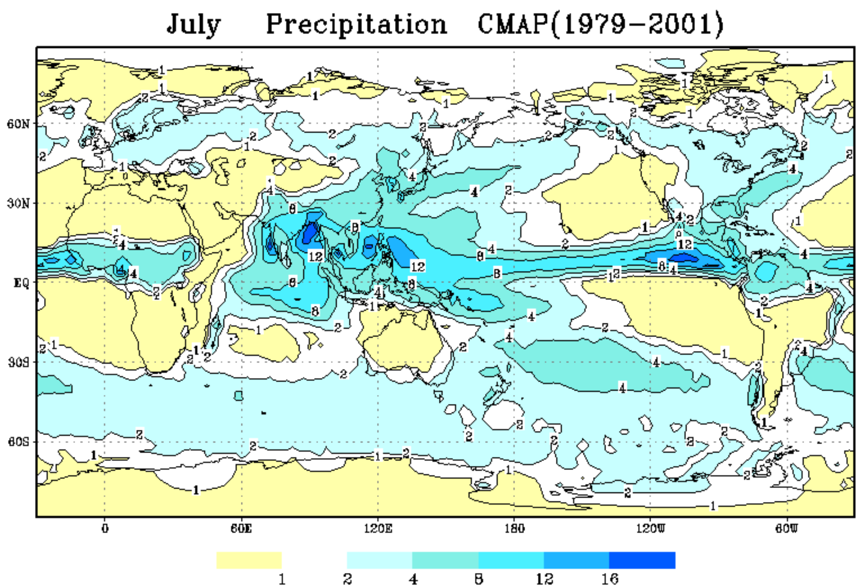

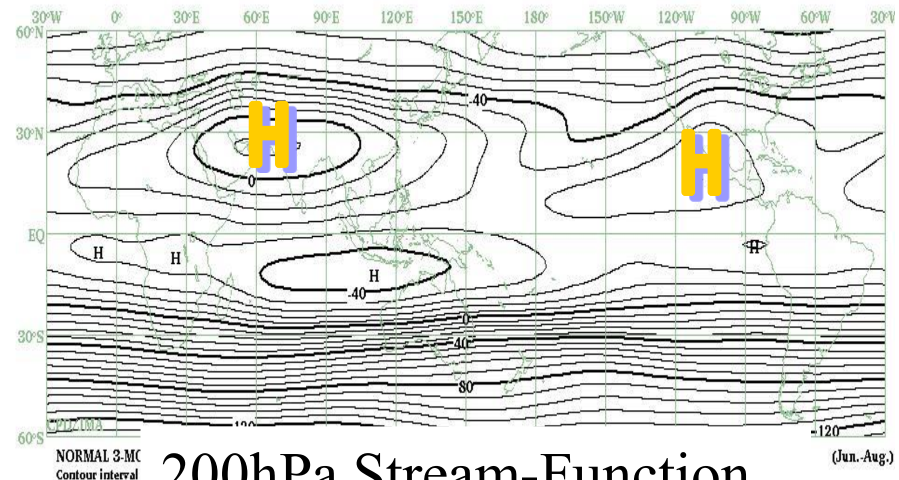

200hPa Stream-Function

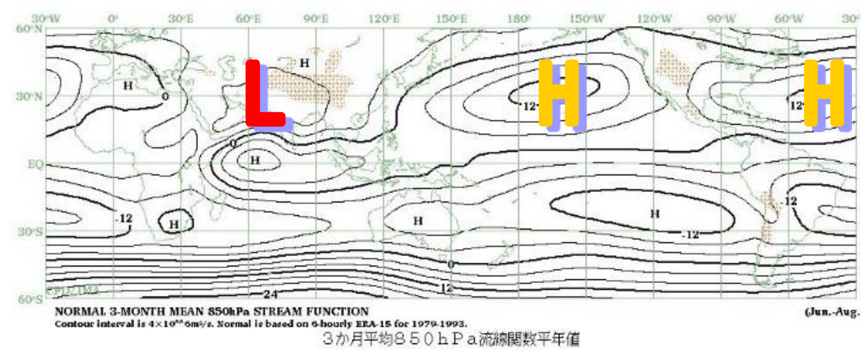

850hPa Stream-Function

Southern Summer Monsoon

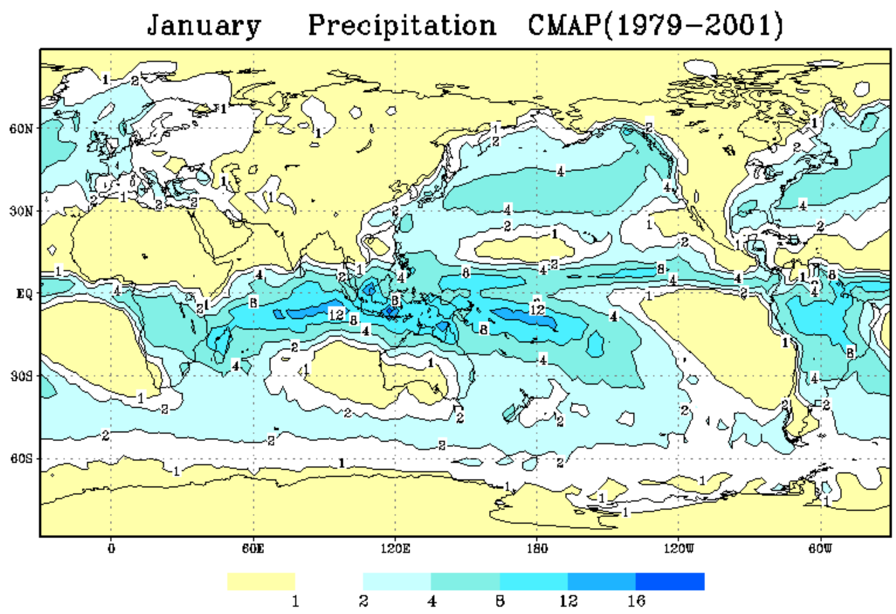

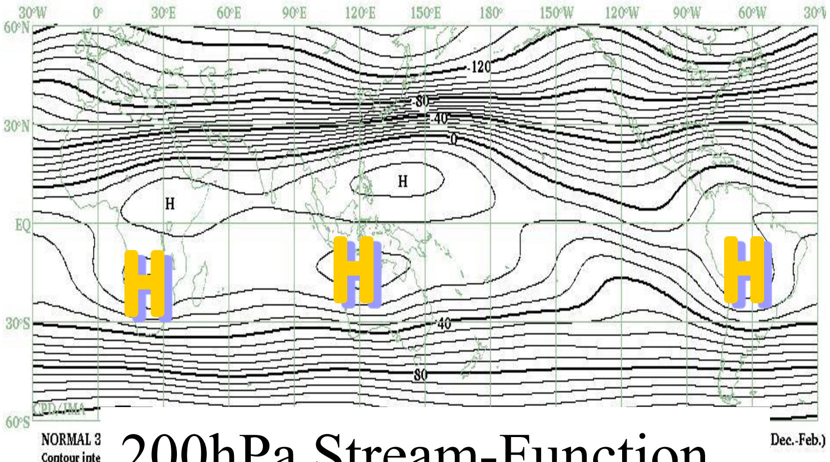

200hPa Stream-Function

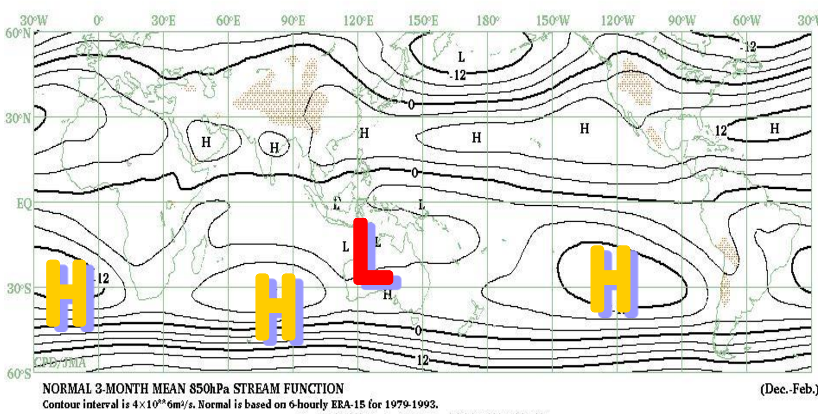

850hPa Stream-Function

Local heating in the tropics forces stationary waves

Diabatic heating in Jan.

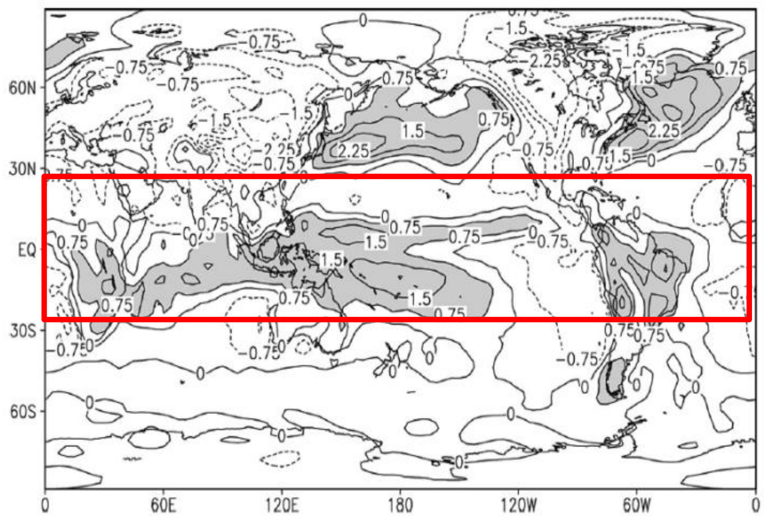

FIG. 8. The column-averaged diabatic heating field in Jan obtained from the NCEP–NCAR reanalysis as described in the appendix. The contour interval is 0.5 K day^{-1}.

Linear response to the heating in the left panel
Eddy stream function at 300hPa

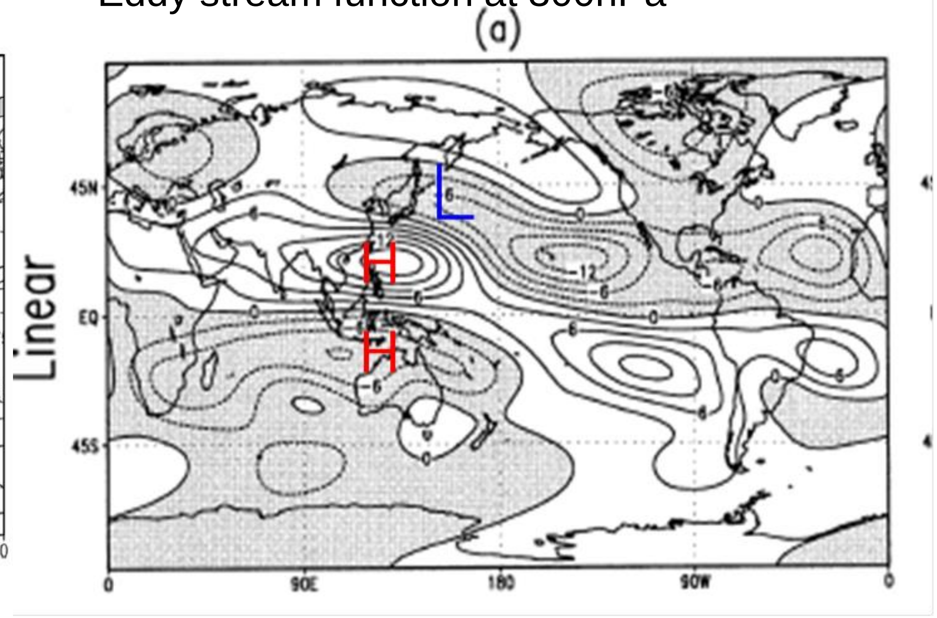

Held et al. (2002)

Seasonal change of precipitation and surface wind

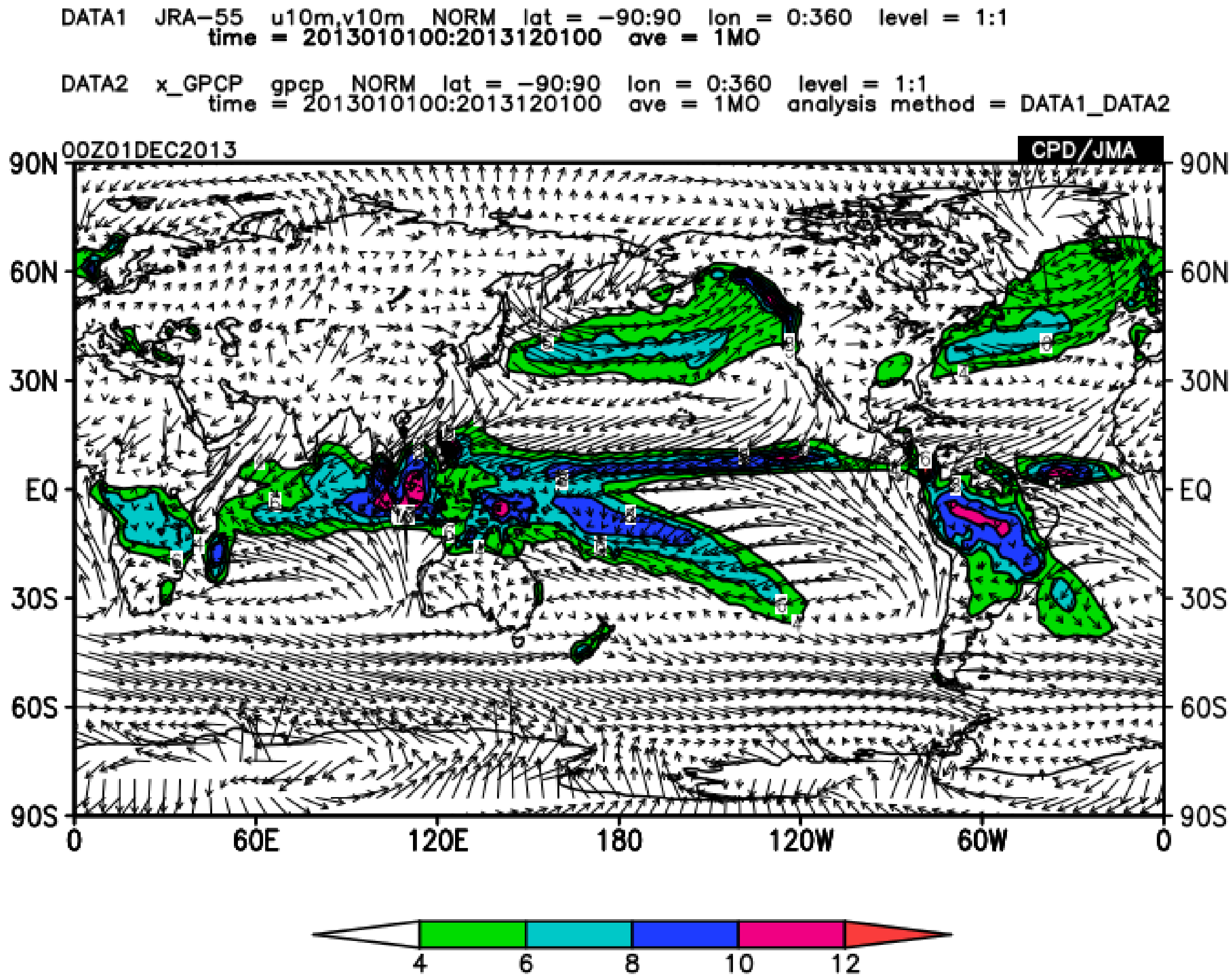

Seasonal change of zonal wind and stream function at 200hPa

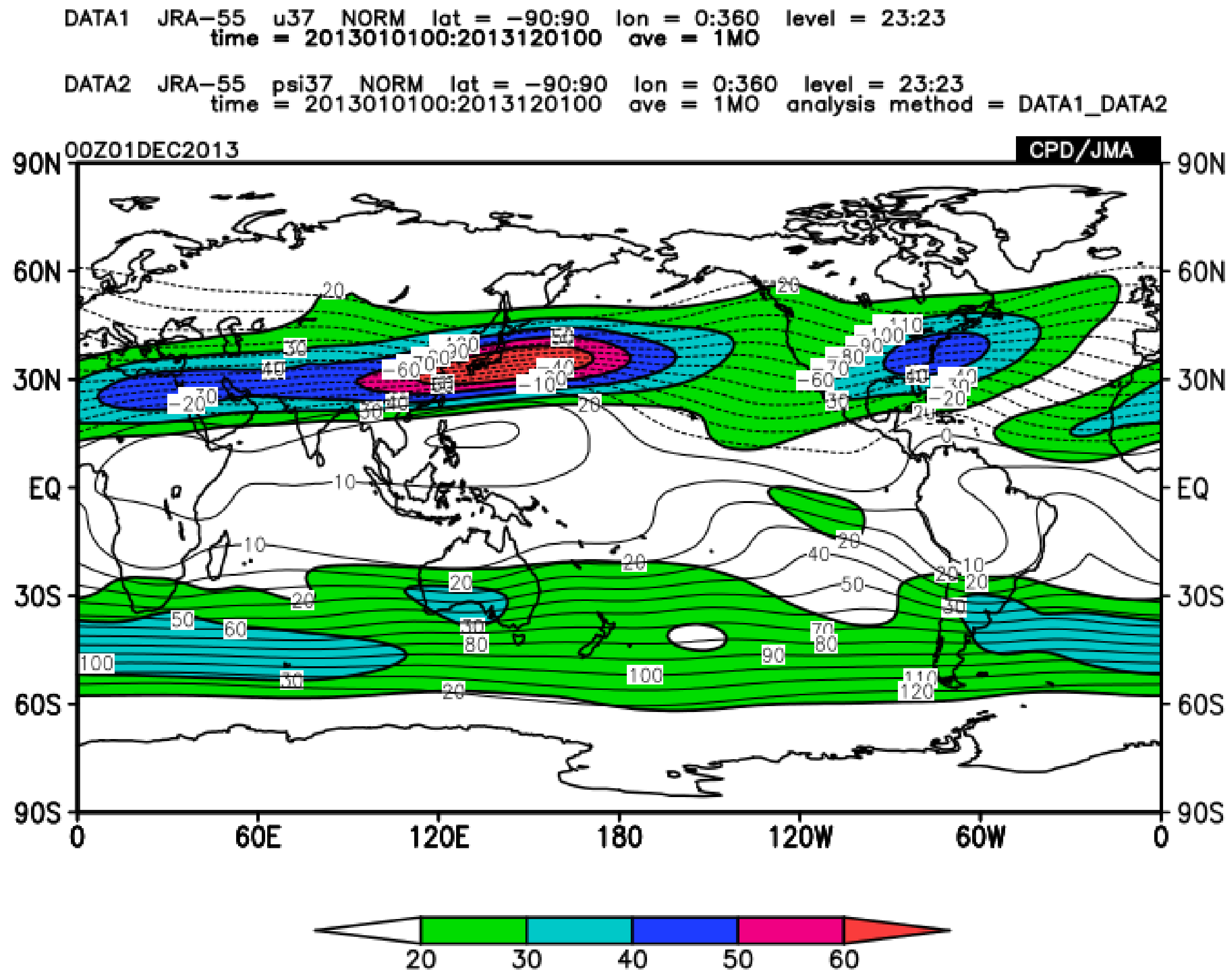

- 1.5 Role of orography on climate

Effect of mountains on climate

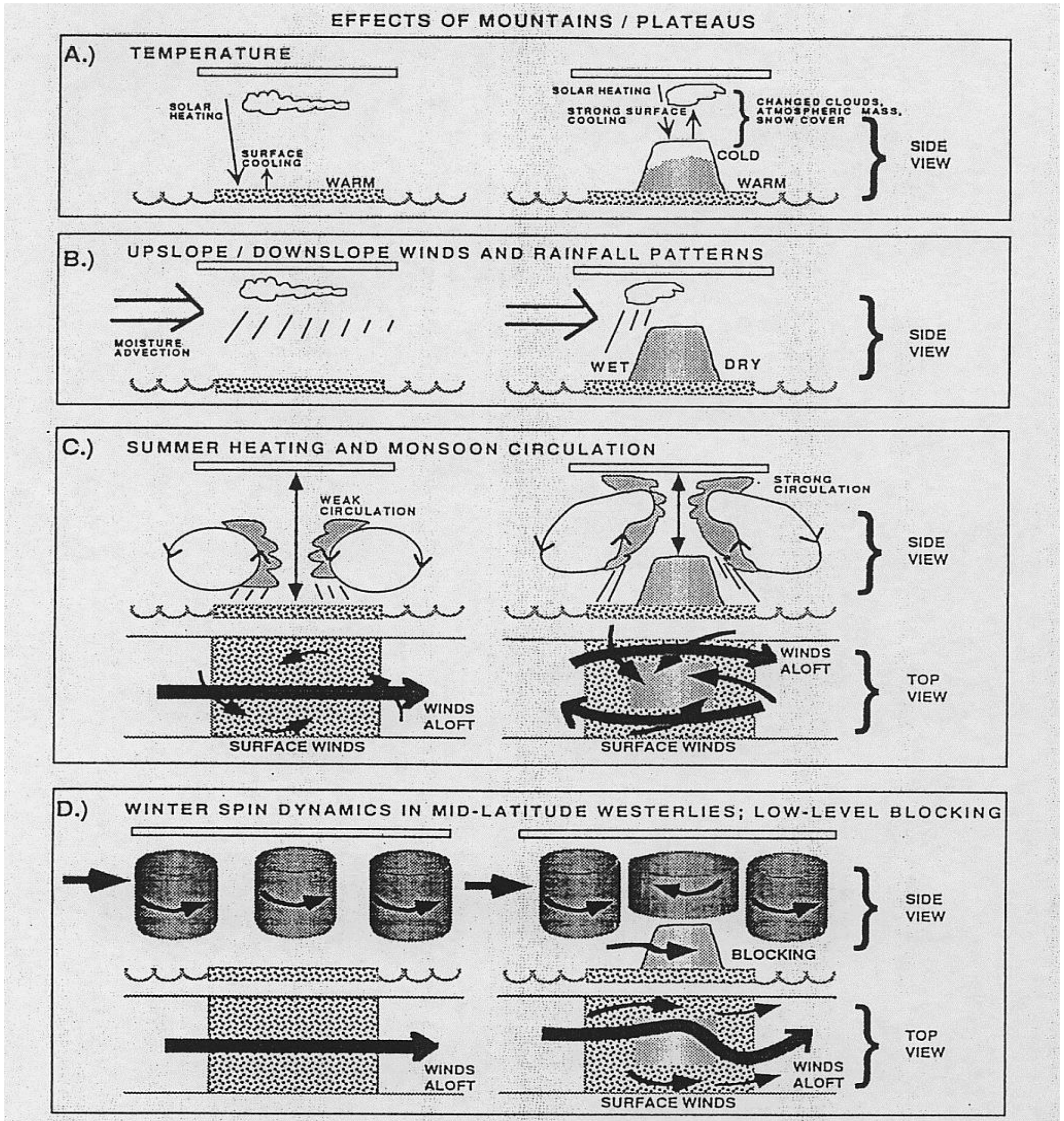

Figure 1. Effects of mountains/plateaus on climate: (*a*) temperature, (*b*) upslope/downslope winds and rainfall patterns, (*c*) summer heating and monsoon circulation, and (*d*) winter spin dynamics in mid-latitude westerlies, and low-level blocking. See text for explanation.

Kutzbach et al. (1993) J.Geology

Effect of mountain: Koppen climate

OBS.

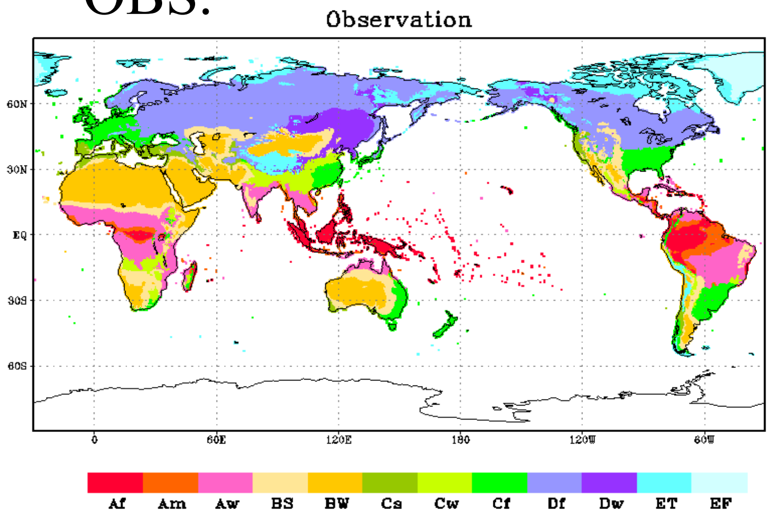

Simulation by Climate Model

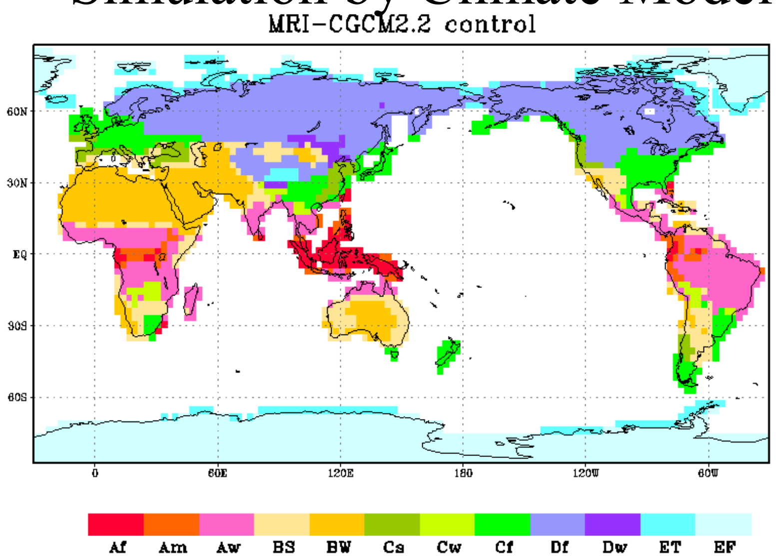

Simulation by Climate Model without mountain

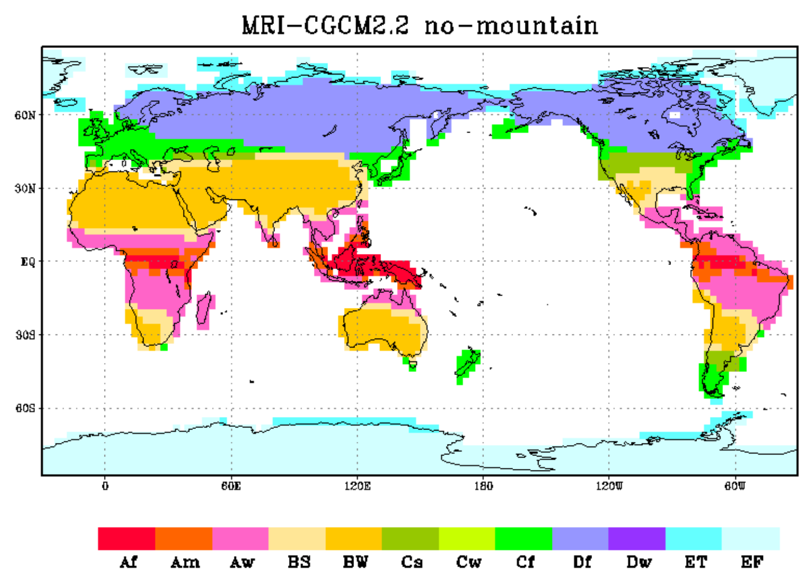

Outline of the lecture

1. Climate System (60 min. + α)
    - 1.1 Introduction
    - 1.2 Radiative Balance
    - 1.3 Horizontal Radiative Imbalance and Circulations
    - 1.4 Seasonal Change
    - 1.5 Role of Orography on Climate
2. Climate Variability (90 min. + α)
    - 2.1 Introduction
    - 2.2 Intraseasonal Variability: Quasi-stationary Rossby wave, MJO and equatorial waves
    - 2.3 Interannual Variability: ENSO, El Nino Modoki, IOD
    - 2.4 Decadal Variability: PDO, ENSO-Monsoon relation
3. Climate change due to anthropogenic forcing (30 min. + α)

- 2.1 Introduction

Causes of Climate Variability

- Natural origin

external: land-sea distribution, orography

solar constant, orbital variations, volcano

internal variability of the climate system

(e.g., air-sea interaction,,,)

- Anthropogenic origin

emission of greenhouse gases, destruction of ozone layer, land surface modification,,, (= climate change)

Various time scales of climate variability

- days to intraseasonal variability
  Blocking, Quasi-stationary Rossby wave
  Madden-Julian Oscillation (MJO)

- seasonal to interannual climate variability
  El Nino/Southern Oscillation (ENSO)
  monsoon variability
  modes of variability (NAO, PNA, WP patterns)

- decadal to interdecadal climate variability

- ocean thermohaline circulation

- glacial and interglacial

N.B. climate system is not in equilibrium

2.2 Intraseasonal Variability

Blocking and Rossby wave,
MJO and equatorial waves

Blocking

- Example: Heatwave by blocking in 2010
- Eastern Europe: late June to late July
- Western Russia: late July to mid August
  - 38.2°C at Moscow on July 30 (15°C higher than climatology)
  - Heavy rainfall and floods over Pakistan
- Hot summer also over Japan

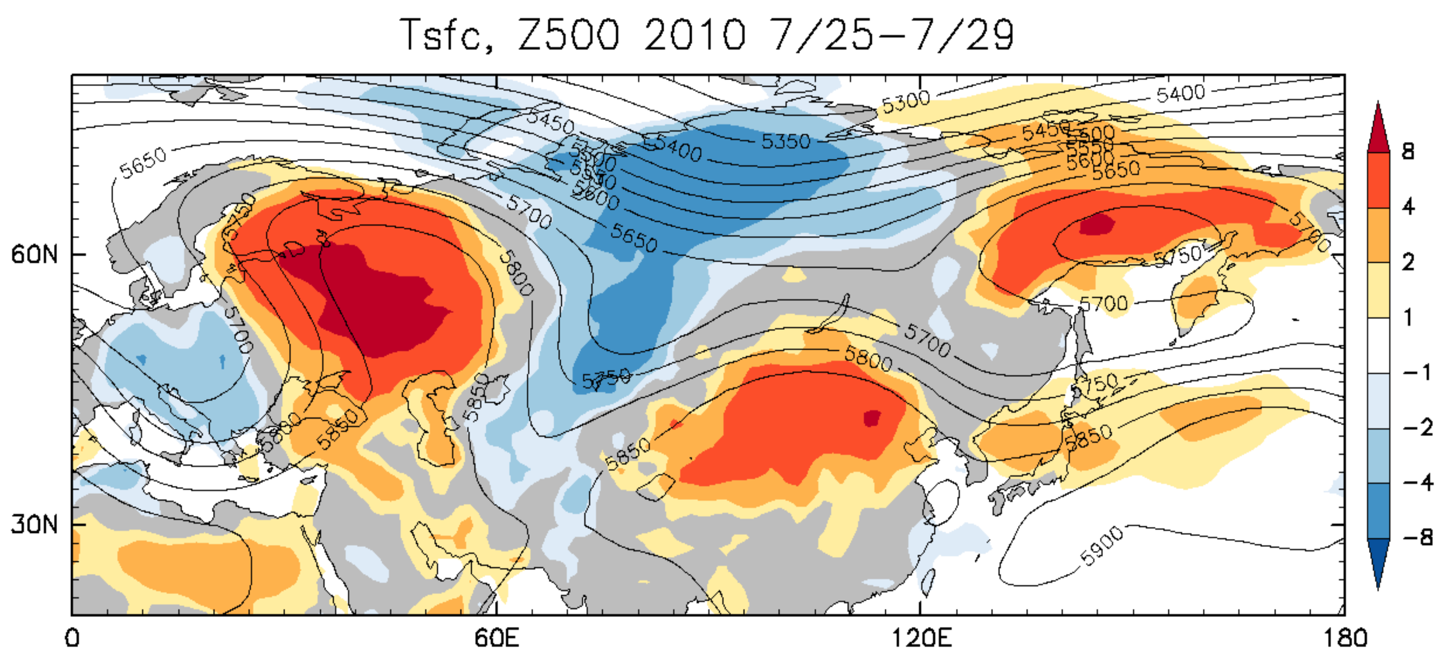

Blocking Climatology

- Blocking events occur over Atlantic to Europe, and Russia to US
- Sometimes it continues over 30 days

Location

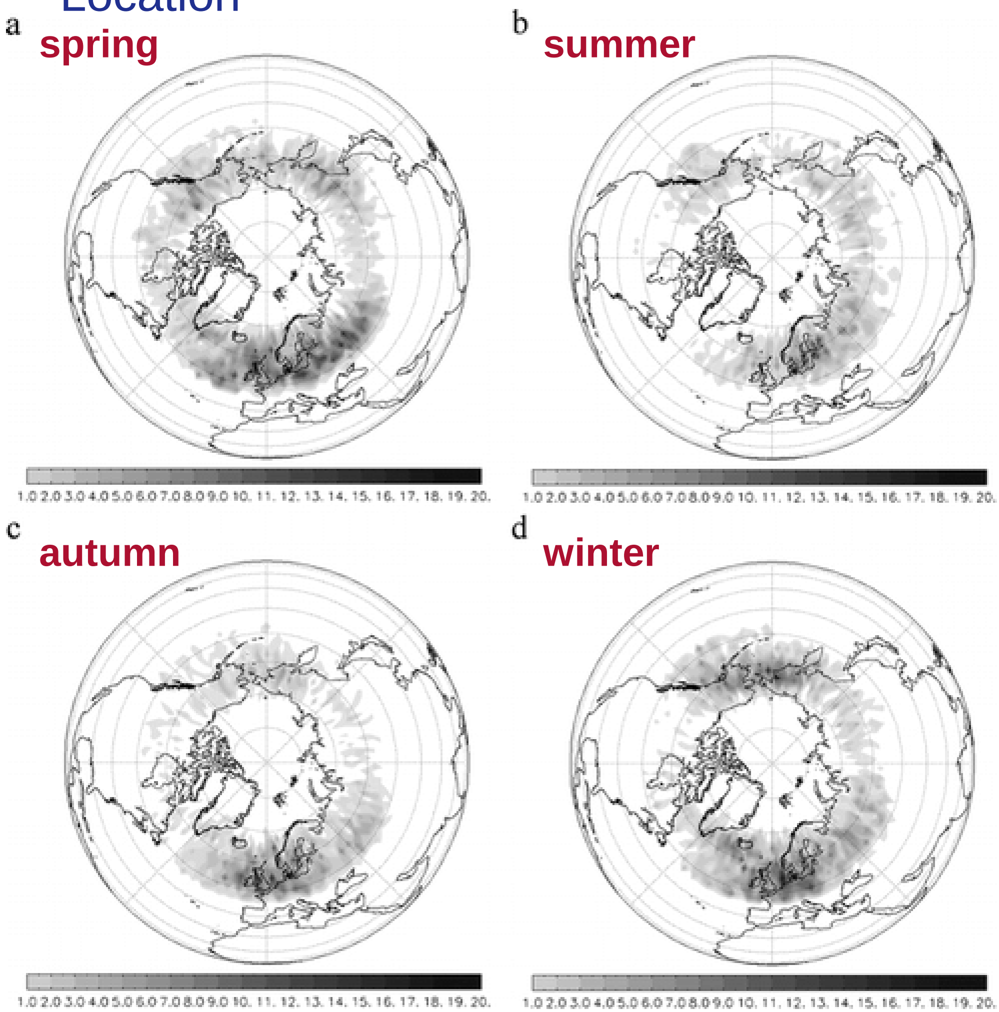

Duration

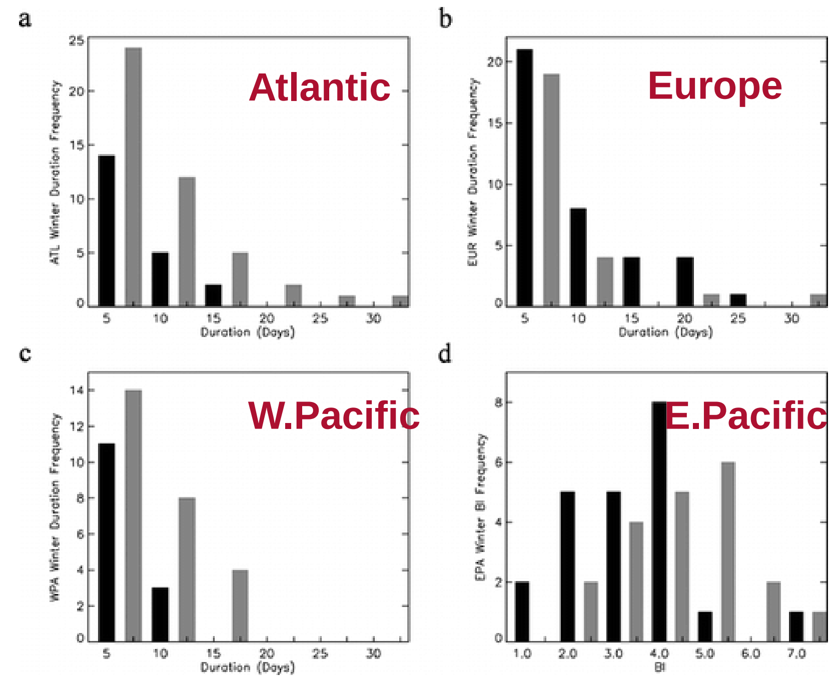

(Barriopedro et al. 2006)

Quasi-stationary Rossby waves

Rossby waves:

are large scale (synoptic and planetary scale) waves in the atmosphere and ocean.

obey the conservation law of potential vorticity.

are dispersive and propagate westward (longer wave is faster).

are stationary if phase speed is the same as westerly wind which advect the waves.

Group velocity of stationary Rossby wave packet is eastward.

Stationary Rossby wave packet tends to propagate trapped by Jet streams.

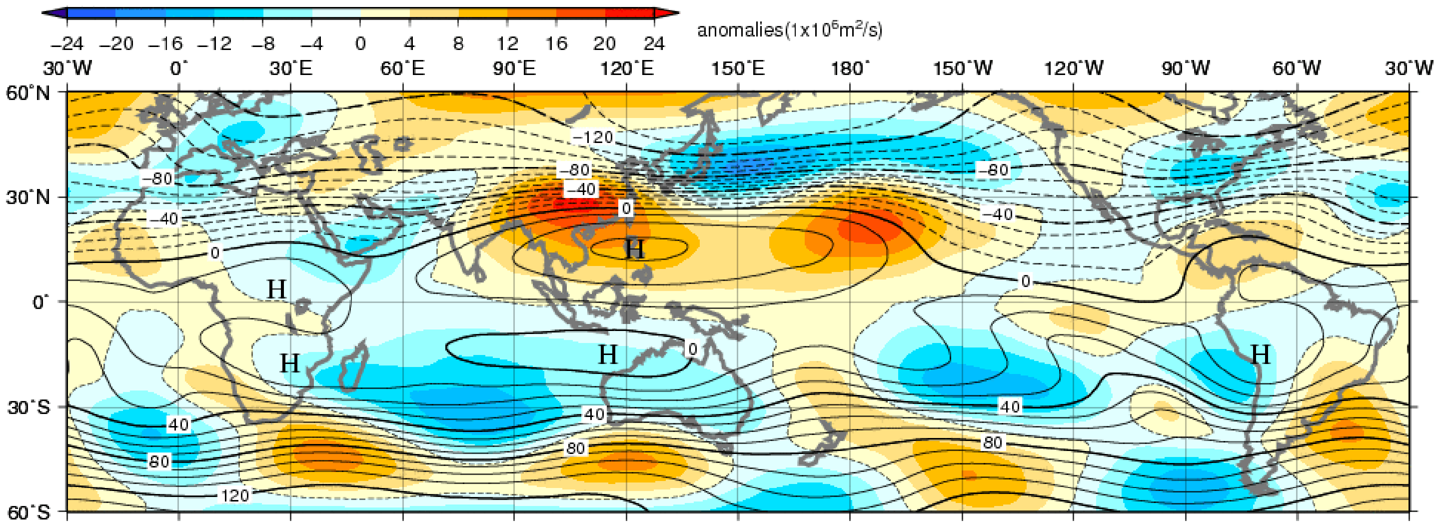

Monthly mean 200 hPa stream function and anomaly (Dec.2005)

The contours show the stream function at intervals of 10×10^6 m^2/s, and the shading shows stream function anomalies.

Anomalies are deviations from the 1981–2010 average.

■ Blocking over the North Atlantic and Rossby wave trains along the Asian jet

5-day mean stream function anomalies at 200hPa 2005.1.18-

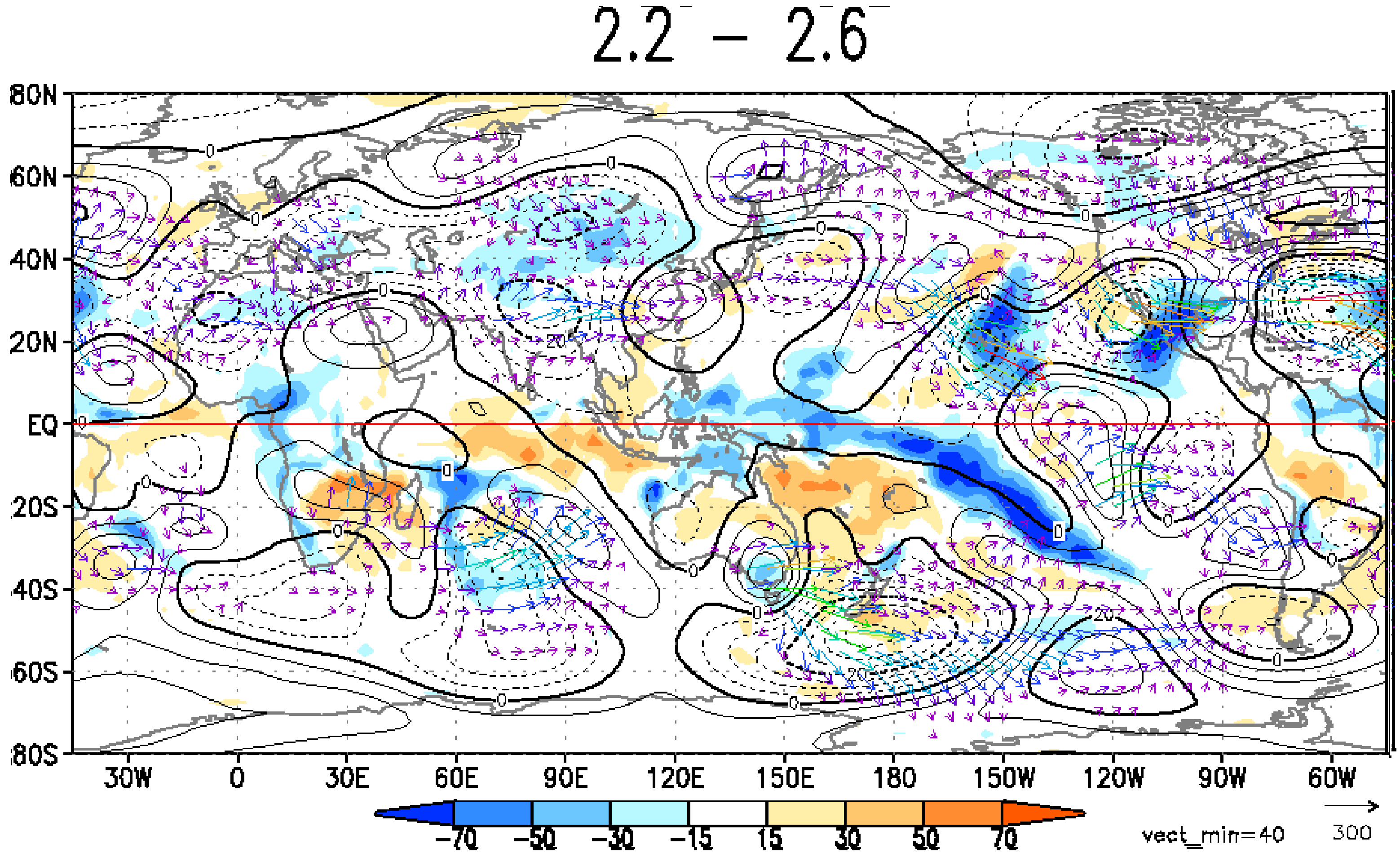

Time cross section of stream function anomalies at 200hPa
x-axis : distance along the red line from a base point (60W,60N)

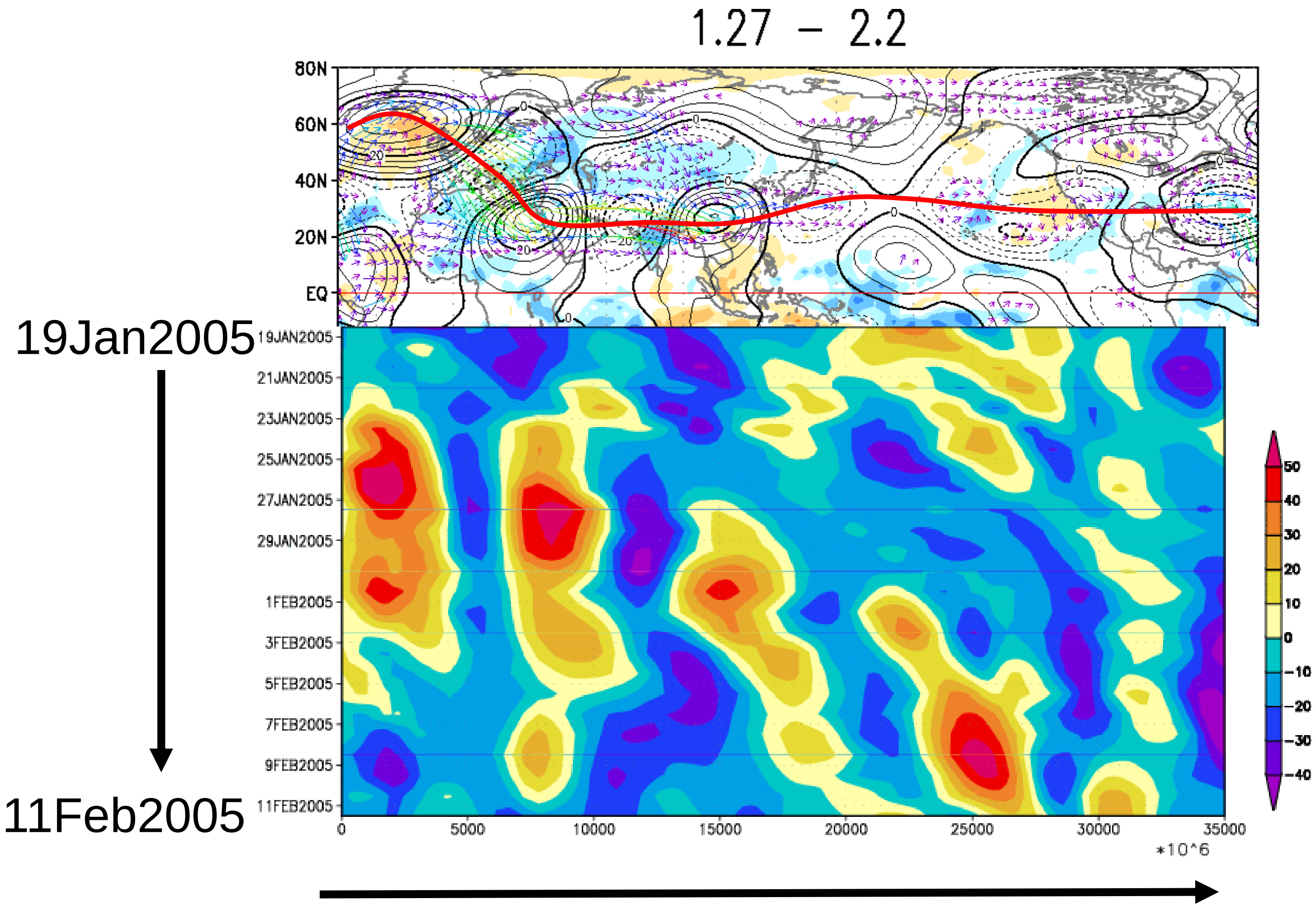

Examples of Quasi-stationary Rossby waves: 2002/1, 2005/2

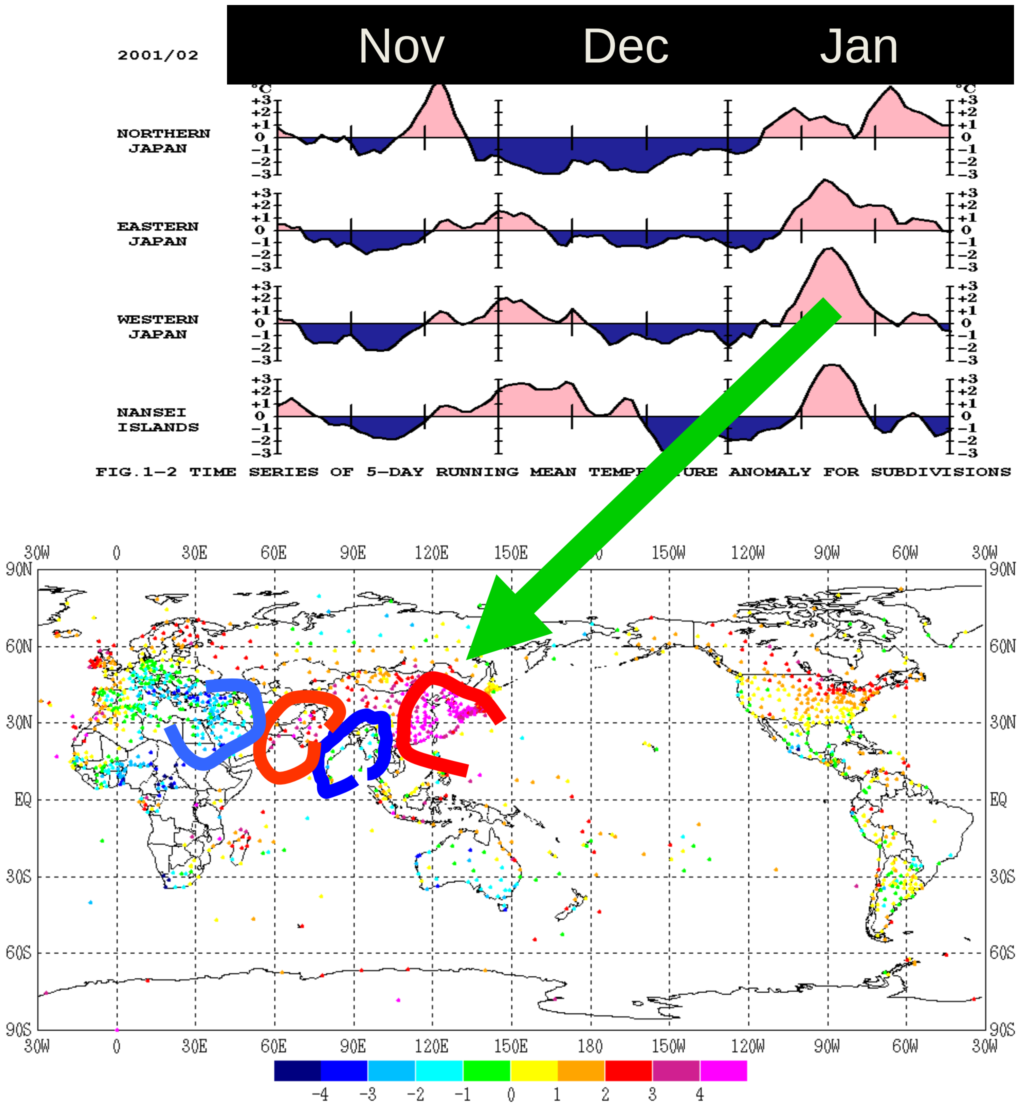

Time sequences of temperature anomalies in Japan (5 day running mean)

2001.11-2002.2

Observed normalized temperature anomalies

2002.1.11-15

Wave train along the Asian jet

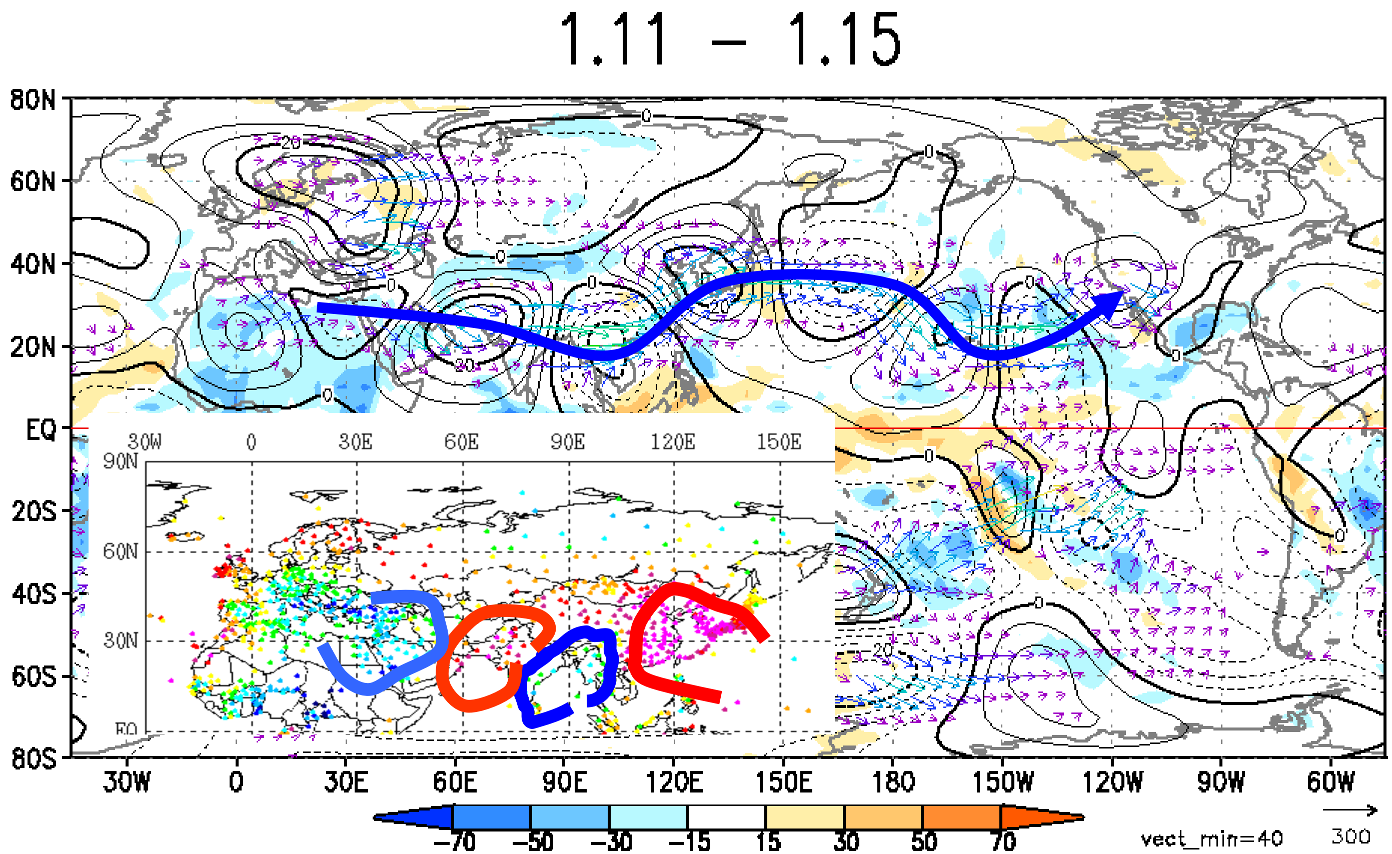

Observed 5-day mean stream function anomalies at 200hPa (contours) 2002.1.11-1.15

Structure of the wave train

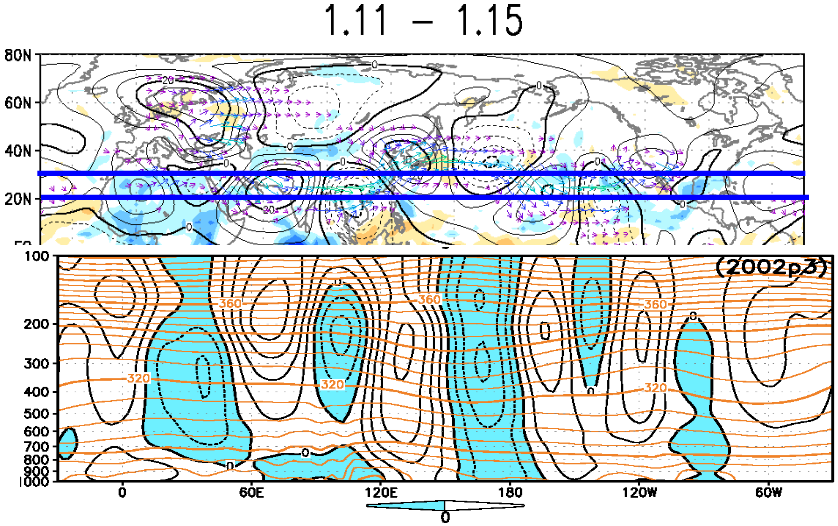

Observed Longitude-height cross section of 20N-30N mean stream function anomalies

2002.1.11-1.15

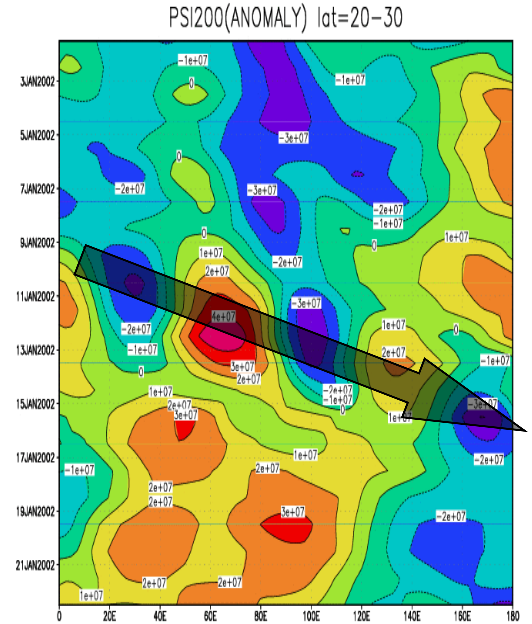

1 JAN

23 JAN

0E

180E

Observed Longitude-time cross section of 20N-30N mean stream function anomalies at 200hPa 2002.1.1-1.23

Equivalent barotropic stationary Rossby wave. Wave length: 70° Group velocity 30° /day

Statistical relationship between 10-day mean temperature in western Japan and wave trains along the Asian jet

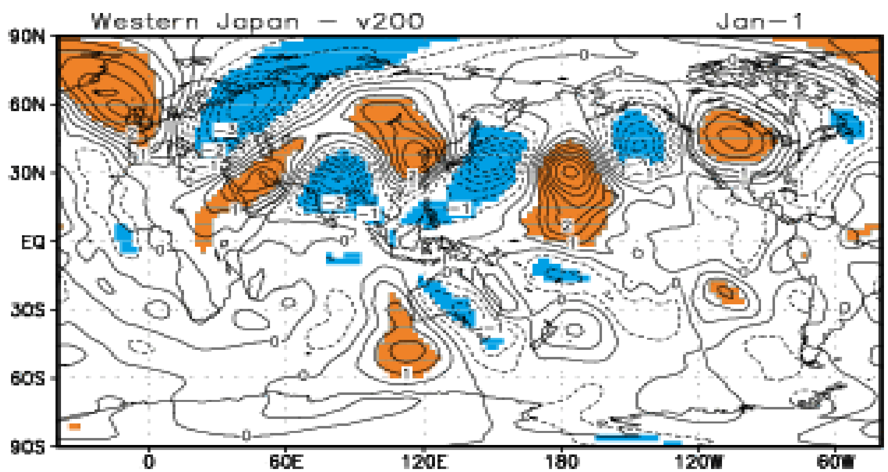

Regression of meridional wind v at 200hPa on 10-day mean temperature in western Japan . 1 Jan.-10 Jan.

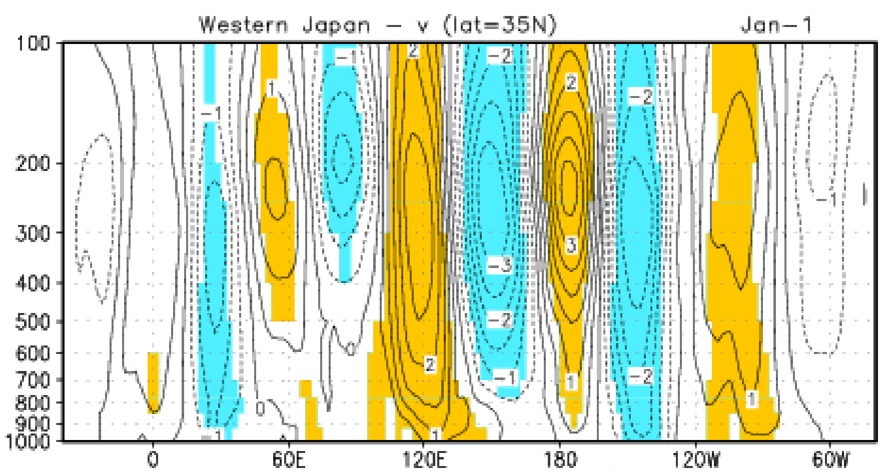

Longitude-height cross section of regression of meridional wind v at 35N

Climatology of stationary Rossby wave packets propagation (1-10 JAN,1971-2000)

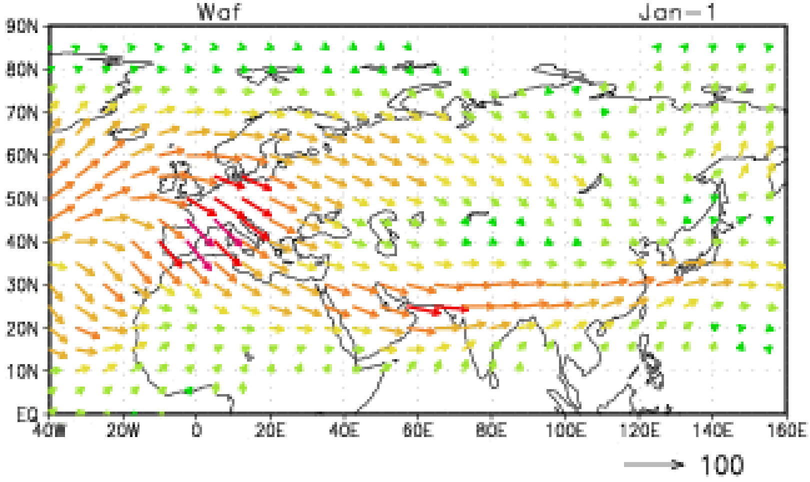

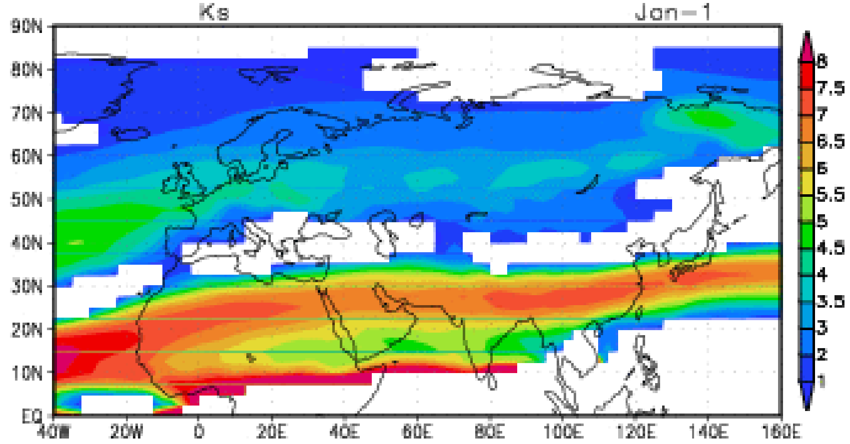

Wave activity flux (Takaya and Nakamura,2001,JAS,608-) at 200hPa

Stationary Rossby wave number Ks (Hoskins and Ambrizzi,1993,JAS,1661-) at 200hPa

Source of Rossby wave train along the Asian jet ?

Decay of Blocking due to Rossby wave radiation

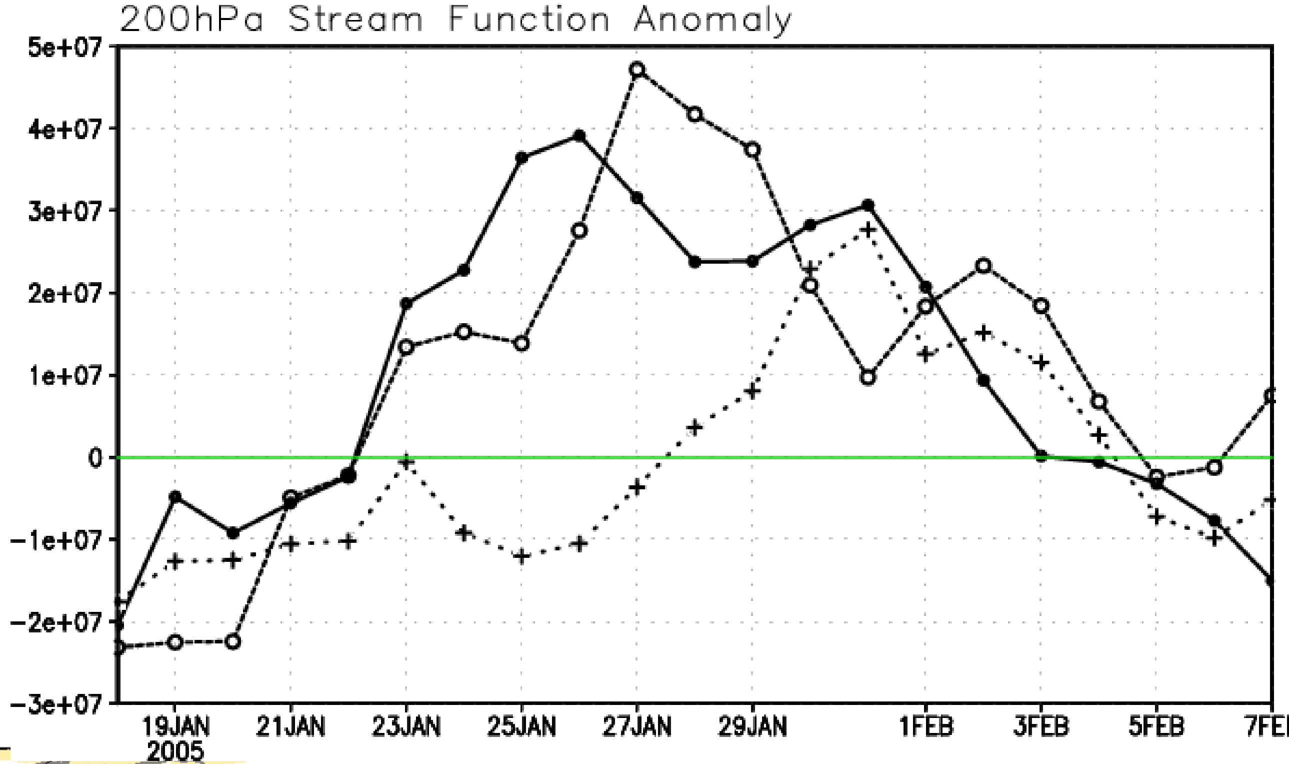

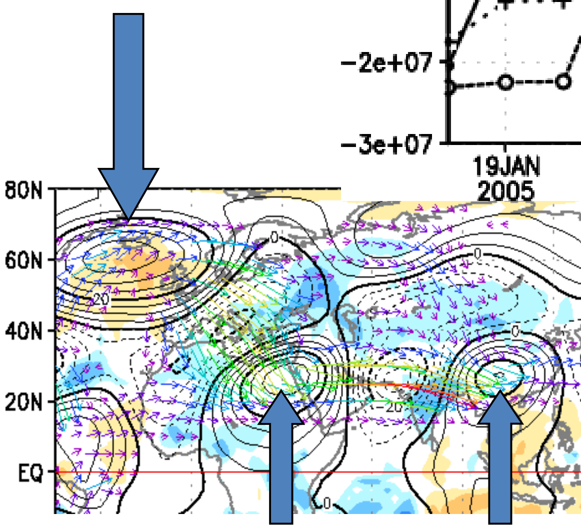

Prediction of development of Blocking

Initial : 20^{th} JAN 2005

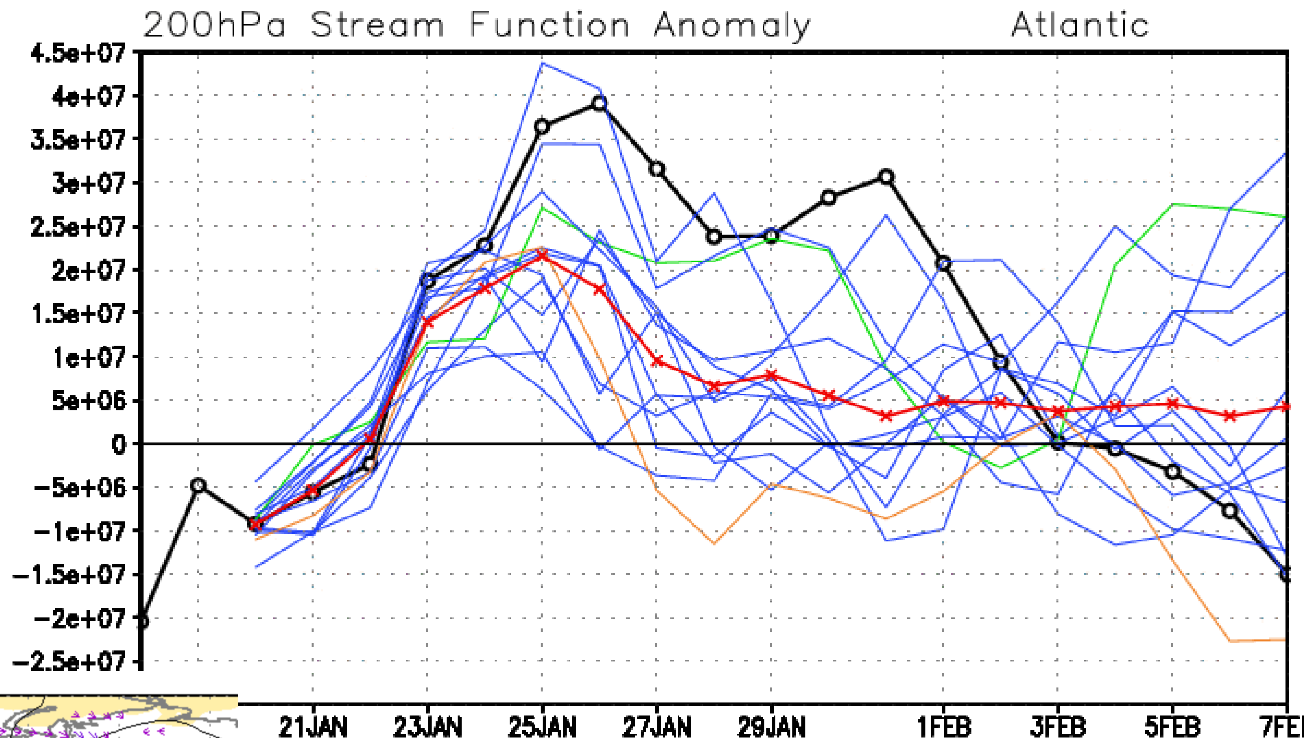

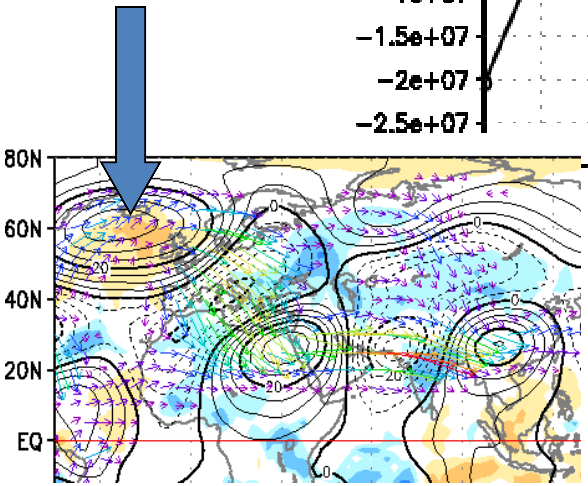

Prediction of decay of Blocking

Initial : 26th JAN 2005

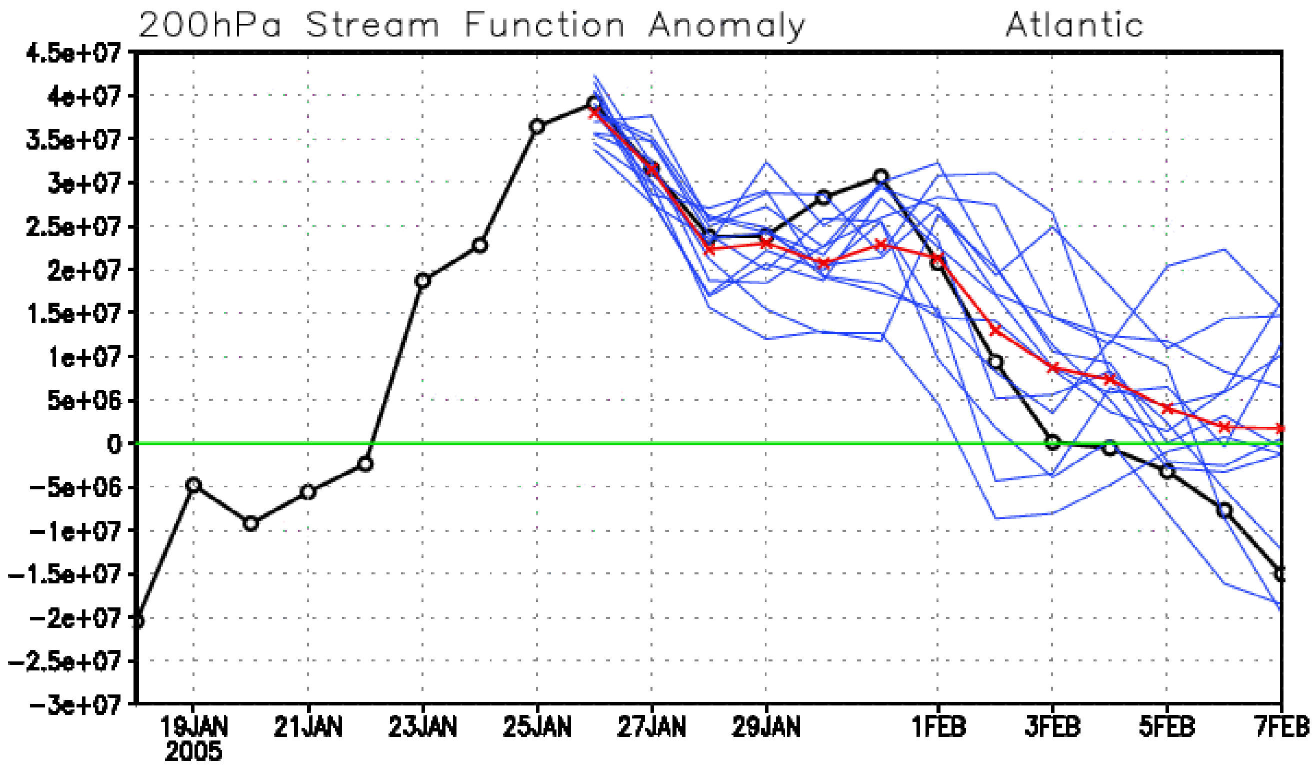

Prediction of decay of Blocking due to Rossby wave radiation

Initial : 26th JAN 2005

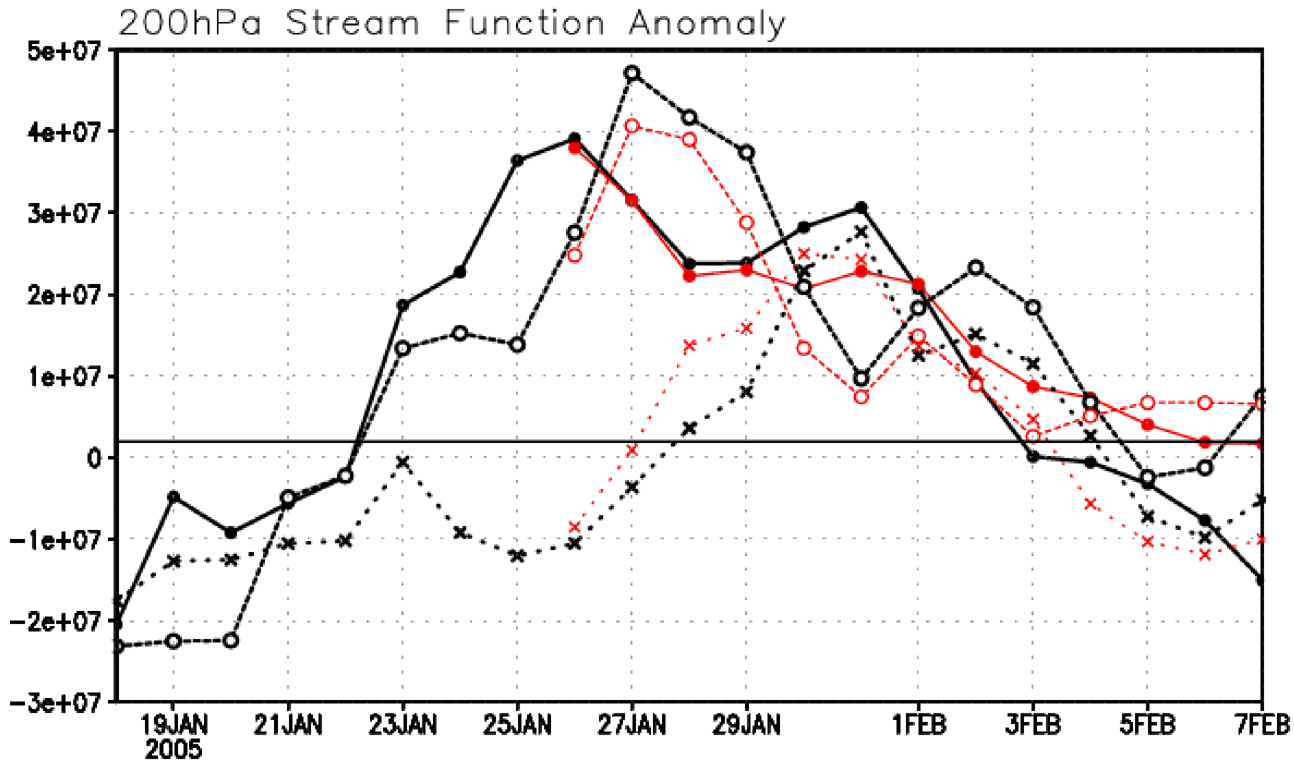

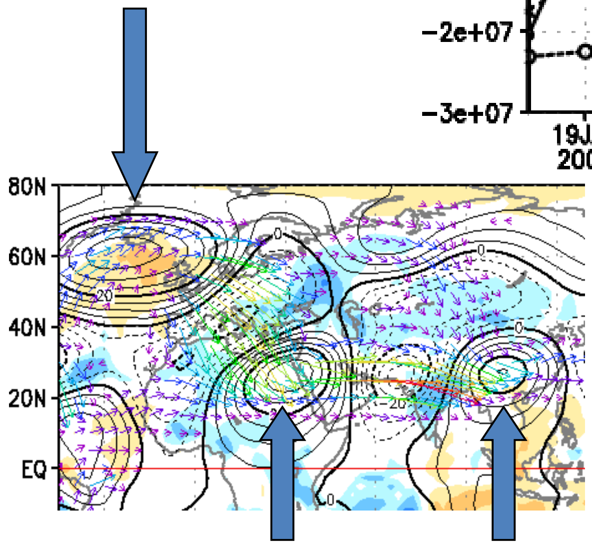

Multi-scale clouds in the tropics

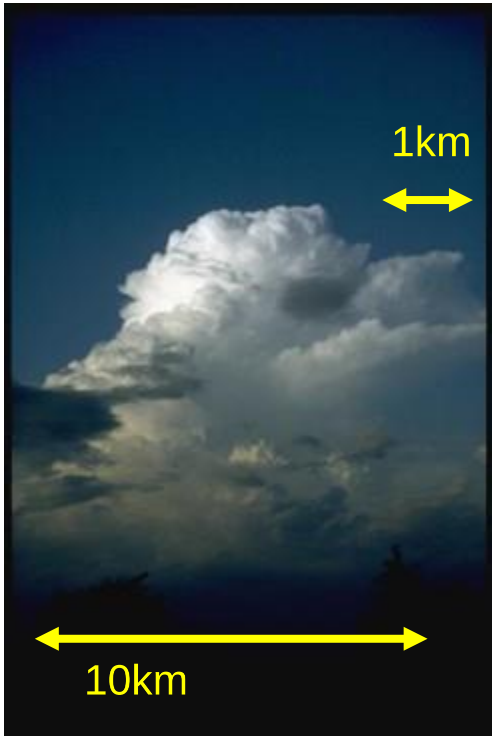

Outgoing Longwave Radiation (OLR) from
MTSAT JMA at 00 UTC Oct. 5, 2005

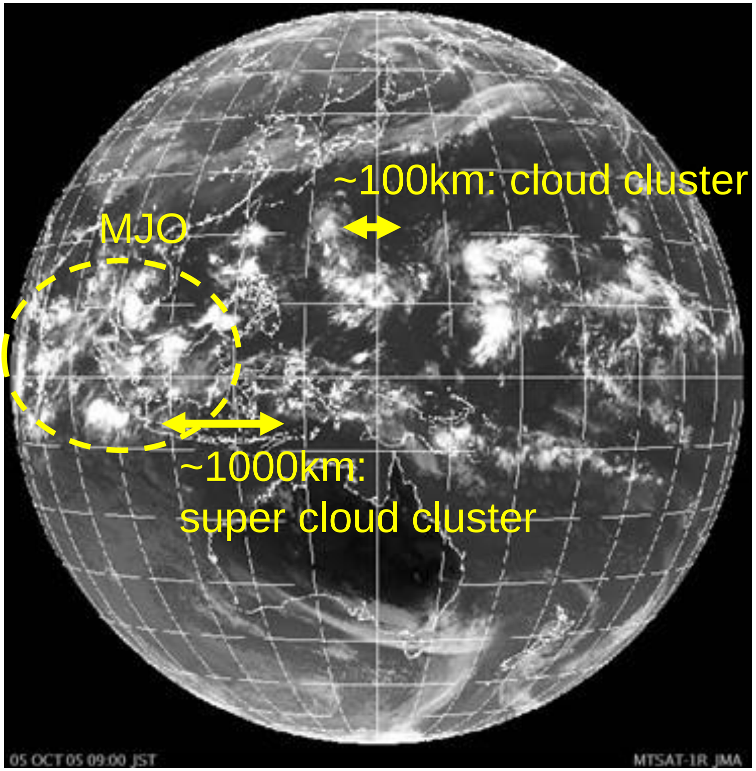

In the tropics, Heavy precipitation -> Deep cloud -> Low cloud-top temperature -> Low OLR

Madden-Julian Oscillation (MJO)

A broad area of active cloud and rainfall propagates eastwards around the equator at intervals of between about 30 to 60 days.

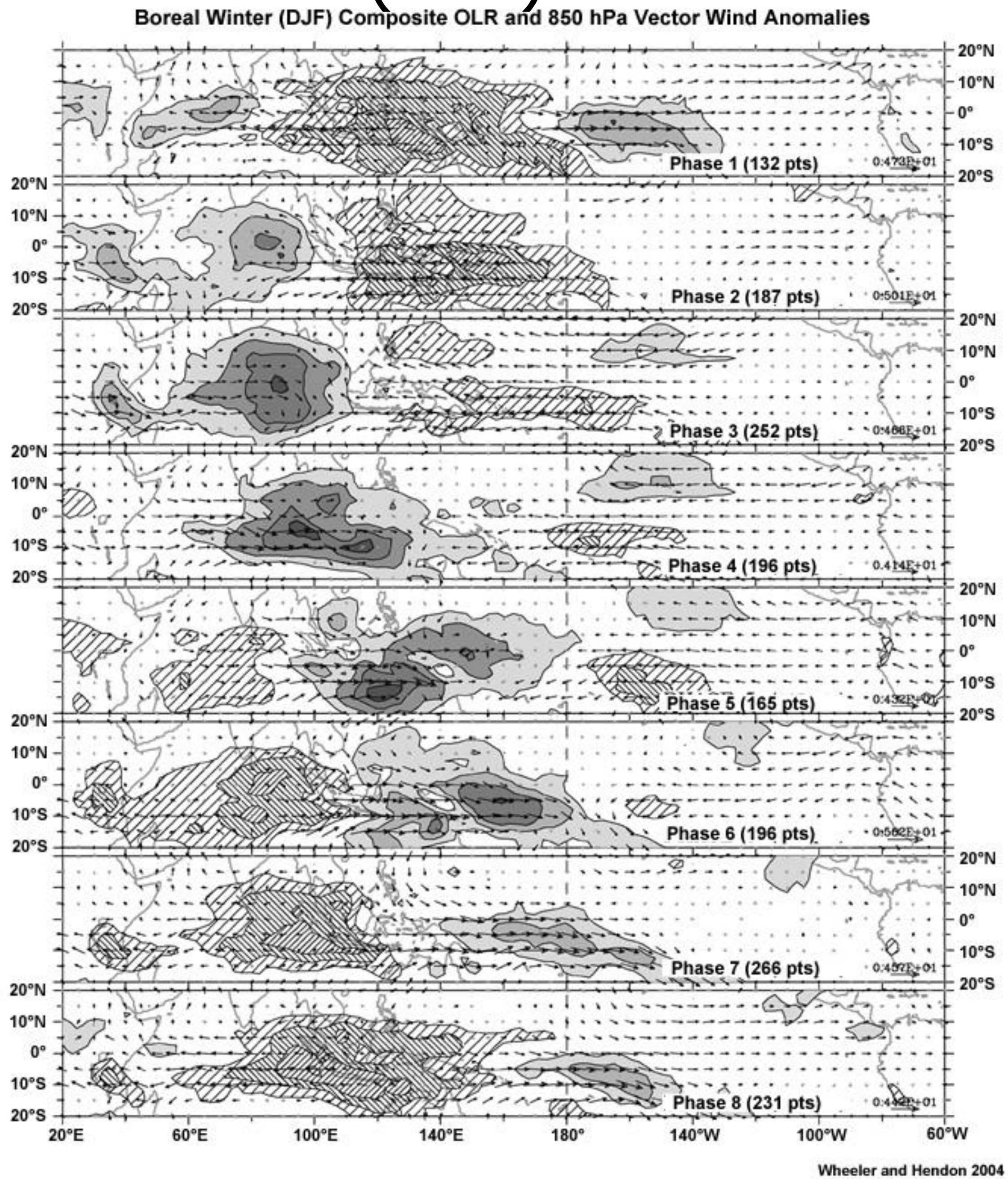

30 - 60 day Period

Madden-Julian Oscillation (MJO)

Surface pressure at Canton Iceland (3S, 172W)

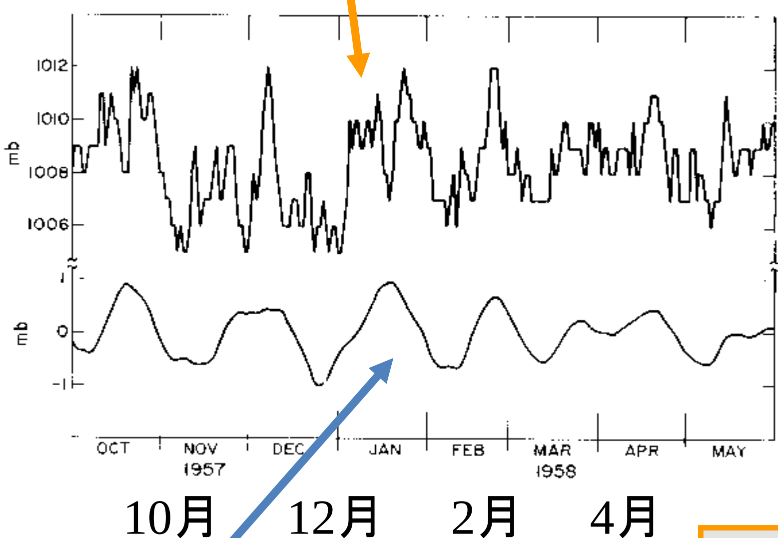

After applying band-pass filter around 45 days

Eastward super cloud cluster detectable by OLR

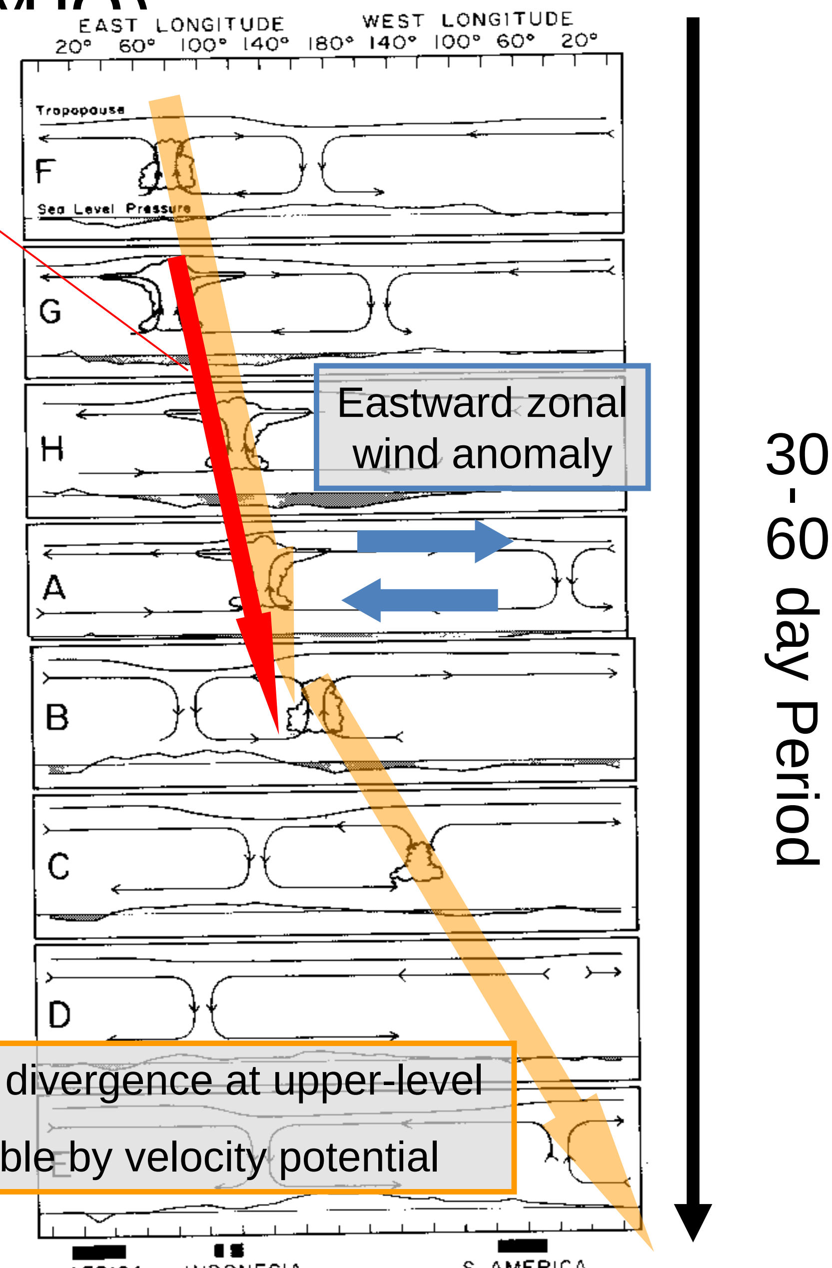

Eastward divergence at upper-level detectable by velocity potential

Madden and Julian (1972)

Schematic structure of MJO

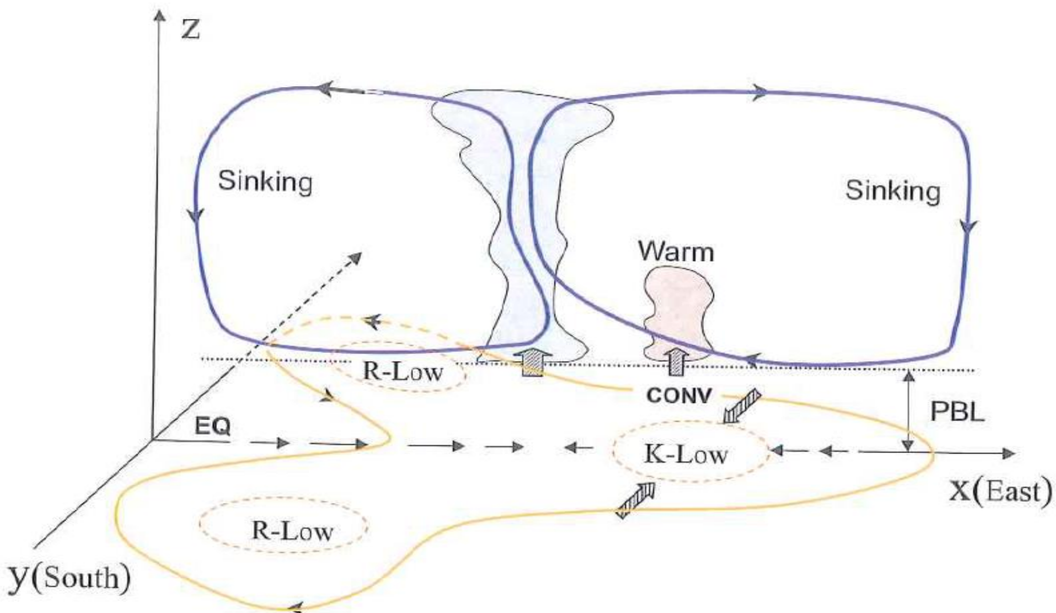

Figure 10.13. Schematic structure of the frictional CID mode, which is the counterpart of observed MJO mode. In the horizontal plane the "K-low" and "R-low" represents the low-pressure anomalies associated with the moist equatorial Kelvin and Rossby waves, respectively. Arrows indicate the wind directions. In the equatorial vertical plane the free-tropospheric wave circulation is highlighted. The wave-induced convergence is in phase with the major convection, whereas the frictional moisture convergence in the "K-low" region is ahead of the major convection due primarily to meridional wind convergence.

From Wang (2005)

Composition maps of stream function at 200hPa and OLR at each phase (1-12) of MJO in winter (DJF)

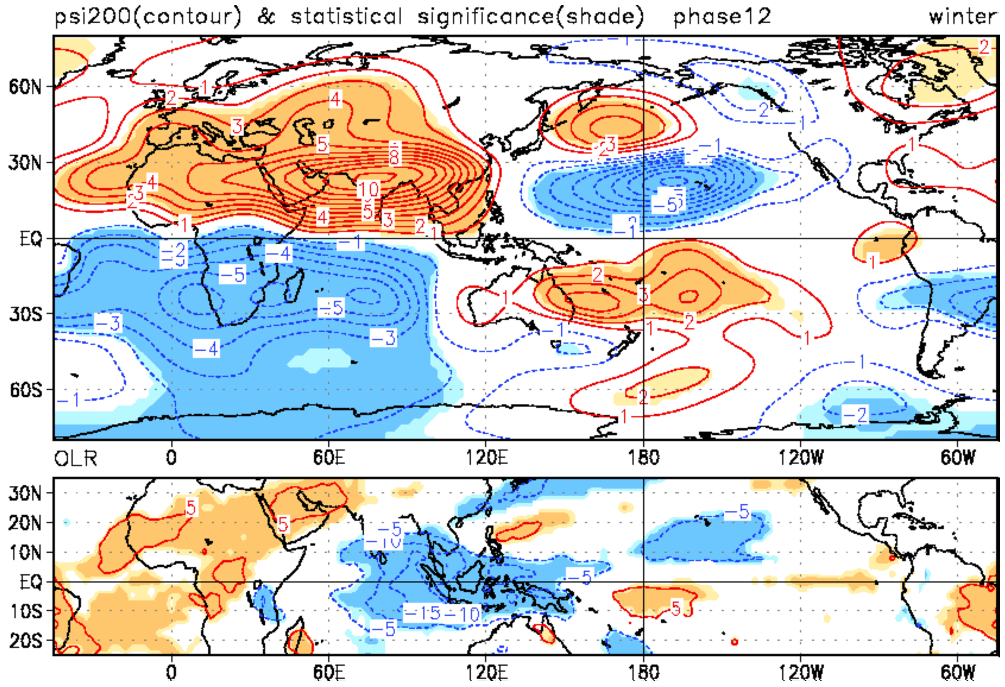

Stream function at 200hPa

OLR

Endoh and Harada (2005)

Equatorial Waves

Kelvin wave

ER: Rossby wave (n=1)

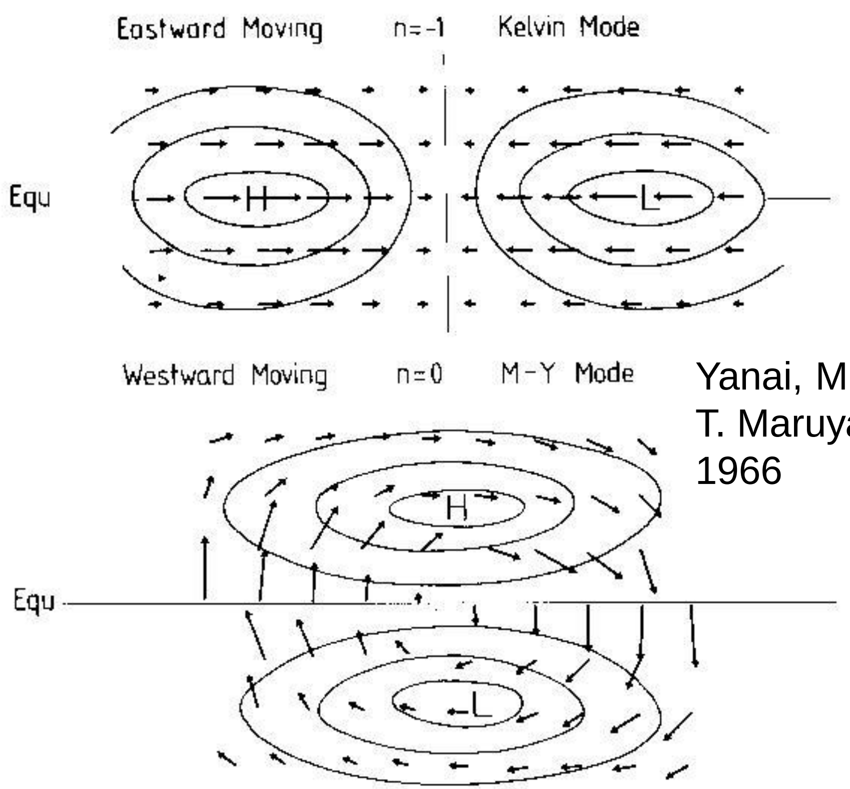

Yanai, M. and T. Maruyama, 1966

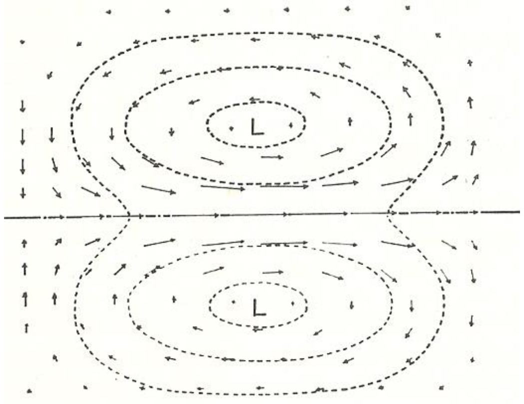

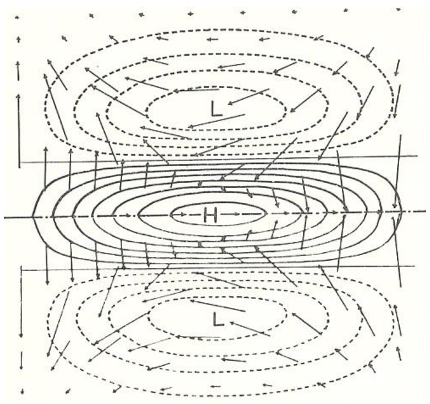

MRG : mixed Rossy-Gravity wave

EIG: eastward propagating inertio-gravity wave (n=1)

Matsuno, T., 1966: Quasi-geostrophic motions in the equatorial area. *J. Meteor. Soc. Japan,* **44,** 25–43.

Convectively coupled equatorial waves

Wave number–frequency power spectrum of the (a) symmetric and (b) antisymmetric component of Cloud Archive User Services (CLAUS) T_b

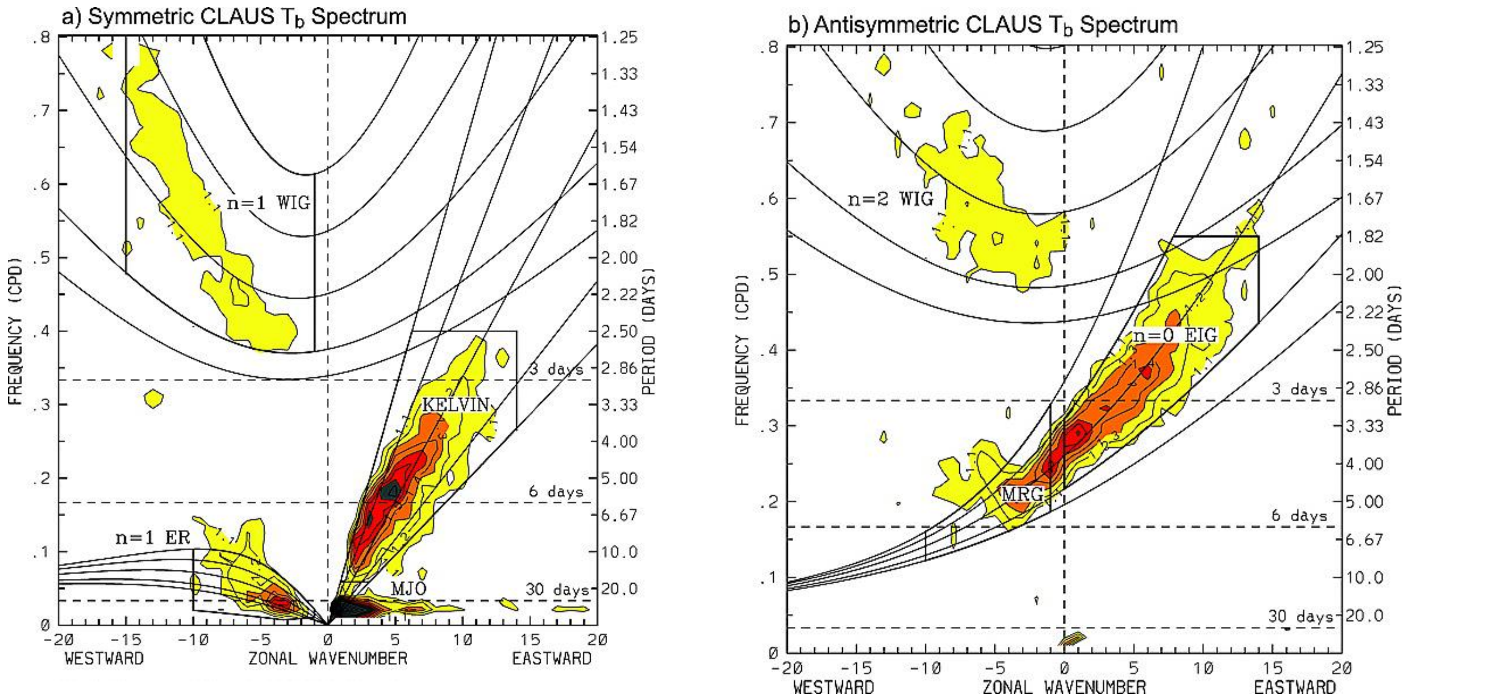

Wave number–frequency power spectrum of the (a) symmetric and (b) antisymmetric component of Cloud Archive User Services (CLAUS) T_b for July 1983 to June 2005, summed from 15° N to 15° S, plotted as the ratio between raw T_b power and the power in a smoothed red noise background spectrum (see WK99 for details). Contour interval is 0.1, and contours and shading begin at 1.1, where the signal is significant at greater than the 95% level. Dispersion curves for the Kelvin, $n = 1$ equatorial Rossby (ER), $n = 1$ and $n = 2$ westward inertio-gravity (WIG), $n = 0$ eastward inertio-gravity (EIG), and mixed Rossby-gravity (MRG) waves are plotted for equivalent depths of 8, 12, 25, 50, and 90 m. Heavy solid boxes represents regions of wave number–frequency filtering

Kiladis et. al.(2009)

Reviews of Geophysics
Volume 47, Issue 2, RG2003, 10 APR 2009 DOI: 10.1029/2008RG000266
http://onlinelibrary.wiley.com/doi/10.1029/2008RG000266/full#rog1687-fig-0001

Decomposition of the equatorial OLR anomalies

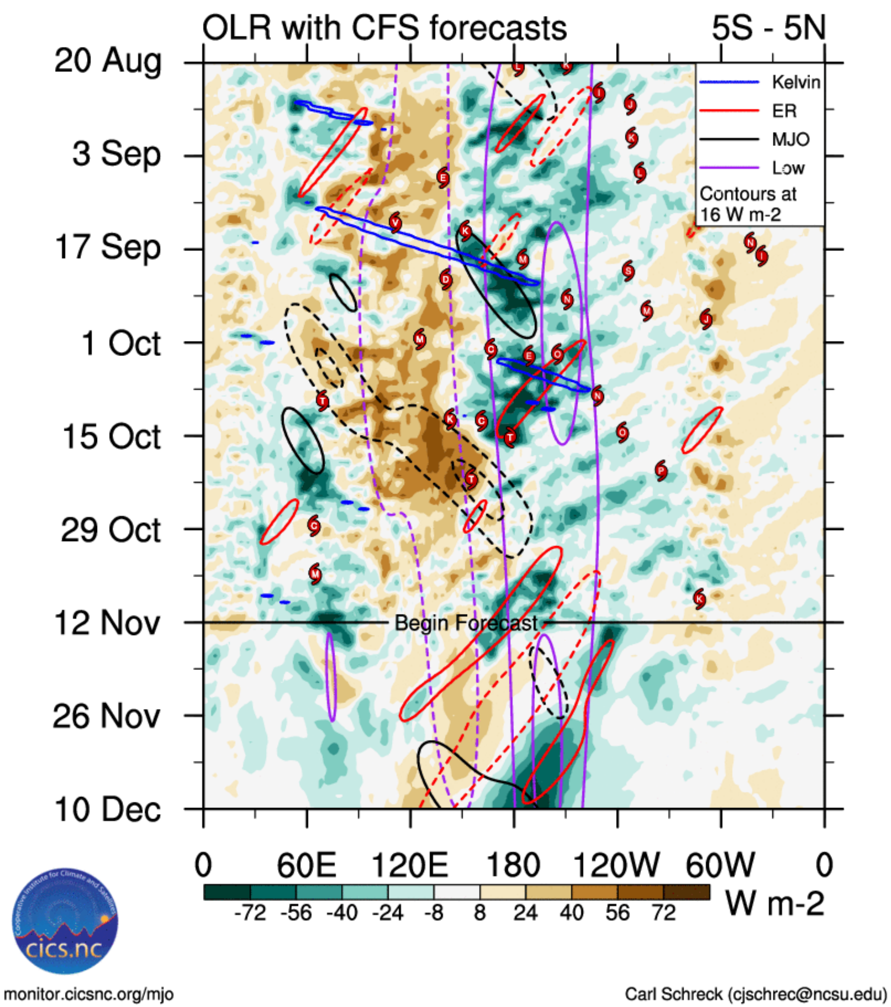

https://monitor.cicsnc.org/mjo/v2/images/spectra.png

Equatorial Rossby wave

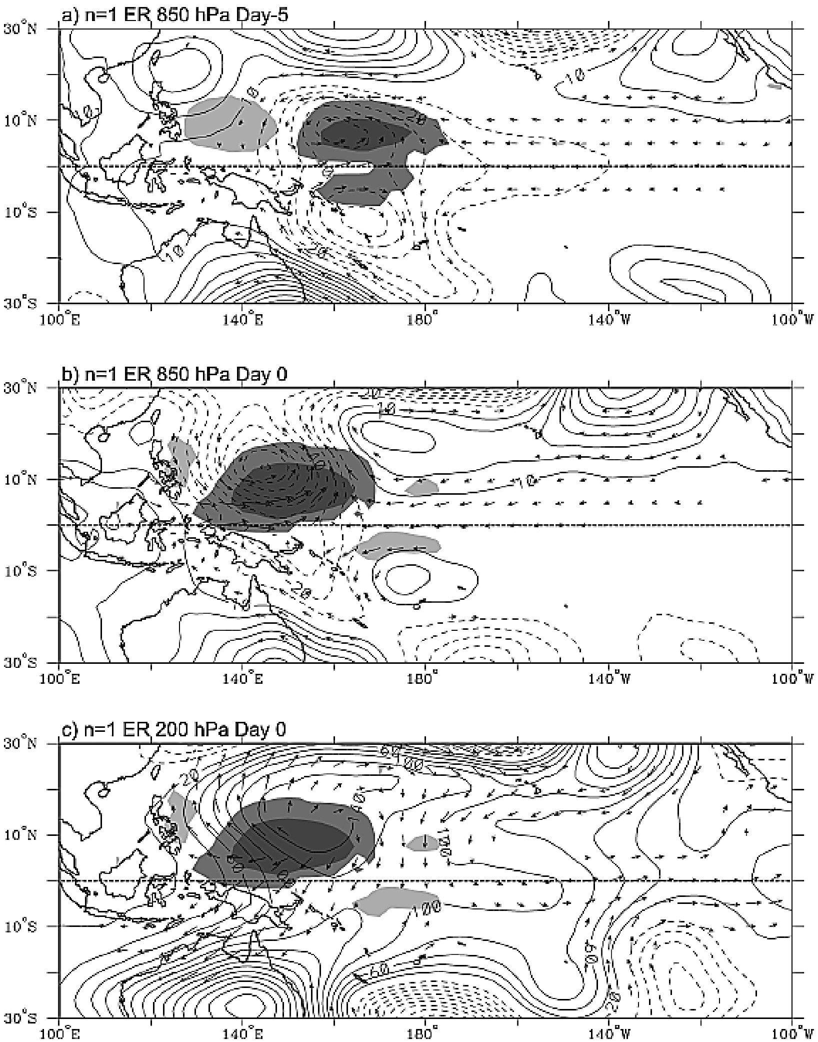

850hPa day= -5

850hPa day= 0

200hPa day= 0

Maps of anomalous T_b (shading), geopotential height (contours), and wind (vectors) associated with a −20 K perturbation in $n = 1$ ER wave T_b at the base point 7.5° N, 152.0° E, for (a) day –5 at 850 hPa, (b) day 0 at 850 hPa, and (c) day 0 at 200 hPa. The contour interval is 10 m in Figures 17a and 17b and 20 m in Figure 17c, with negative contours dashed. Dark (light) shading is for negative (positive) T_b perturbations of ±10 K and 3 K. T_b and wind vectors are locally significant at the 95% level, with the largest vectors around 2 m s^{-1}.

Kiladis et. al.(2009)

Impact of MJO (Example for Japan)

DJF Temperature Anomaly over Japan

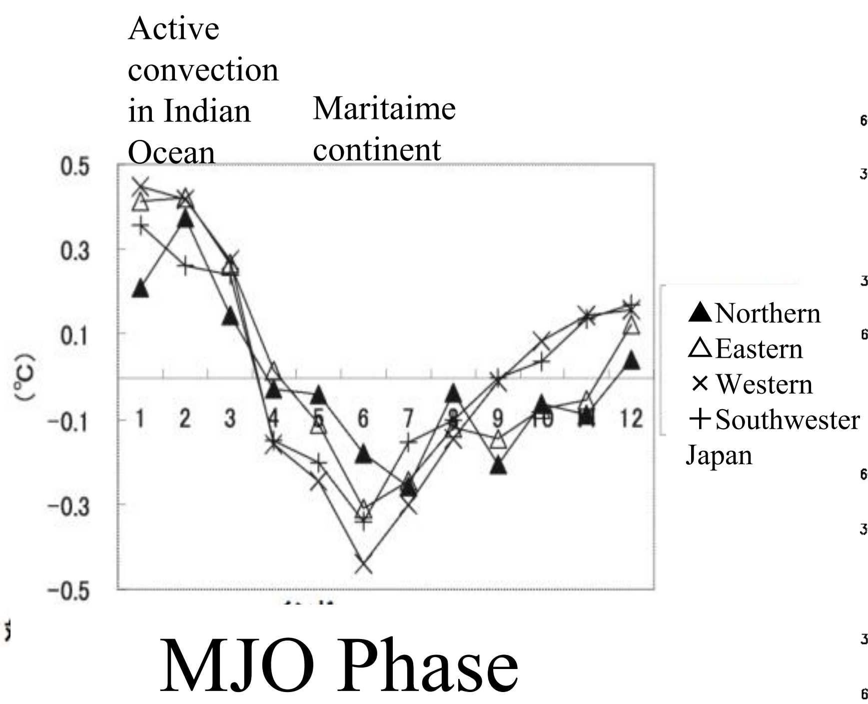

Endo and Harada (2008)

Composition maps of MJO in DJF

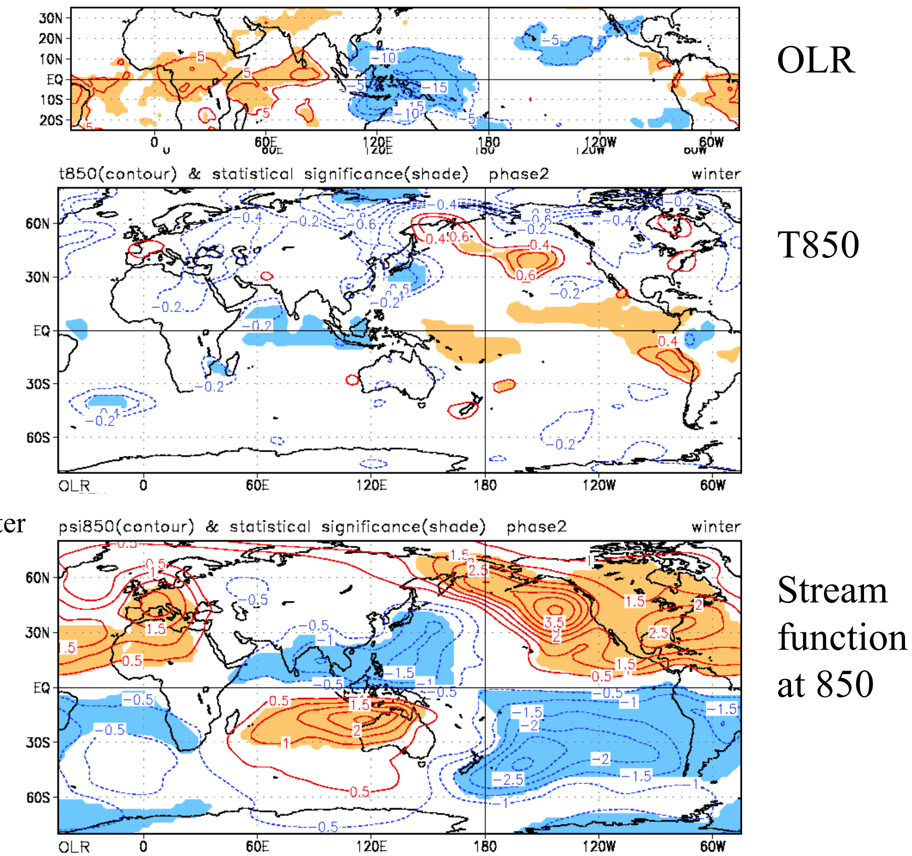

Endoh and Harada (2005)

- MJO predictability is not so much.

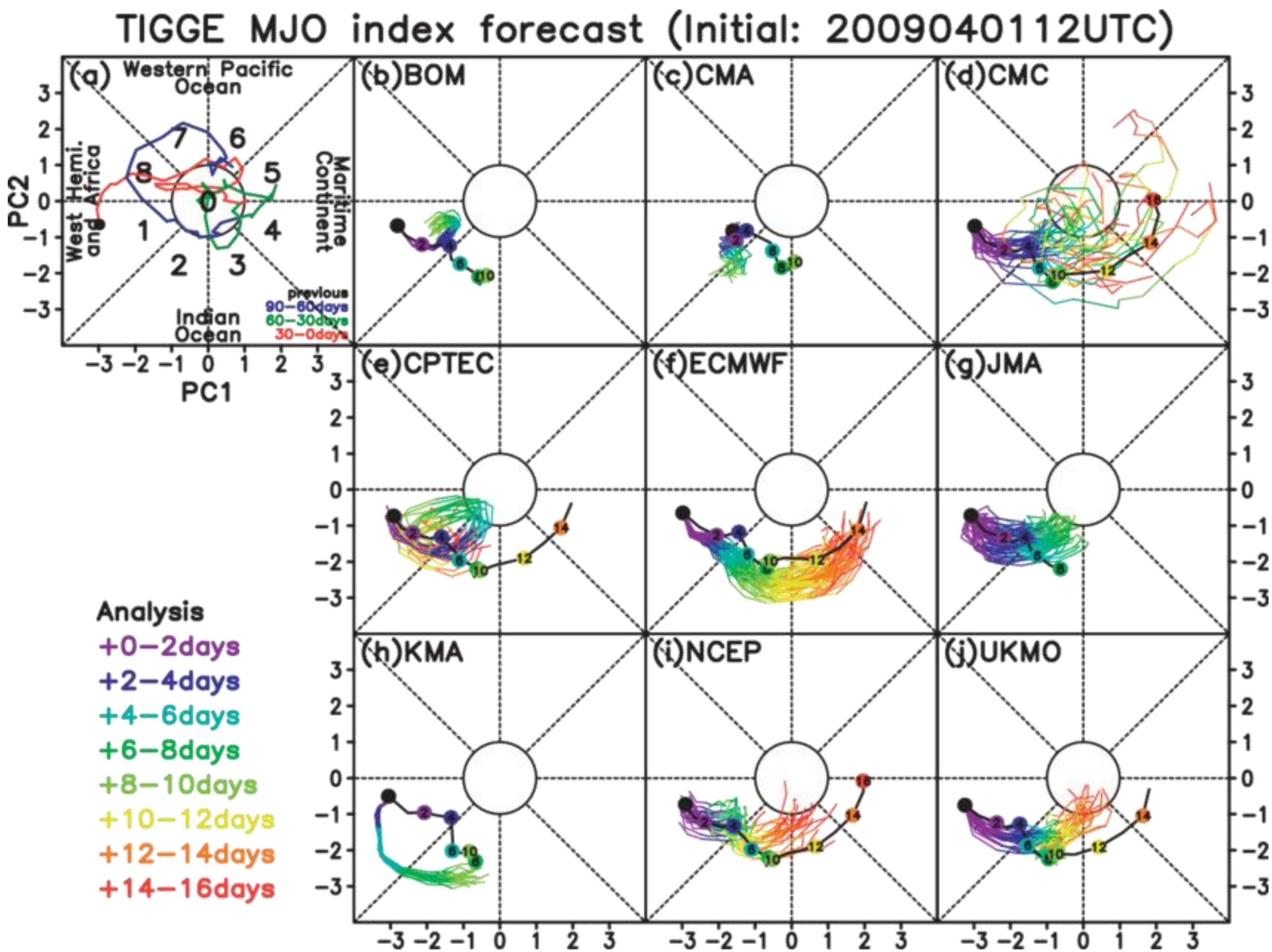

Matsueda and Endo (2011)

- 2.3 Interannual Variability

ENSO, El Niño Modoki, IOD

El Niño and Southern Oscillation (ENSO)

Why is El Niño/La Niña important ?

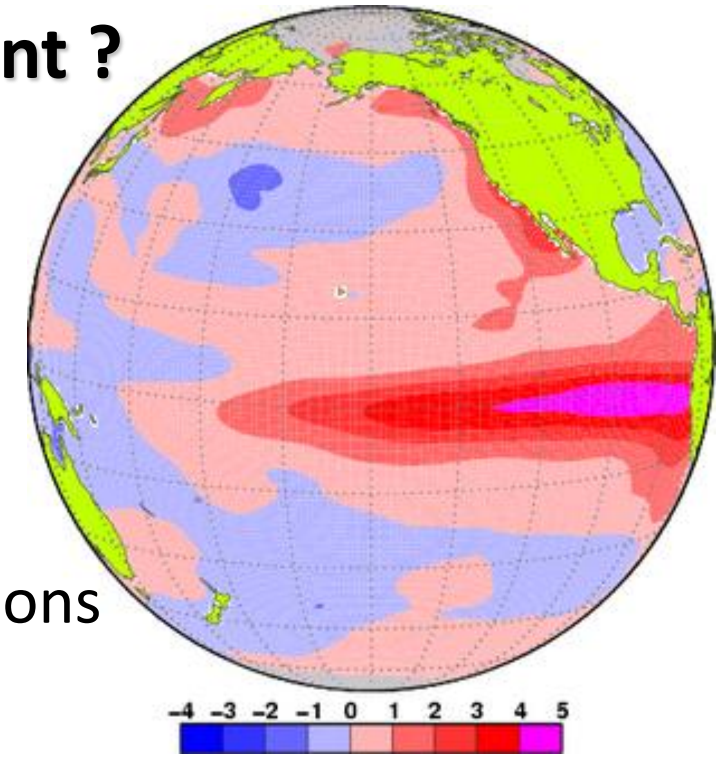

1. Predominant inter-annual climate variability
2. Big Impact on the world climate
3. Predictable with one or two seasons lead time

The prediction of El Niño or La Niña is a base of our long range forecast. First, we check the ENSO conditions and then discuss our long range forecast.

Normal condition in the equatorial Pacific Ocean

Trade wind, a persistent easterly atmospheric flow blowing over the equatorial Pacific Ocean, sustains warmer-western, cooler-eastern sea surface condition.

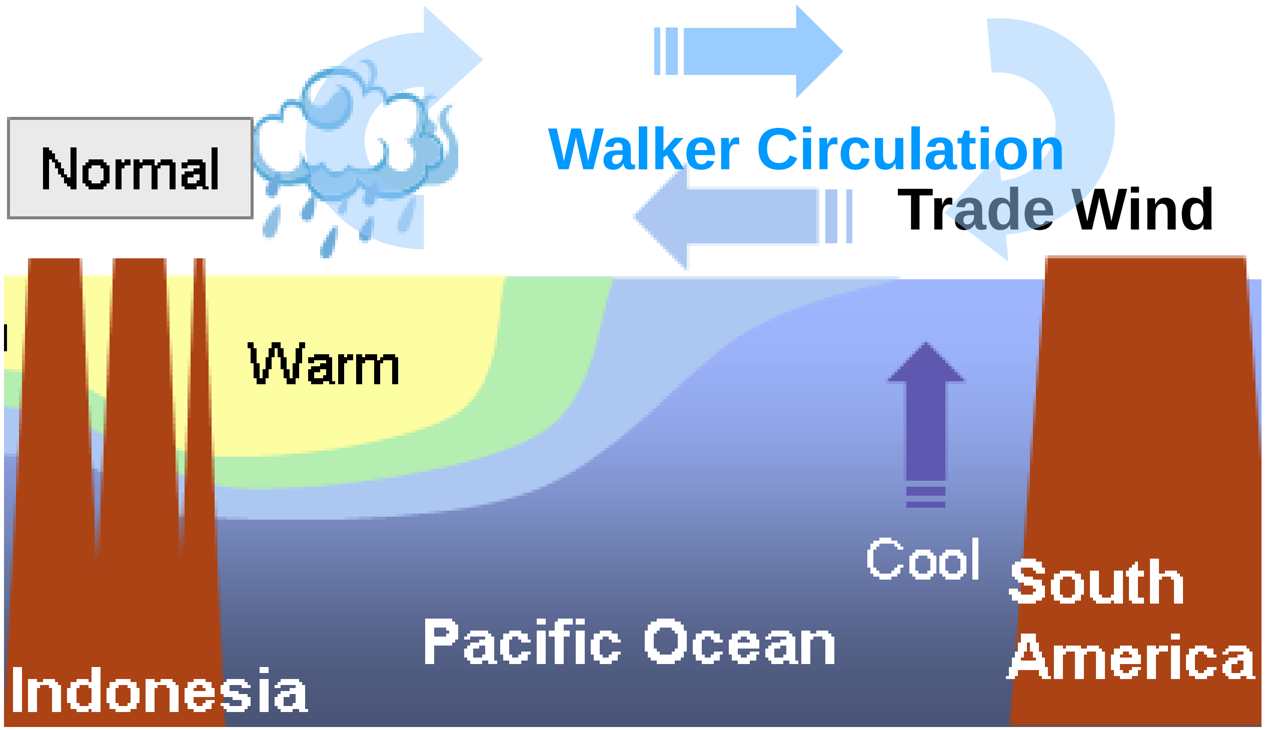

Japan Meteorological Agency

Sea surface temperature (SST)

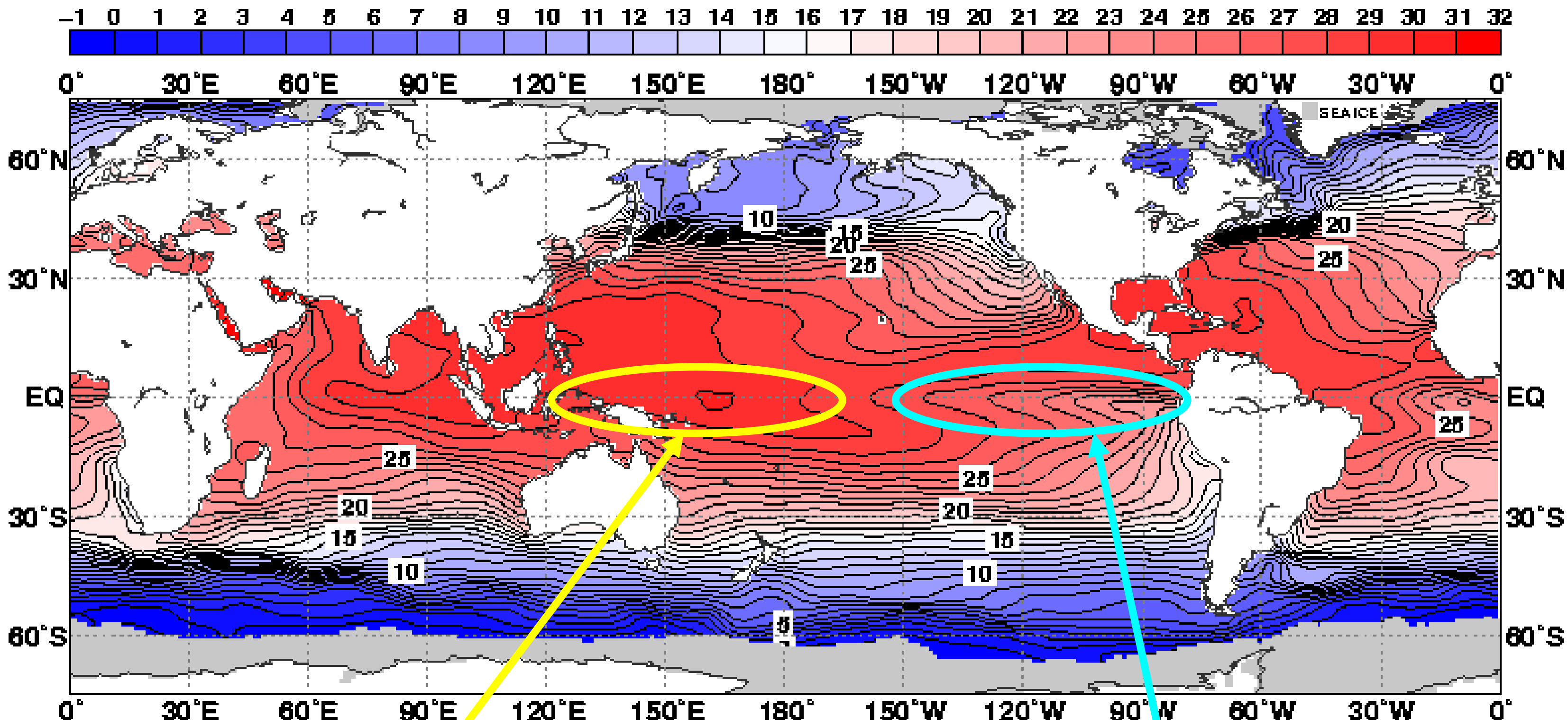

warmer in the west
(typically around 30ºC)

cooler in the east
(typically around 22ºC)

1-month mean sea surface temperature observed in July 2005 when the conditions in the equatorial Pacific Ocean stayed close to normal.

Atmosphere-ocean interaction during El Niñ

気象庁
Japan Meteorological Agency

Normal condition

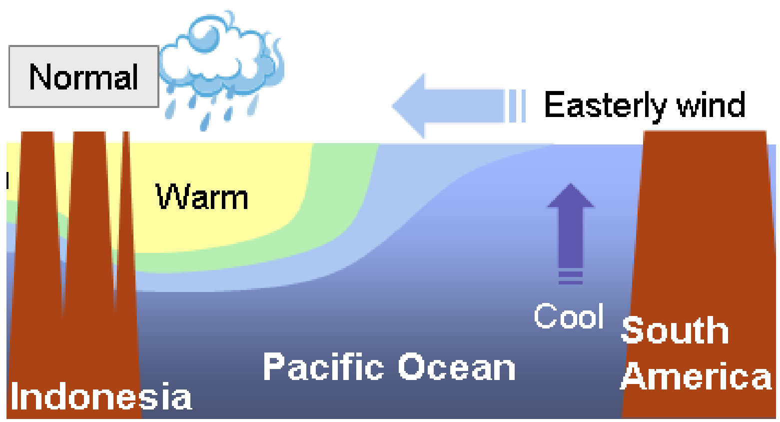

El Niño condition

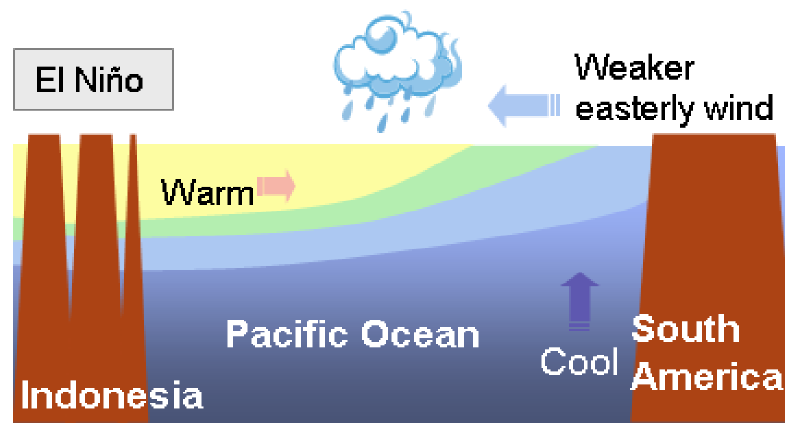

Warmer SST in the eastern Pacific → Eastward shift of active convection

↑ ↓

Eastward shift of warm water ← Weaker easterly trade wind

El Niño + Southern Oscillation = ENSO

Atmosphere-ocean interaction during La Niña

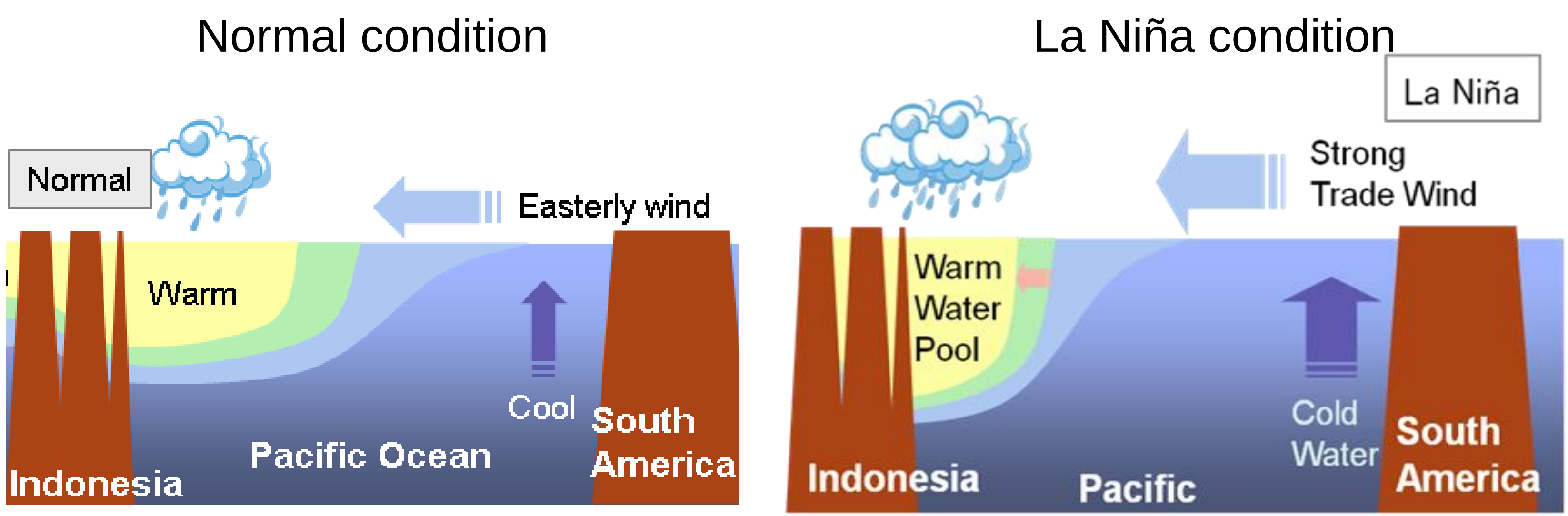

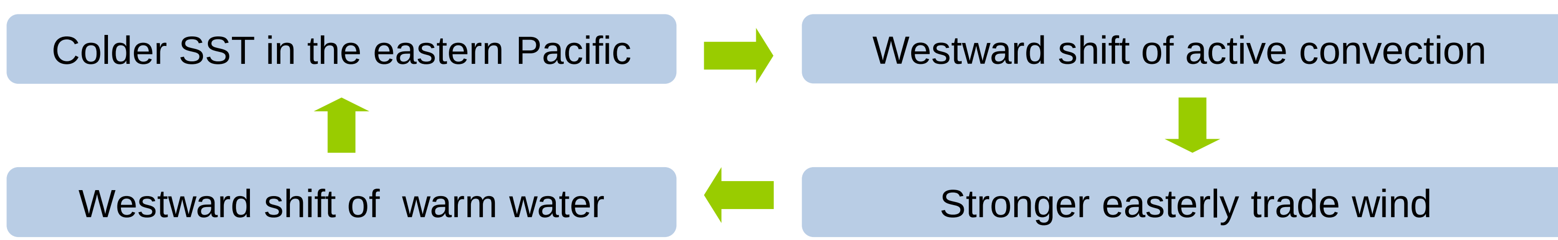

“El Niño”(“La Niña”) refers to:

A large-scale ocean climate phenomenon linked to a periodic rise (fall) in sea surface temperatures across the central to east equatorial Pacific

El Niño (NOV1997)

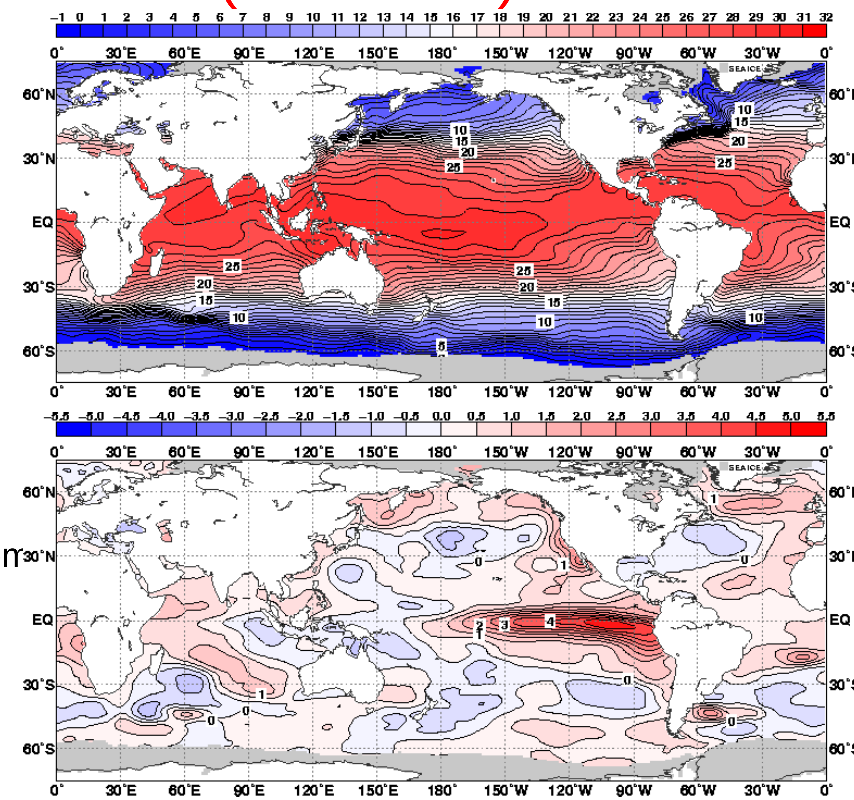

La Niña (NOV1988)

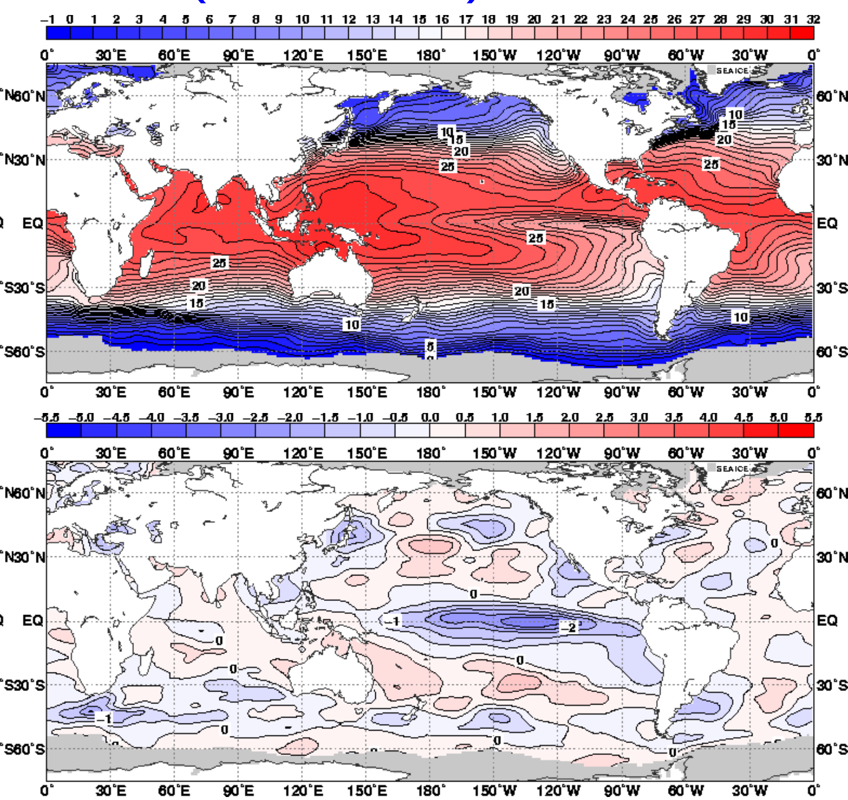

sea surface temperature

departure from normal

Look deep into the sea

SST anomaly in 27OCT1997

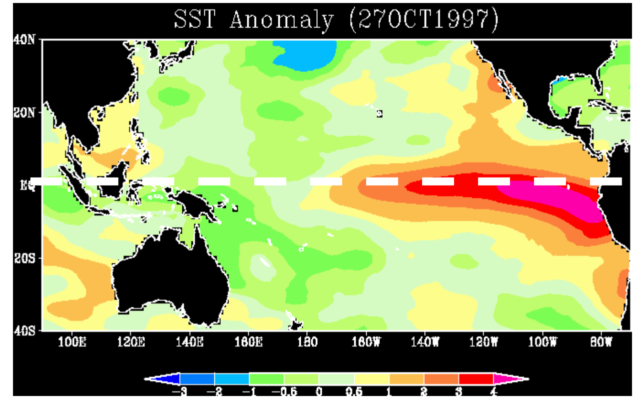

Subsurface temperatures in the equatorial Pacific in 1996/12-98/12

m

depth

200

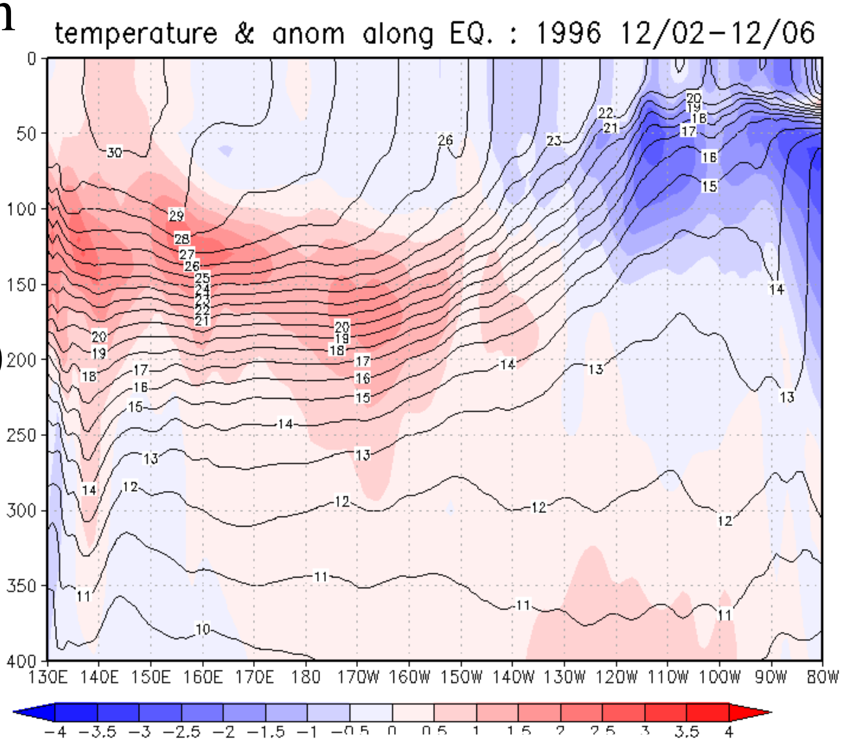

Longitude

Contour: sea temperature (°C)
Shade:anomaly (°C)

Japan Meteorological Agency

1997/98 El Niño development and decay – hovmoeller plots

SST anomaly

OHC anomaly

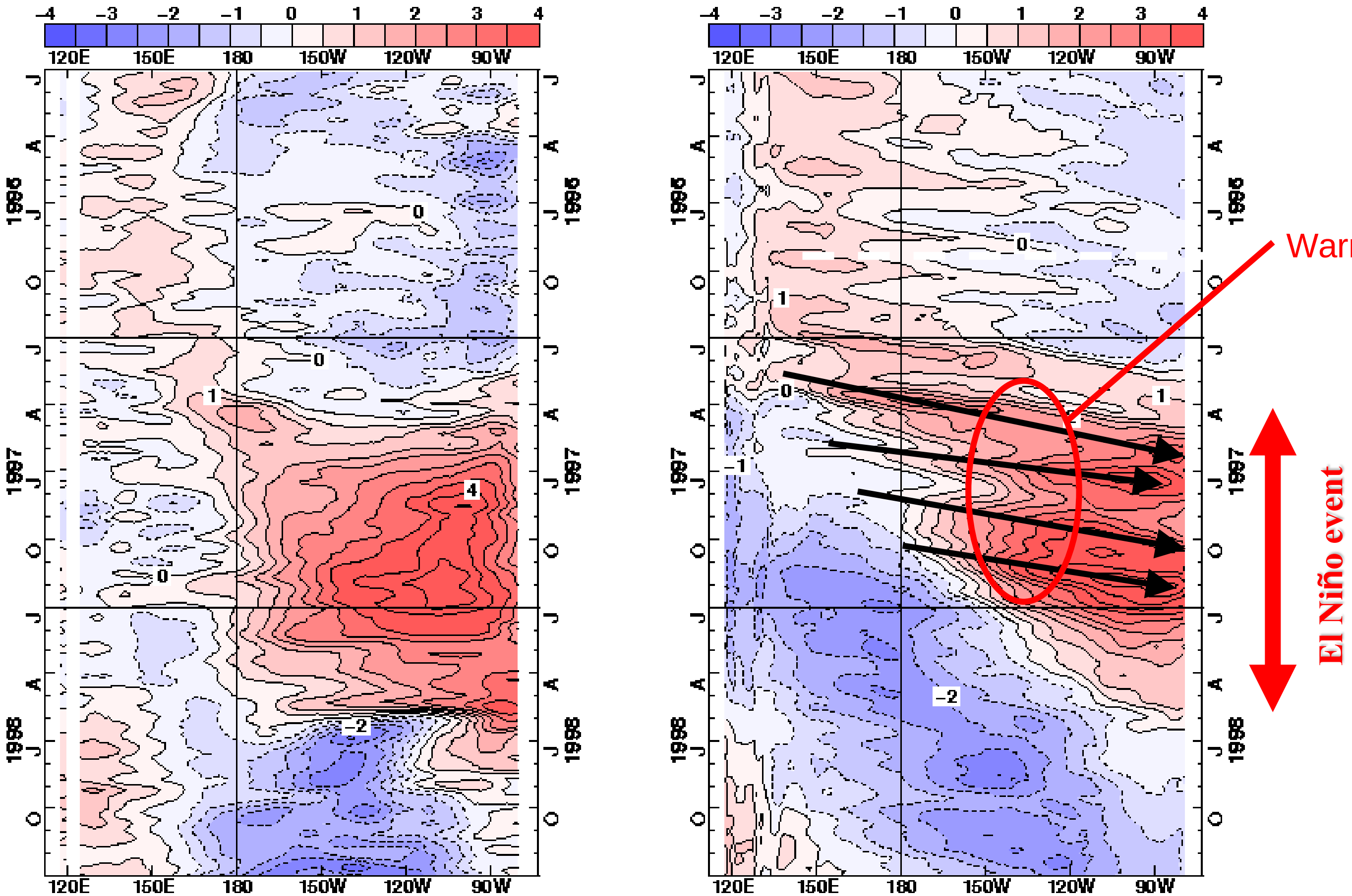

OHCs are defined as vertically averaged temperatures of top 300m.

Positive feedback

Hövmoeller (Longitude-time section) in equatorial Pacific

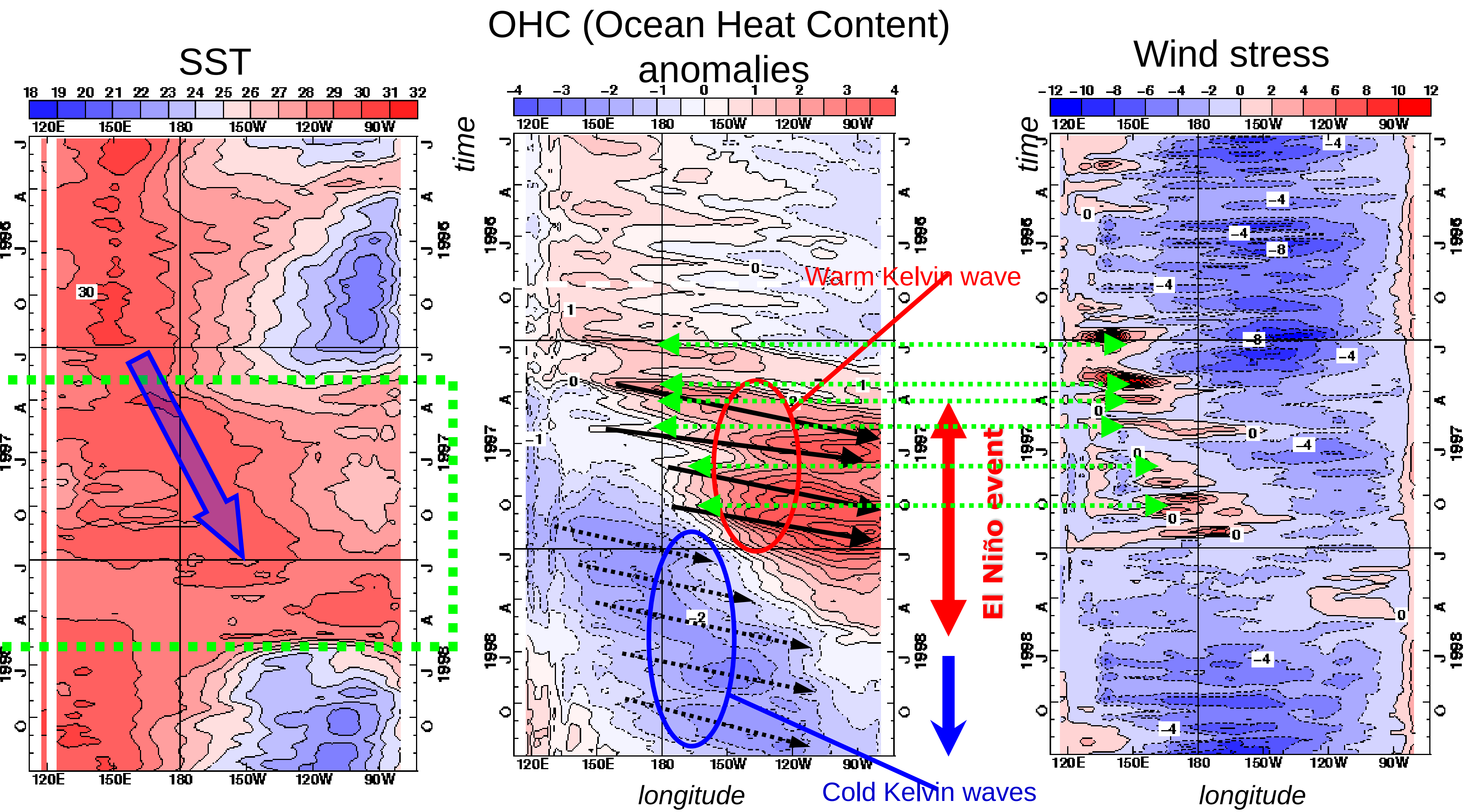

OHCs are defined as vertically averaged temperatures from sea surface to 300-m depth

ENSO is huge heat variation in the climate system

	Atmosphere	Ocean
Density	$1.2\text{–}1.3\,kgm^{-3}$	$10^3 kgm^{-3}$ ：atom. X 800
Mass(per 1 m^2)	（Top ～ Surface） $10^4 kgm^{-2}$	（Surface ～10m depth） $10^4 kgm^{-2}$ ：Mass of the atmosphere is the same as that of same as that of ocean with 10m depth
Specific heat	$10^3 Jkg^{-1}K^{-1}$	$4\times10^3 Jkg^{-1}K^{-1}$ ：atom. X 4
Heat capacity (per 1 m^2)	（Top ～ Surface） $10^7 JK^{-1}m^{-2}$	（Surface ～2.5m depth） $10^7 JK^{-1}m^{-2}$ ：Heat capacity of the atmosphere is the same as atmosphere is the same as that of ocean with 2.5m

“1K in 250m depth ocean” is near equal to “100K in the atmosphere”

* from Gill 1982

Historical look at SST variations

5-month running mean SST departures from normal in the JMA's El Niño monitoring region for 1950-2016

red: El Niño period

blue: La Niña period

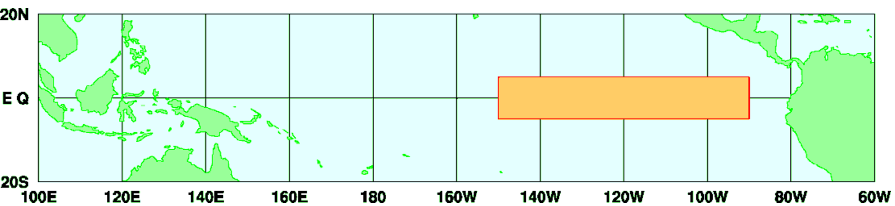

SST Deviation at NINO.3 (5S-5N,150W-90W)

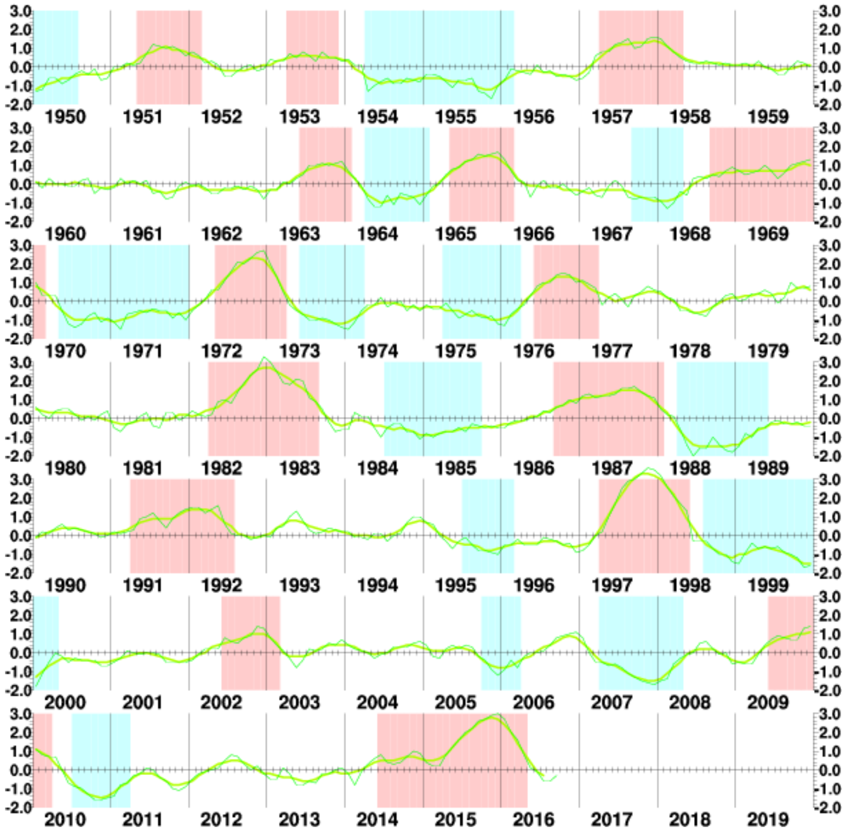

El Niño and La Niña impact on the world climate

Walker Circulation along the equator during El Nino (lower panel) and La Nina (upper panel)

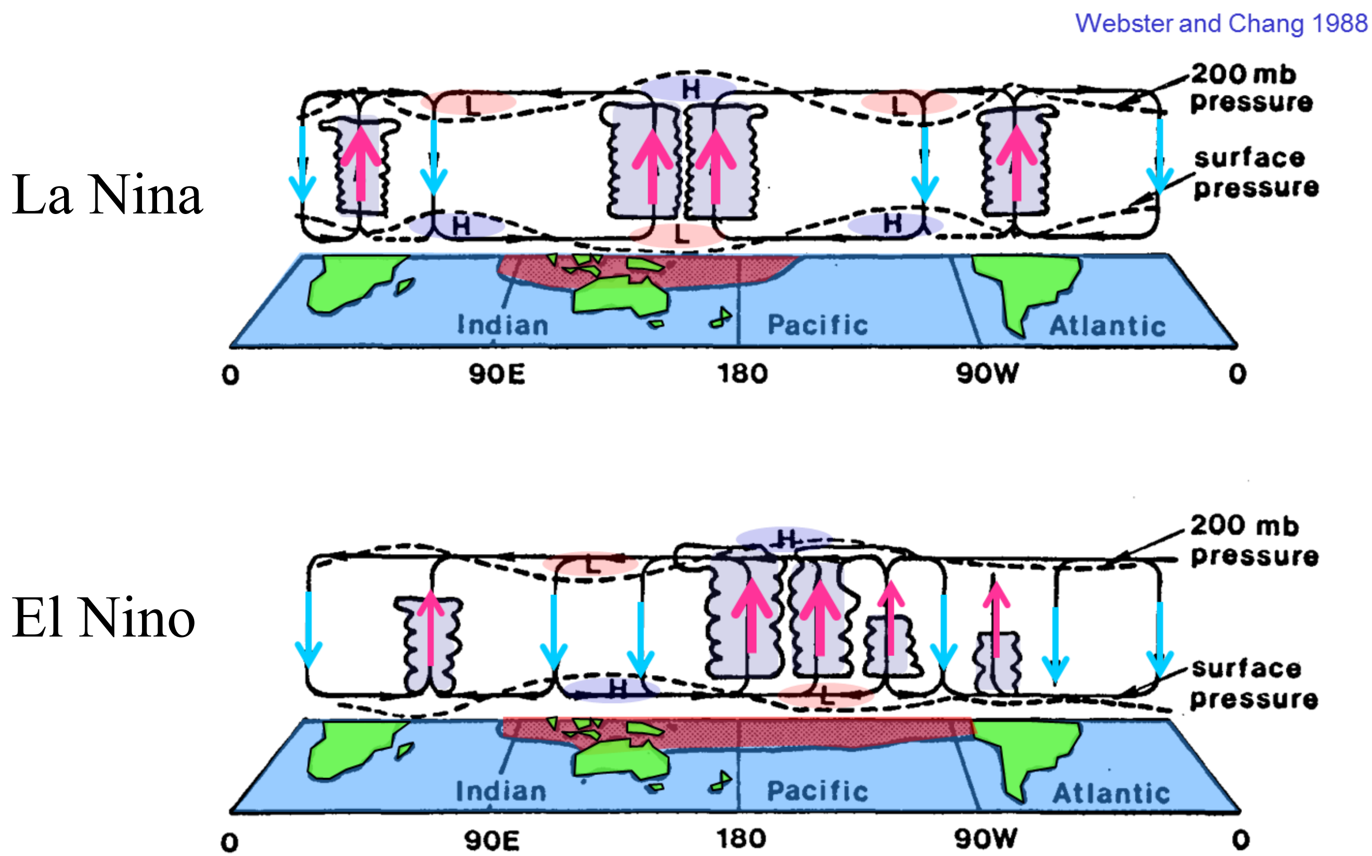

FIG. 1. Schematic view of the Walker Circulation along the equator during El Niño (lower panel) and La Niña (upper panel) periods that occur at the extremes of the Southern Oscillation. The shaded areas indicate sea surface temperatures warmer than 27°C and the dashed lines show relative horizontal pressure variations in the lower and upper troposphere. (From Webster, 1983)

Precipitation in 1997/98 winter(DJF)

Upper：1997/98, lower：normal

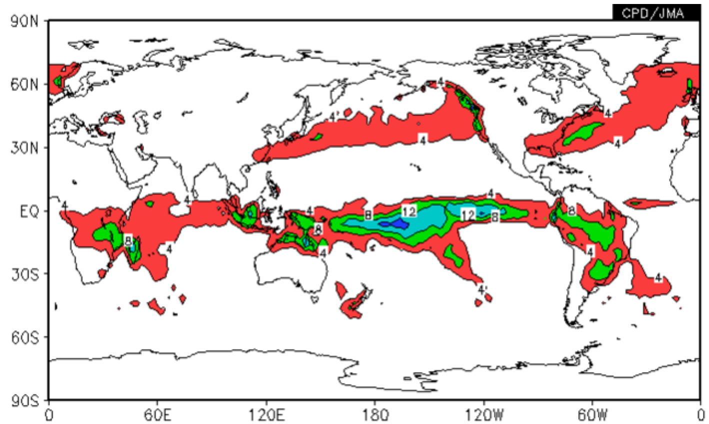

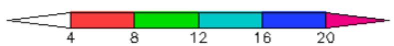

mm/day

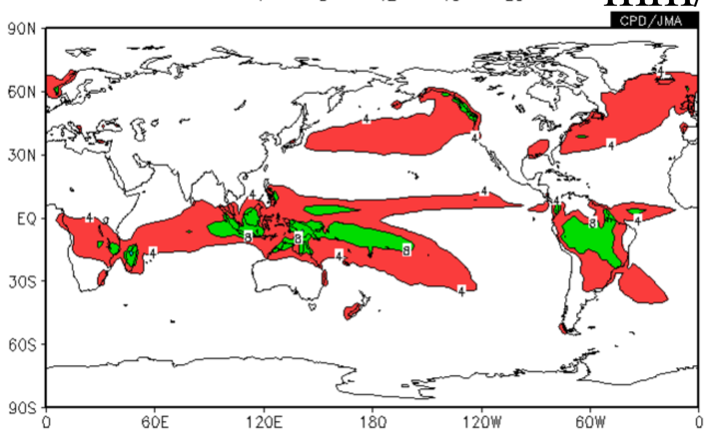

Anomalies in 1997/98

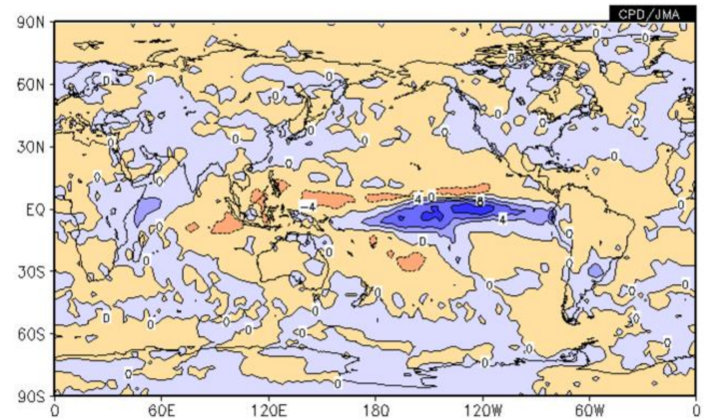

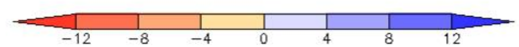

mm/day

Atmospheric heating by condensation

Latent heat

: $2.5 \times 10^{6} \mathrm{Jkg}^{-1}$

Heat capacity of the atmosphere (per $1\mathrm{m}^2$)

: $10^{7} \mathrm{JK}^{-1}\mathrm{m}^{-2}$

→

4kg/day(=4mm/day) condensation heats the atmosphere 1K/day

Global atmospheric response to condensation heating in the central equatorial Pacific

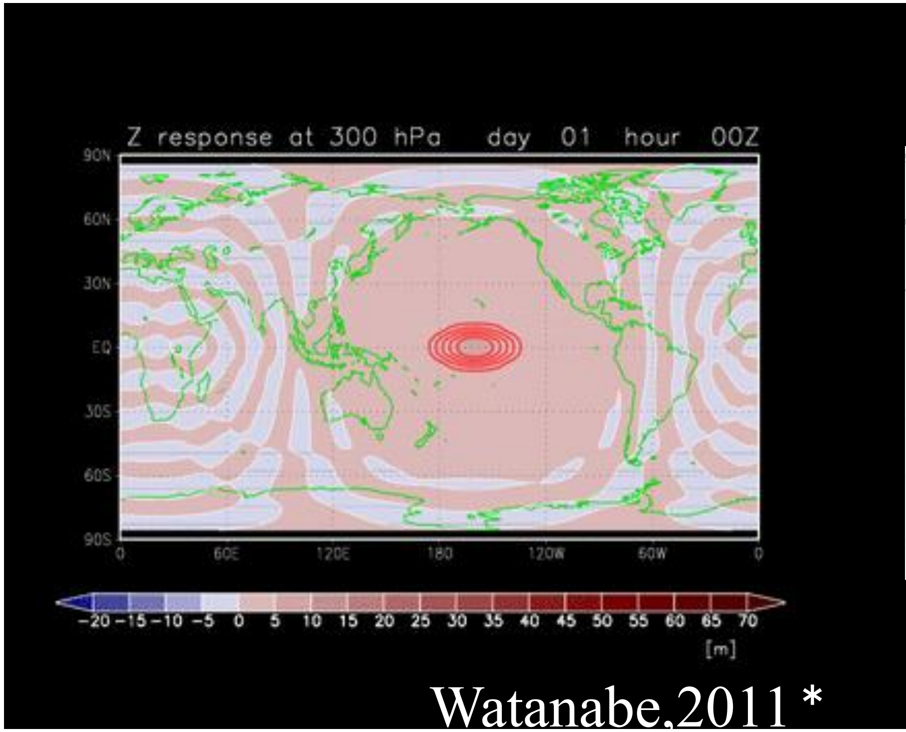

LBM simulation of response to condensation heating in the central equatorial Pacific.

Geopotential height at 300hPa

* from his presentation in "Twelfth Joint Meeting for the Seasonal Prediction of the East Asian Winter Monsoon"

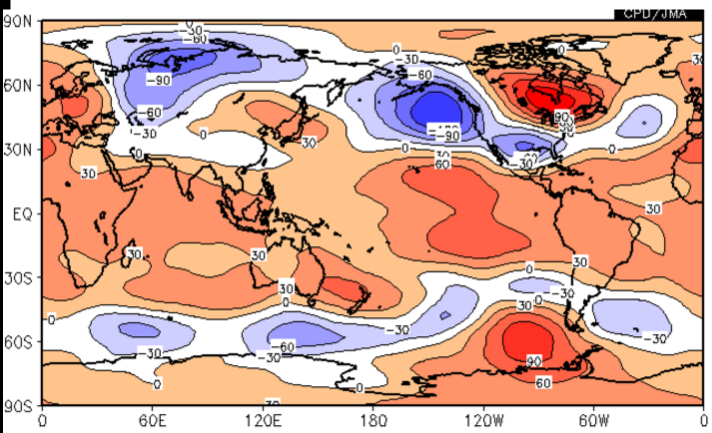

Geopotential height anomalies at 300hPa in 1997/98 winter (DJF).

Localized condensation heating in the tropics force stationary Rossby waves which propagate to the mid-high latitudes.

Impact of ENSO on Global average surface temperature

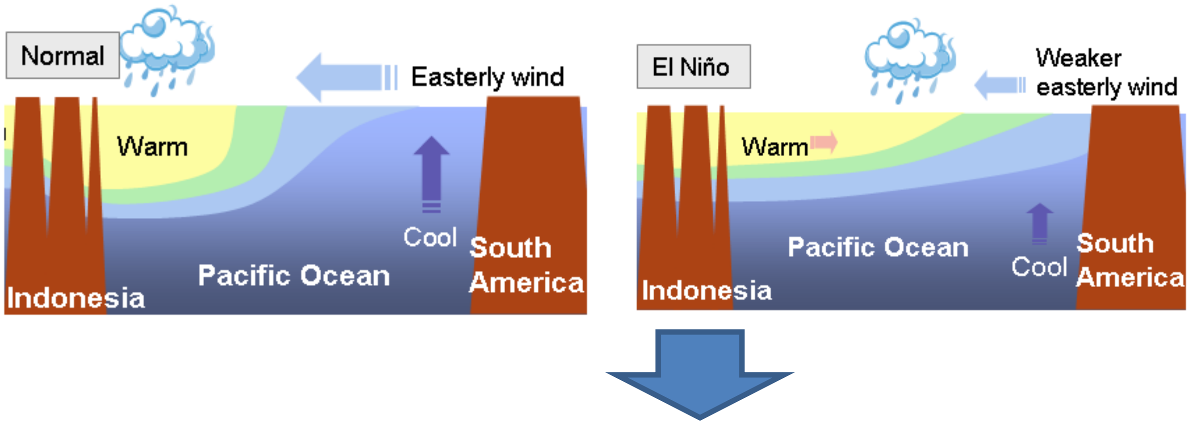

Sub-surface sea temperature in the equatorial Pacific is warmer than normal during El Nino

Global average surface temperature anomalies (1950-2015)

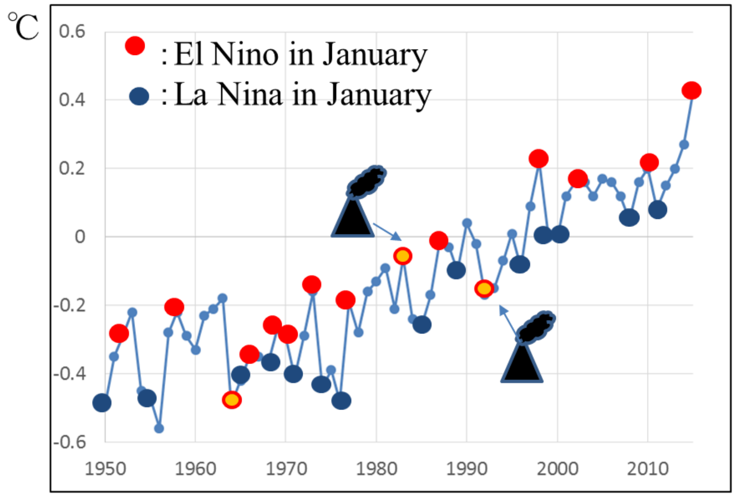

Global average monthly surface temperature tends to raise 0.09 °C per Nino3.4 with three months lag (Trenberth, 2002).

Impact of ENSO on zonal average temperature and circulation

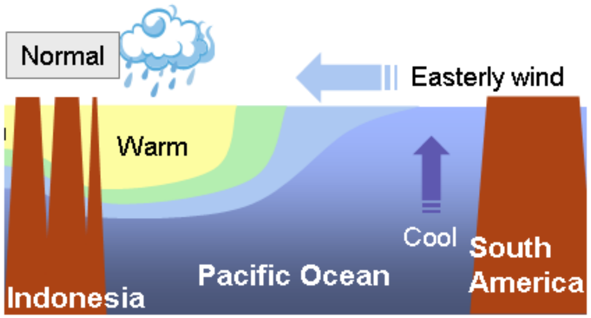

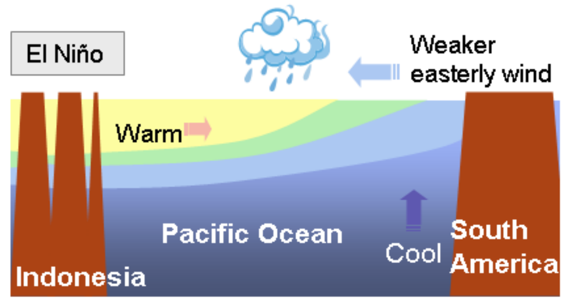

Sub-surface sea temperature in the equatorial Pacific is warmer than normal during El Nino

Temperature in JFM

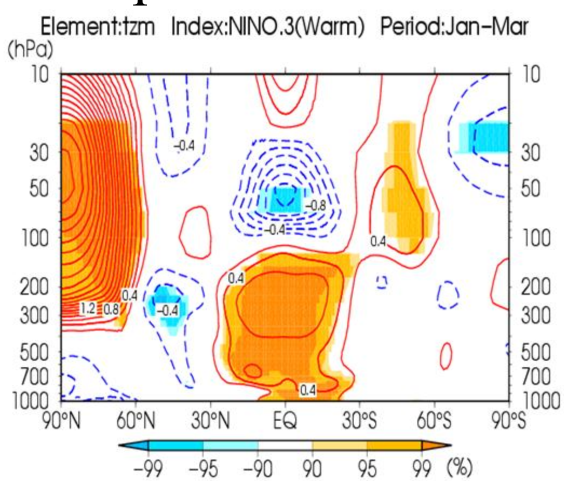

Zonal Wind in JFM

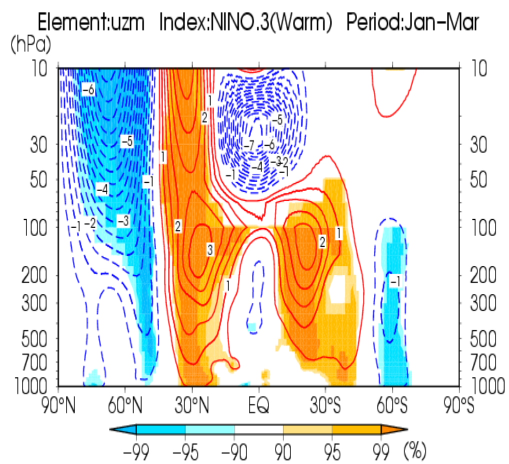

Composite maps in El Nino years

Temperature is higher in the tropics in the troposphere during El Nino.

Temperature gradient between the tropics and mid-latitudes is greater during El Nino

Zonal wind in the sub-tropics is stronger during El Nino

Statistical relationship between NINO.3 and atmospheric circulation fields in DJF

SST

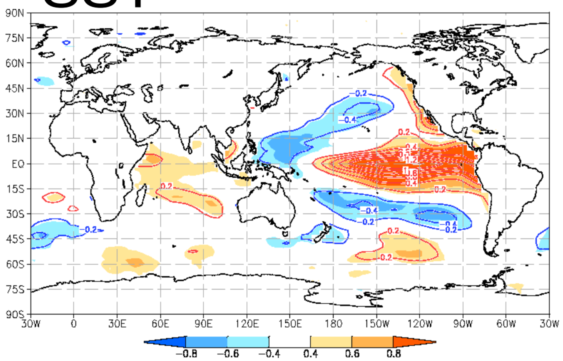

OLR

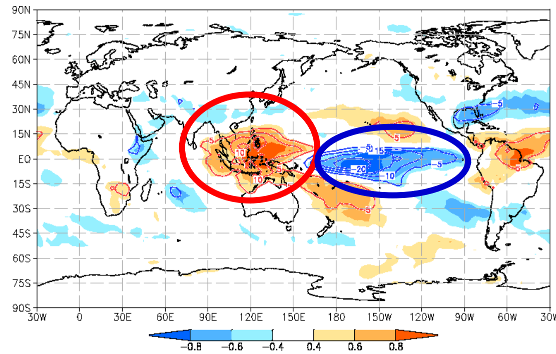

Sea Level Pressure

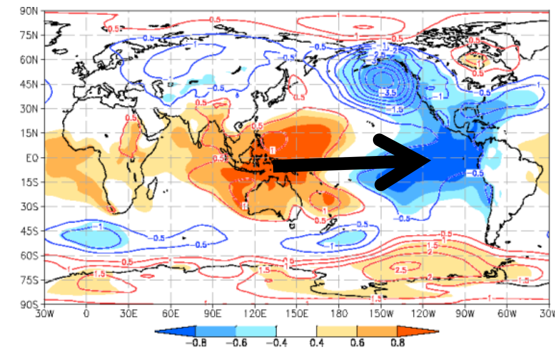

Velocity Potential at 200hPa

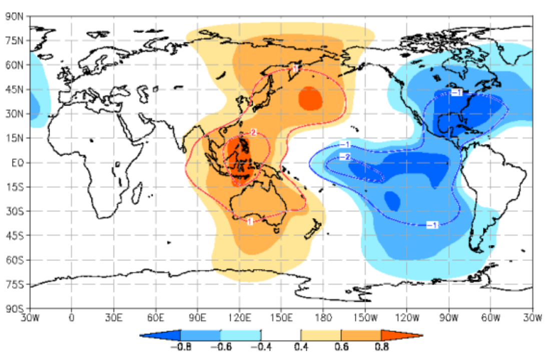

Stream Function at 850hPa

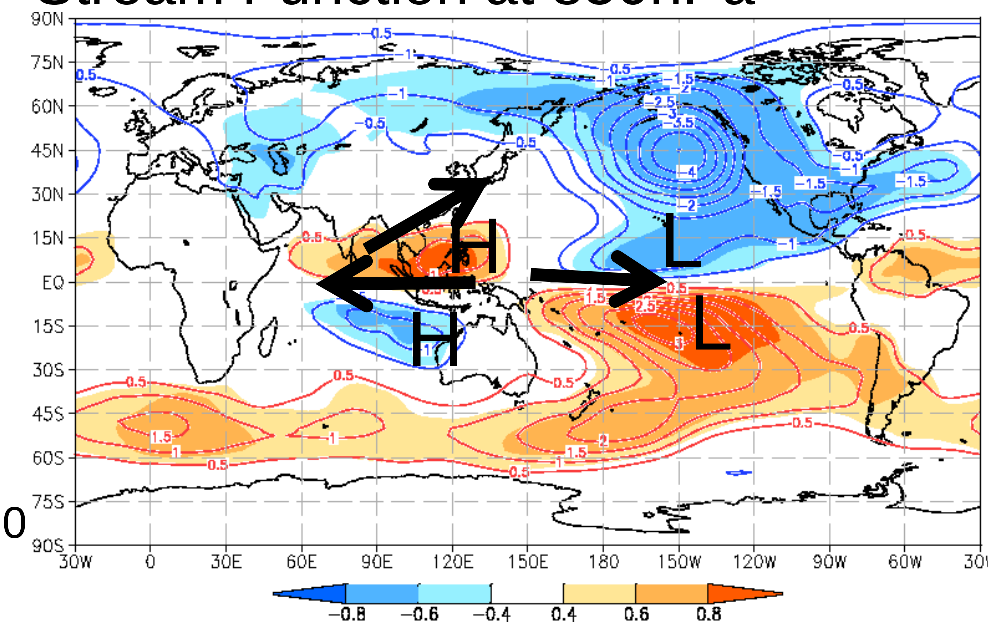

Contours show atmospheric circulation anomalies when normalized NINO.3 is+1.0
Shadings show correlation coefficients.

Some simple solutions for heat-induced tropical circulation

Quarterly Journal of the Royal Meteorological Society
Volume 106, Issue 449, July 1980, Pages: 447–462, A. E. Gill

Symmetric Heating Anomaly about the equator

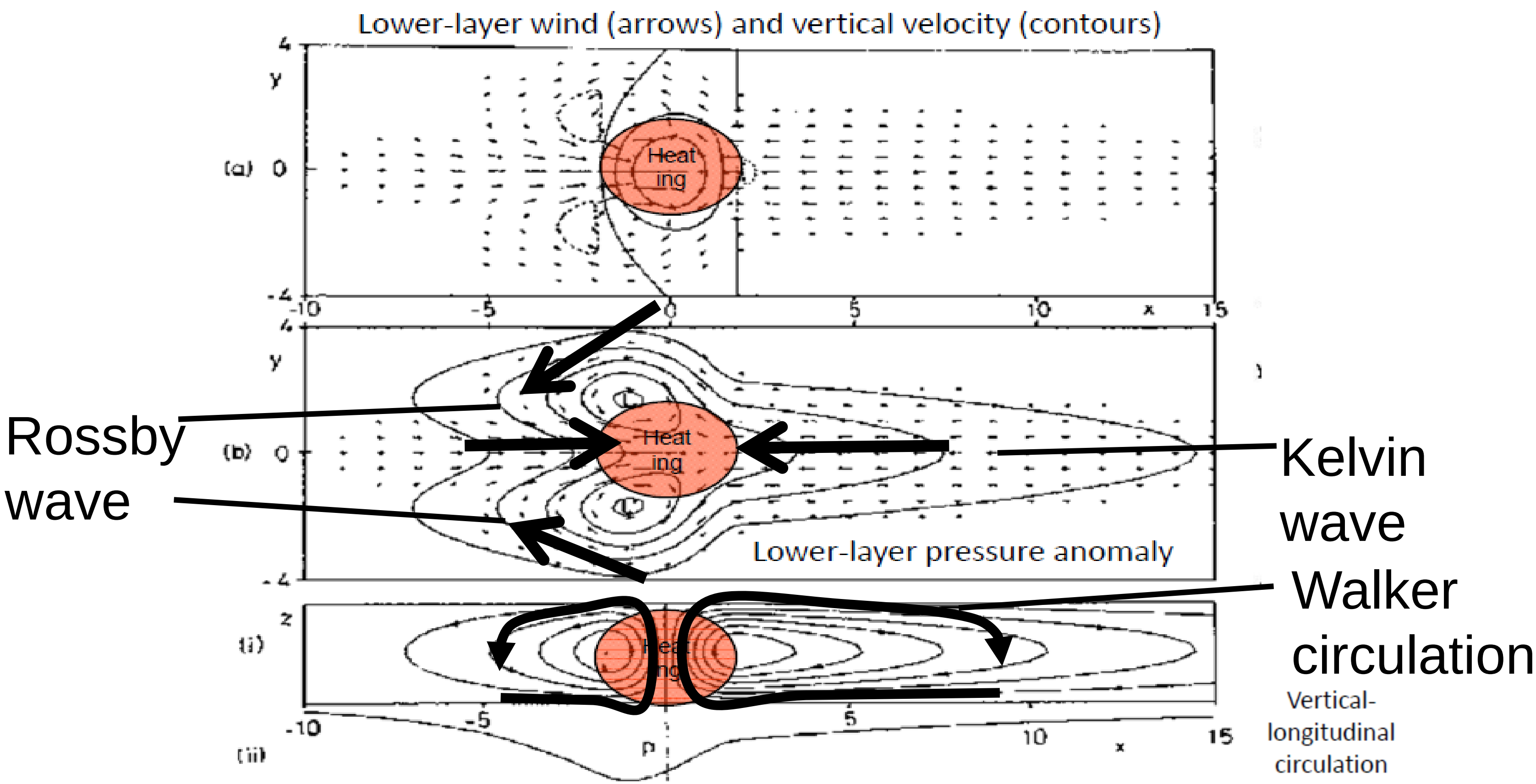

Climate tendencies during El Nino/La Nina

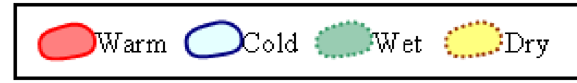

EL in boreal summer

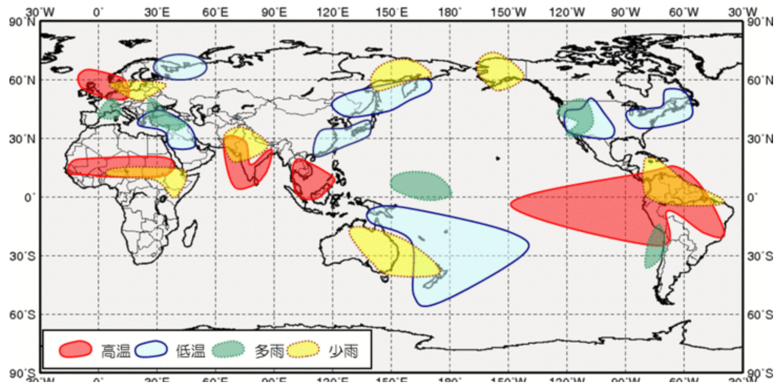

EL in boreal winter

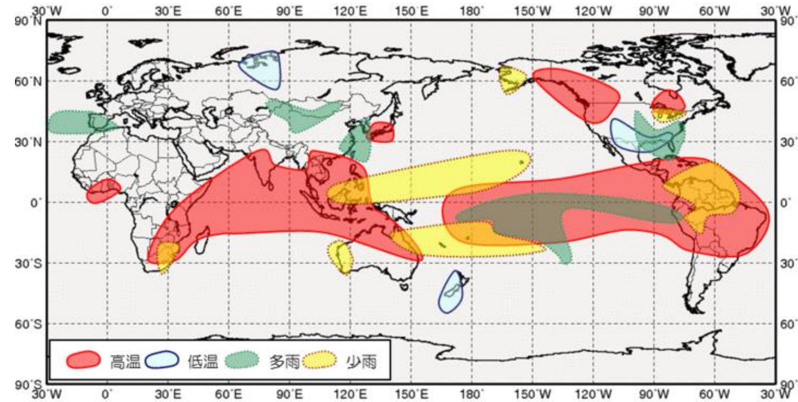

LA in boreal summer

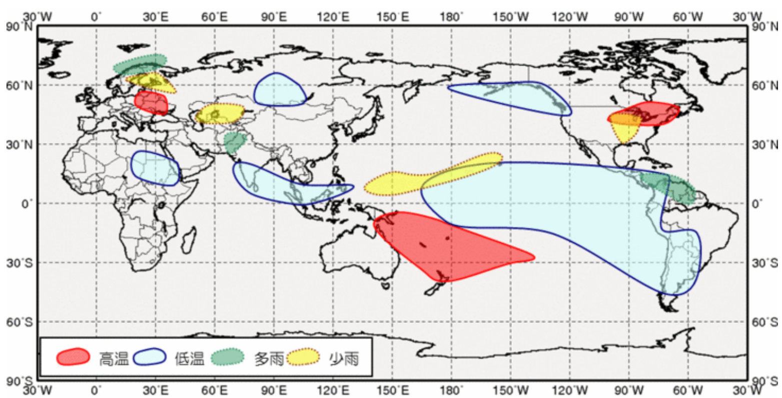

LA in boreal winter

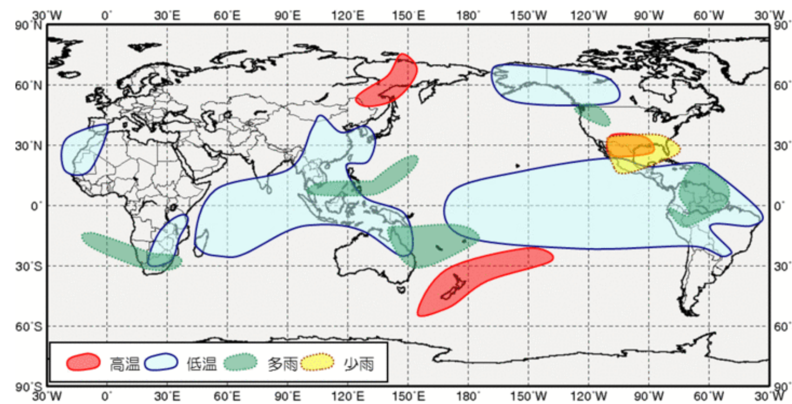

The maps show the regions where climate tendencies observed during El Niño/La niña episodes are statistically significant in boreal summer/winter.

Example of ENSO prediction

Initial :1997.8.29,　Valid time : 1997.12～1998.2

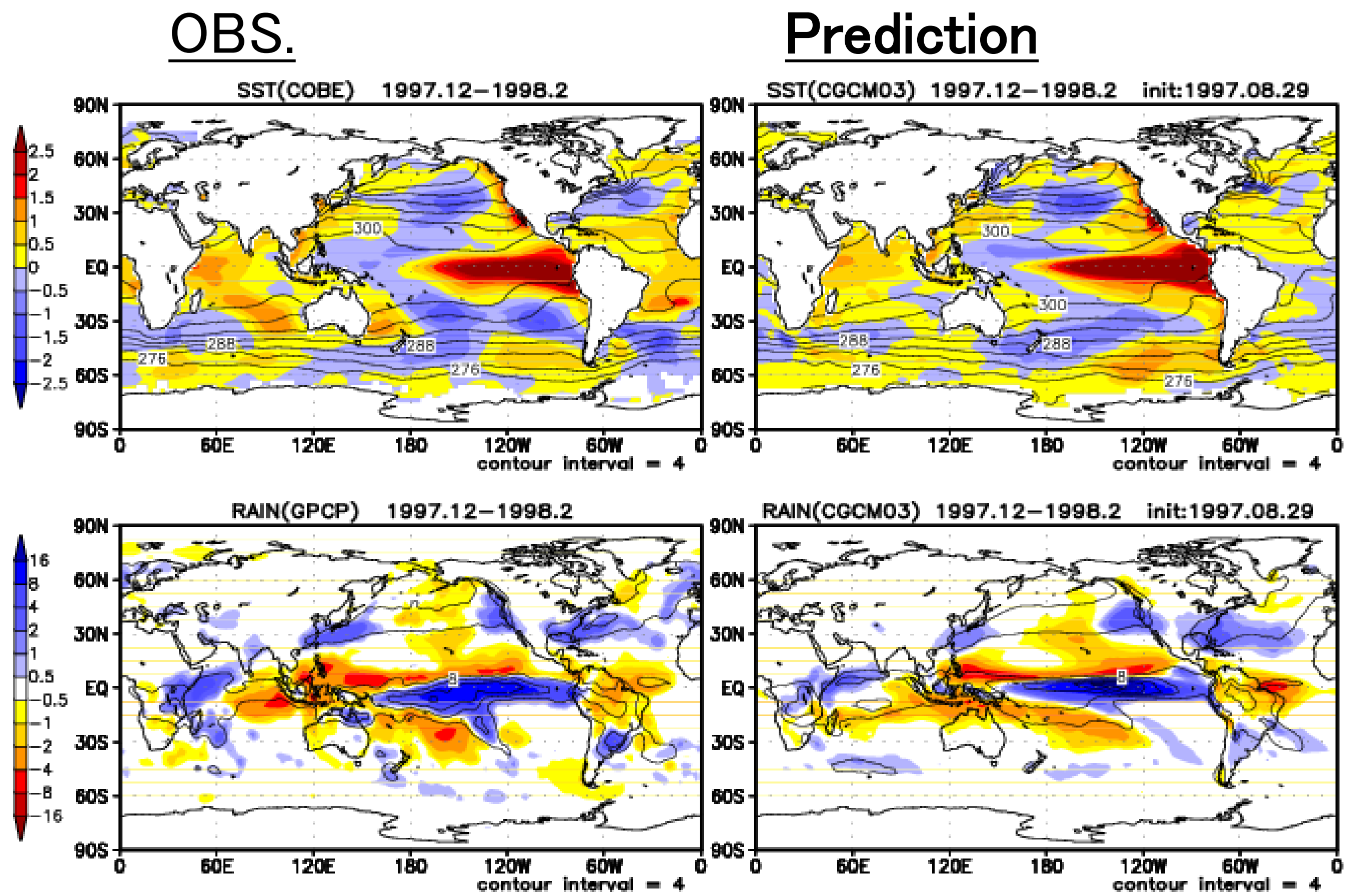

Contour : SST
Shade:
SST anomaly

Contour :
Precipitation
Shade:
Precipitation anomaly

Lingering impacts of ENSO through change in SST in Tropical Indian Ocean (TIO)

SST in TIO tends to raise associated with El Nino with one-season lag

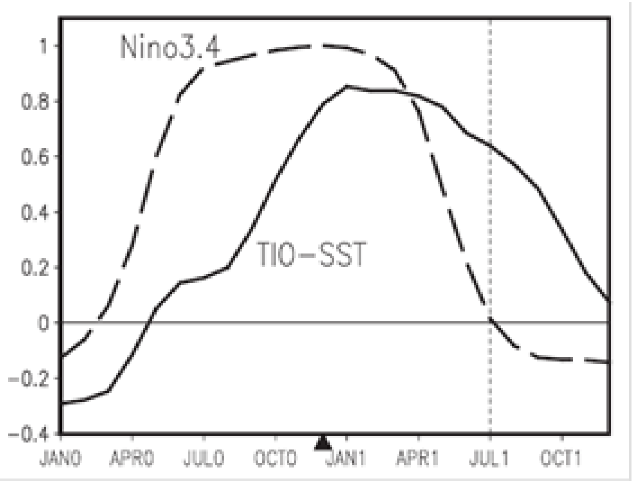

Fig. 1. Correlation of tropical Indian Ocean (40-100°E, 20°S-20°N) SST (solid) with the Nino3.4 (170°W-120°W, 5°S-5°N) SST index for Nov(0)-Dec(0)-Jan(1). Numerals in parentheses denote years relative to El Nino: 0 for its developing and 1 for decay year. The dashed curve is the Nino3.4 SST auto-correlation as a function of lag. The black triangle denotes Dec(0), the peak phase of ENSO.

Warm SST in TIO has impact on atmospheric circulation in Asia Pacific region in JJA

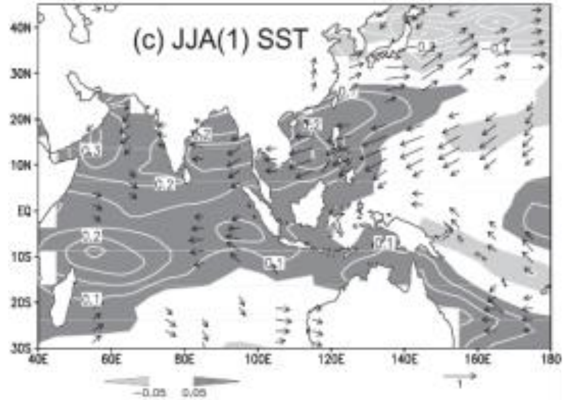

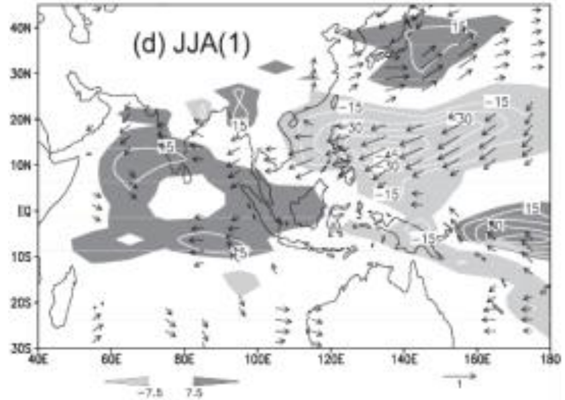

Xie et al.(2009)

El Niño Modoki & CP El Niño

Nature,2009

The El Niño with a difference

Karumuri Ashok and Toshio Yamagata

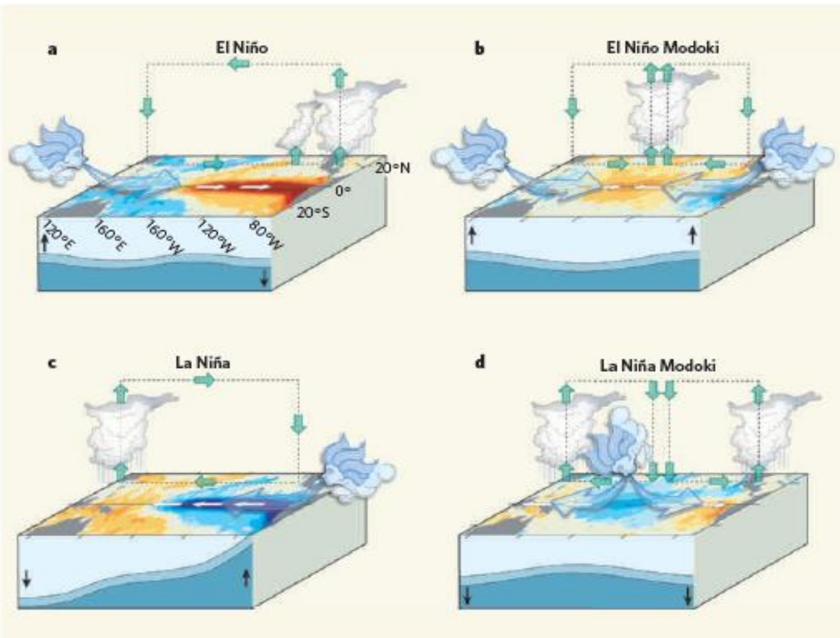

Figure 2 | Anomalous conditions in the tropical Pacific. **a**, An El Niño event is produced when the easterly winds weaken; sometimes, in the west, westerlies prevail. This condition is categorized by warmer than normal sea surface temperatures (SSTs) in the east of the ocean, and is associated with alterations in the thermocline and in the atmospheric circulation that make the east wetter and the west drier. **b**, An El Niño Modoki event is an anomalous condition of a distinctly different kind. The warmest SSTs occur in the central Pacific, flanked by colder waters to the east and west, and are associated with distinct patterns of atmospheric convection. **c**, **d**, The opposite (La Niña) phases of the El Niño and El Niño Modoki respectively. Yeh *et al.*[3] argue that the increasing frequency of the Modoki condition is due to anthropogenic warming, and that these events in the central Pacific will occur more frequently if global warming increases.

Nature,2009

El Niño in a changing climate

Sang-Wook Yeh[1], Jong-Seong Kug[1], Boris Dewitte[2], Min-Ho Kwon[3], Ben P. Kirtman[4] & Fei-Fei Jin

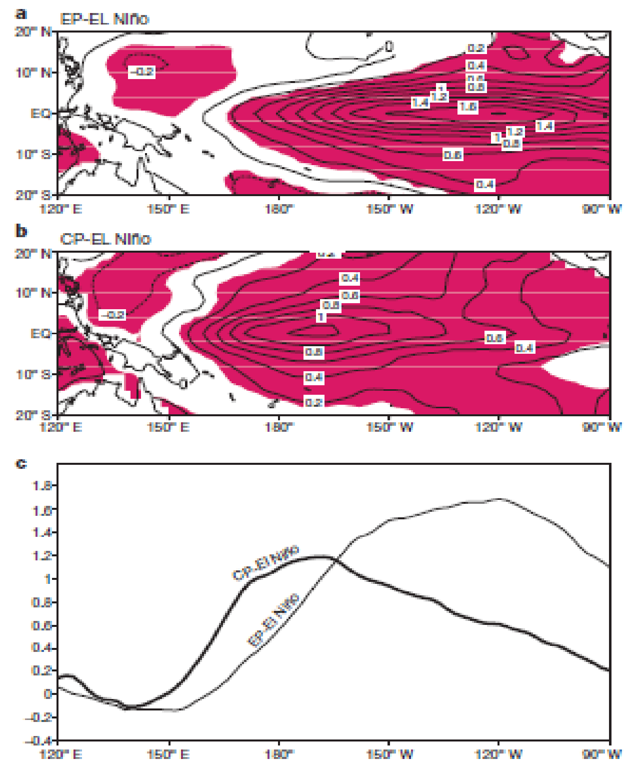

Figure 1 | Deviations of mean SST for the two characteristics of El Niño from the 1854–2006 climatology. **a**, The EP-El Niño; **b**, the CP-El Niño. The contour interval is 0.2 °C and shading denotes a statistical confidence at 95% confidence level based on a Student's *t*-test. **c**, The zonal structure for the composite EP-El Niño (thin line) and CP-El Niño (thick line) averaged over 2 °N to 2 °S.

ENSO-Monsoon relation

Severe droughts in India have always been accompanied by El Niño events. SST anomalies in the central equatorial Pacific are more effective in focusing drought-producing subsidence over India.

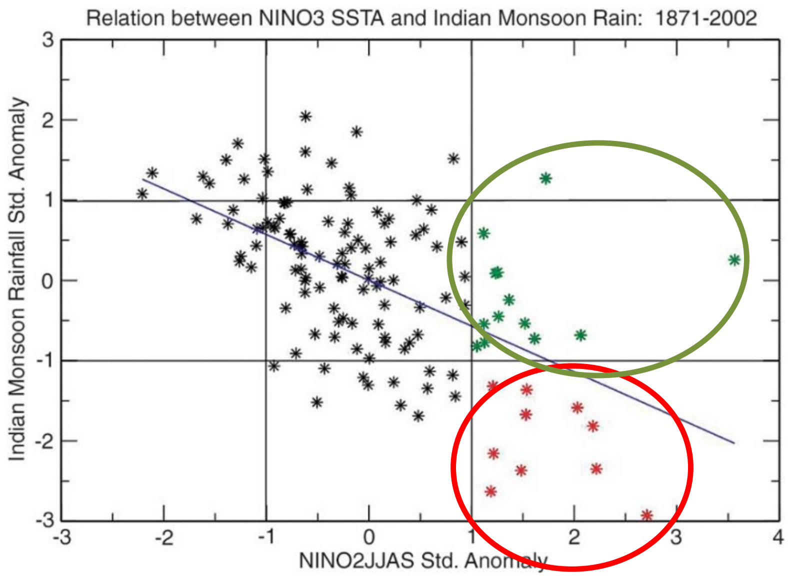

Plot of standardized, all-India summer [June to September (JJAS)] monsoon rainfall and summer NINO3 anomaly index. Severe drought and drought-free years during El Niño events (standardized NINO3 anomalies > 1) are shown in red and green, respectively.

Kumar et al.(2006)

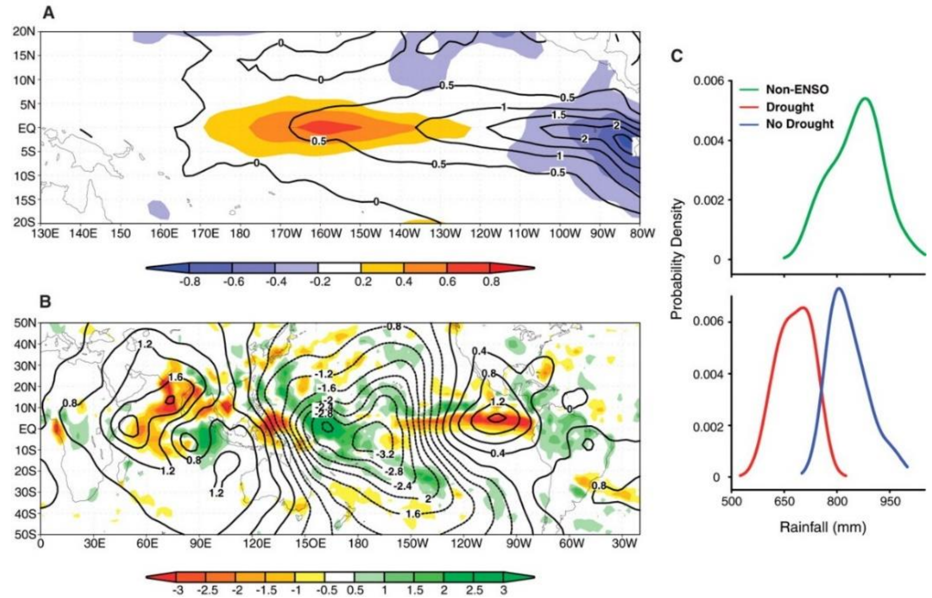

(**A**) Composite SST difference pattern between severe drought (shaded) and drought-free El Niño years. Composite SST anomaly patterns of drought-free years are shown as contours. (**B**) Composite difference pattern between severe drought and drought-free years of velocity potential (contours) and rainfall (shaded). (**C**) PDF of all-India summer monsoon rainfall from severe-drought (red curve) and drought-free (blue curve) years associated with El Nino occurrence and from the non-ENSO years (green curve). SST and velocity potential composite differences are based on 1950 to 2004, rainfall composites are based on 1979 to 2004, and PDFs are based on 1873 to 2004.

A dipole mode in the tropical Indian Ocean

Saji et al., Nature 1999

N. H. Saji*, B. N. Goswami†, P. N. Vinayachandran* & T. Yamagata*‡

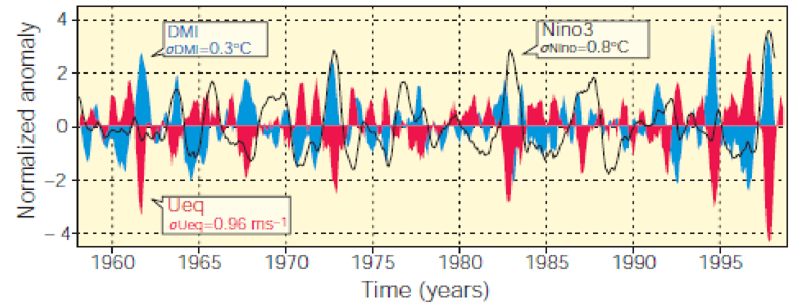

Figure 1 Dipole mode and El Niño events since 1958. Plotted in blue, the dipole mode index (DMI) exhibits a pattern of evolution distinctly different from that of the El Niño, which is represented by the Nino3 sea surface temperature (SST) anomalies (black line). On the other hand, equatorial zonal wind anomalies U_{eq} (plotted in red) coevolves with the DMI. All the three time series have been normalized by their respective standard deviations. We have removed variability with periods of 7 years or longer, based on harmonic analysis, from all the data sets used in this analysis. In addition, we have smoothed the time series using a 5-month running mean.

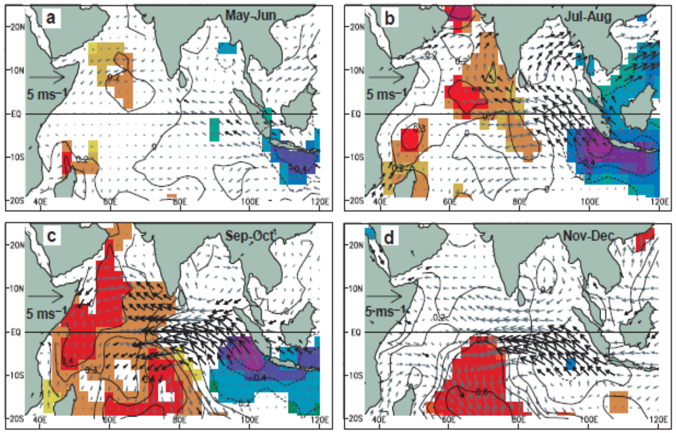

Figure 2 A composite dipole mode event. **a–d**, Evolution of composite SST and surface wind anomalies from May–June (**a**) to Nov–Dec (**d**). The statistical significance of the analysed anomalies were estimated by the two-tailed *t*-test. Anomalies of SSTs and winds exceeding 90% significance are indicated by shading and bold arrows, respectively.

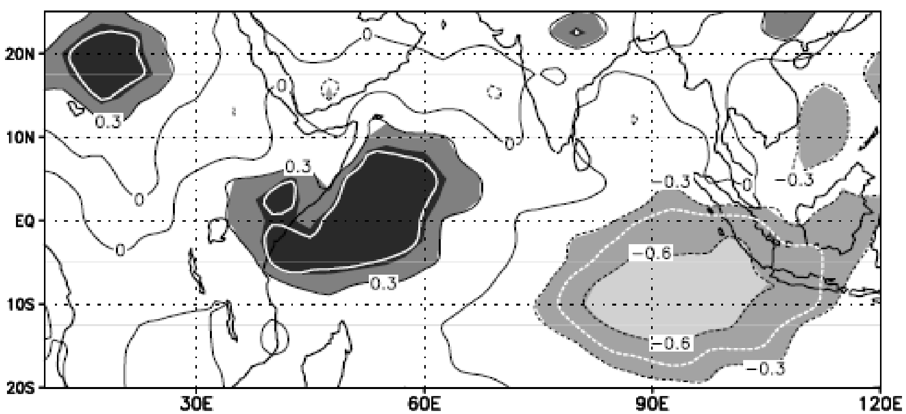

Figure 4 Rainfall shifts northwest of the OTCZ during dipole mode events. The map correlates the DMI and rainfall to illustrate these shifts. The areas within the white curve exceed the 90% level of confidence for non-zero correlation (using a two-tailed *t*-test).

Vol. 25: 151–169, 2003 | CLIMATE RESEARCH Clim Res | Published December 5

Possible impacts of Indian Ocean Dipole mode events on global climate

N. H. Saji[1,3,*], T. Yamagata[1,2]

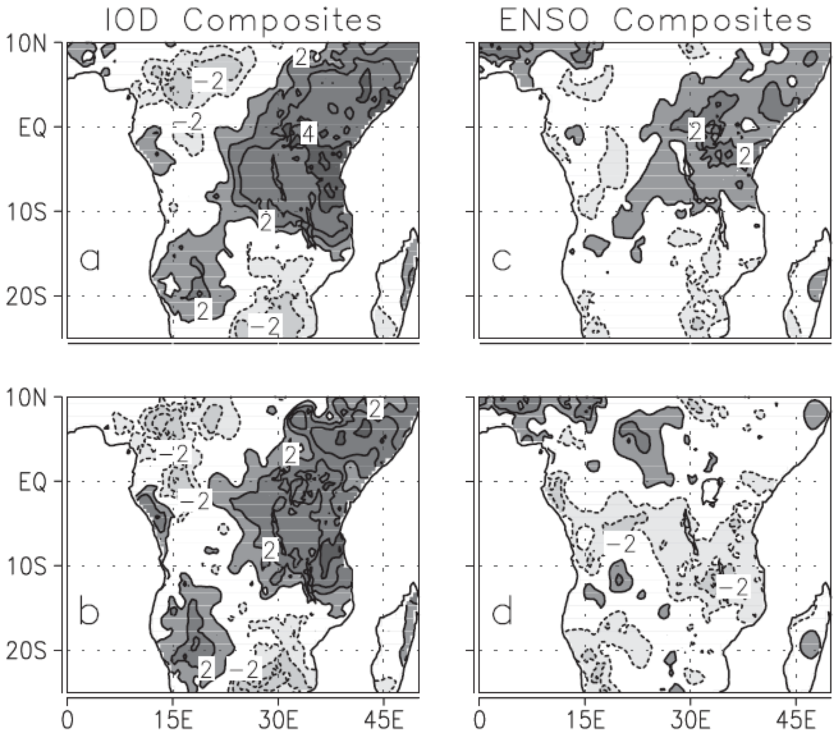

Fig. 1. Composite OND rain anomaly over Africa for (a) 19 IOD events, (b) 11 ENSO-independent IOD events, (c) 20 ENSO events and (d) 12 IOD-independent ENSO events. The composite anomaly was normalized by the standard deviation of rain during OND. Contours given at ±1, ±2, etc.

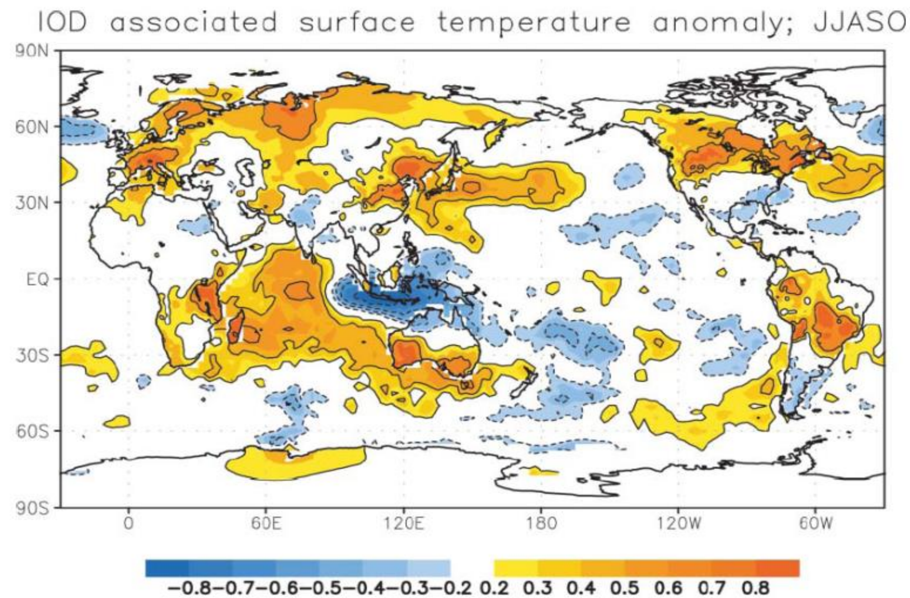

Fig. 21. Partial correlation of land and sea-surface temperature on DMI independent of Nino3 during JJASO

- 2.4 Decadal Variability

PDO, AMO,ENSO-Monsoon relation

Pacific Decadal Oscillation (PDO)

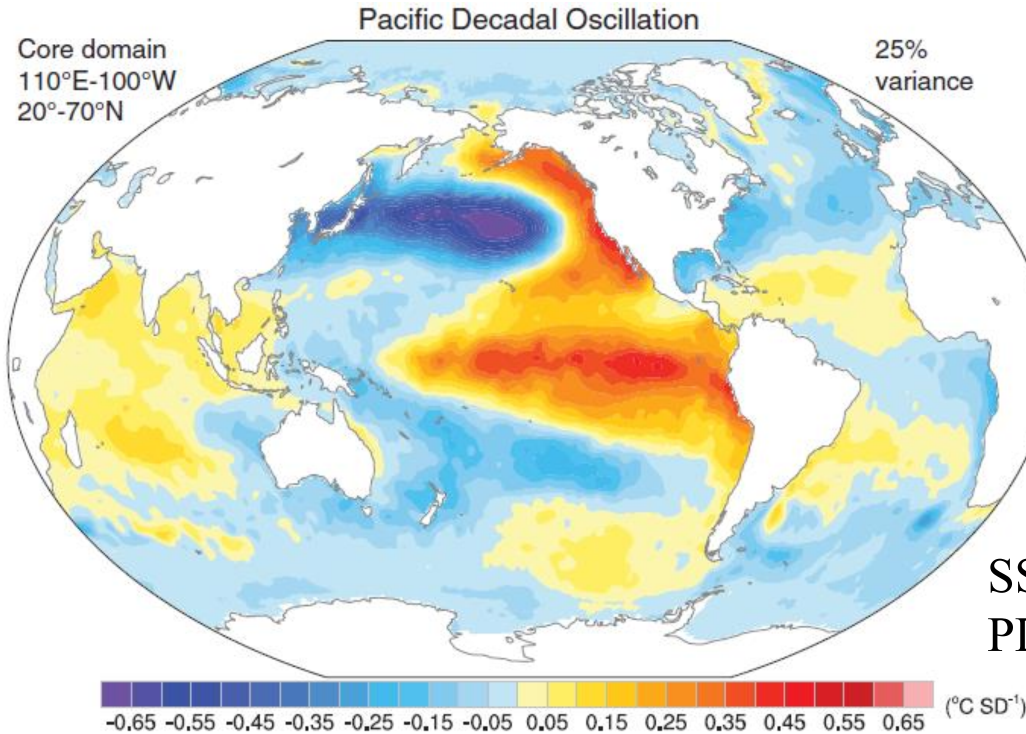

Trenberth and Fasullo (2013)

SST pattern regressed on PDO index

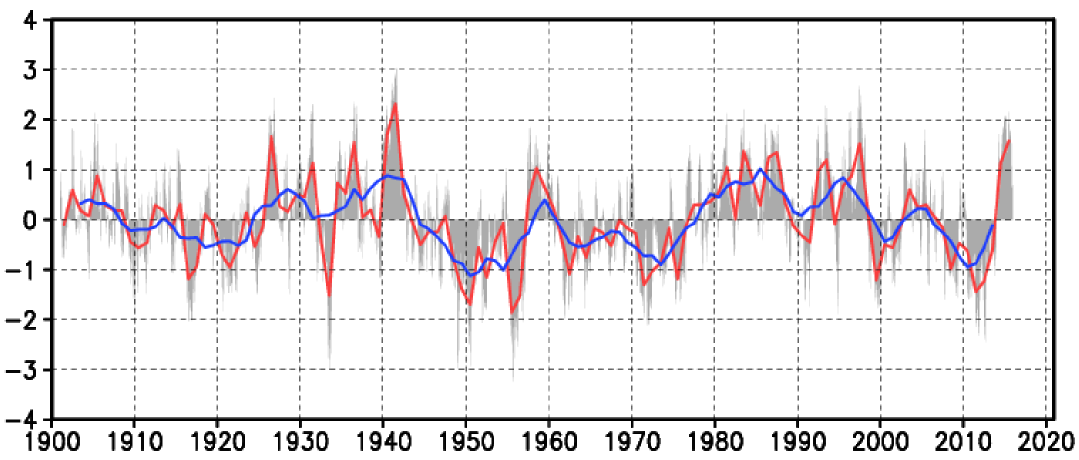

PDO index

(from JMA website)

PDO and local climate

Zonal wind

Dec/Jan/Feb

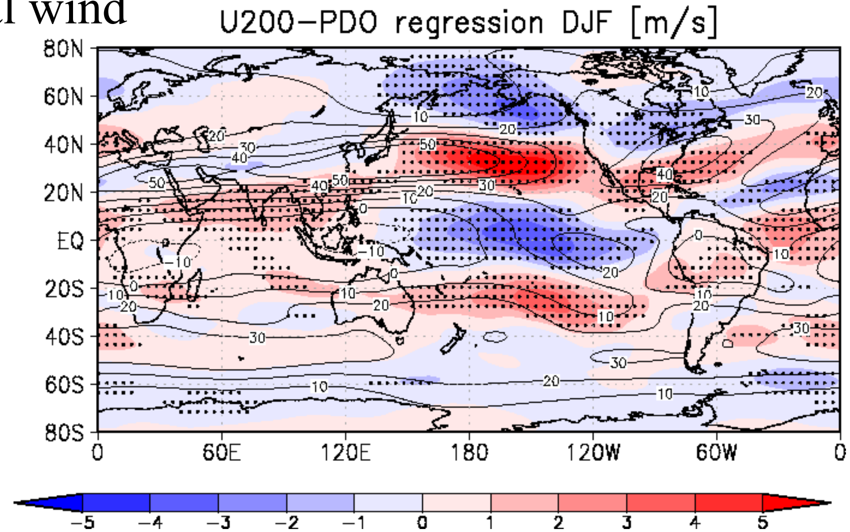

Jun/Jul/Aug

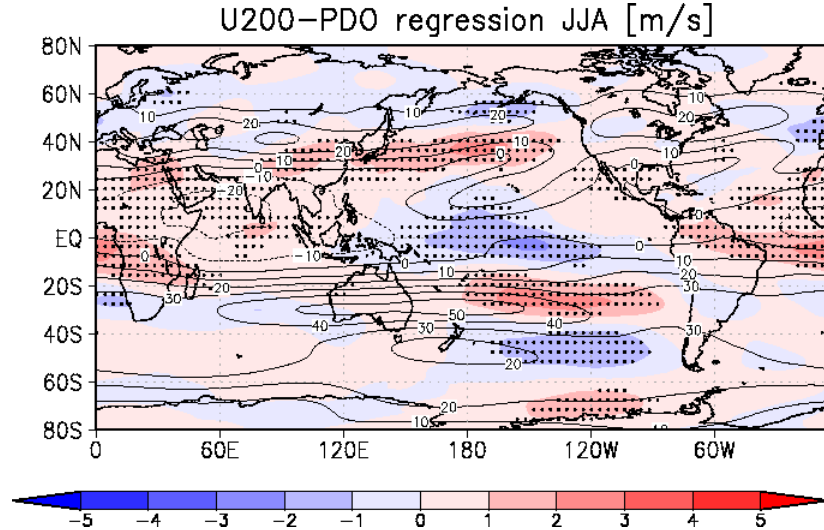

Temperature

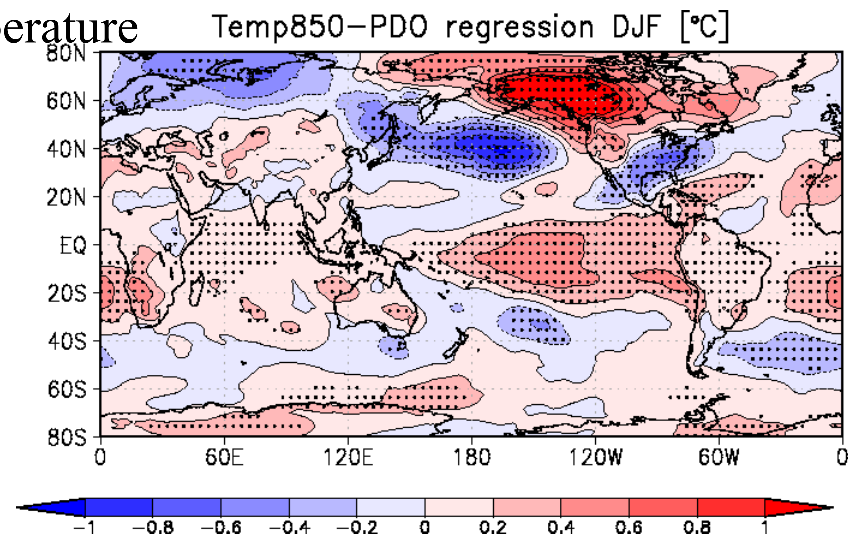

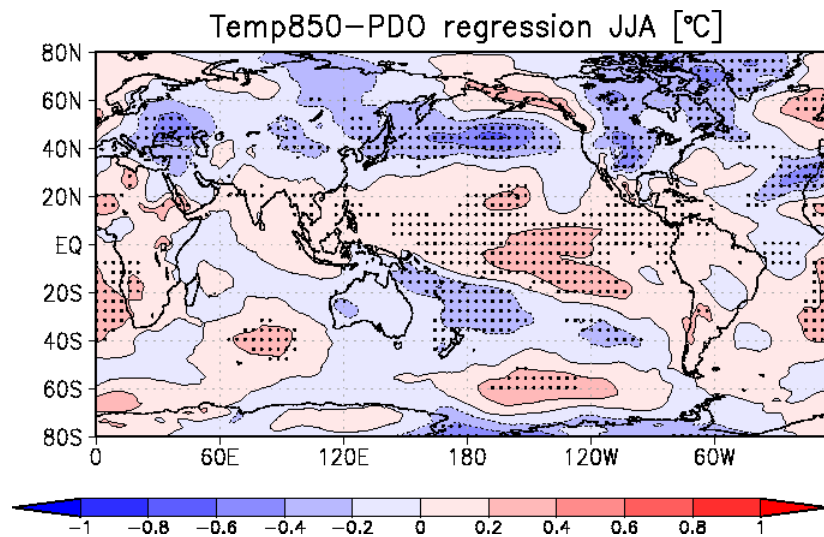

(from JMA website)

Global Warming Slowdown and PDO

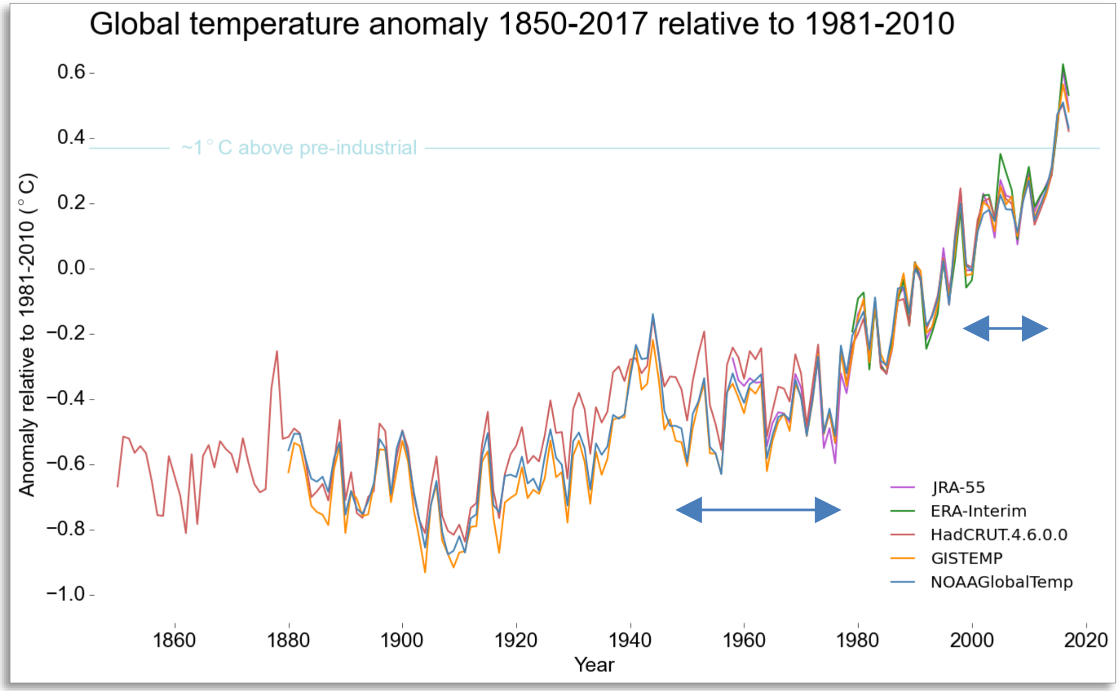

Phases of global warming slowdown ("hiatus") correspond to the negative phase of PDO index

PDO index

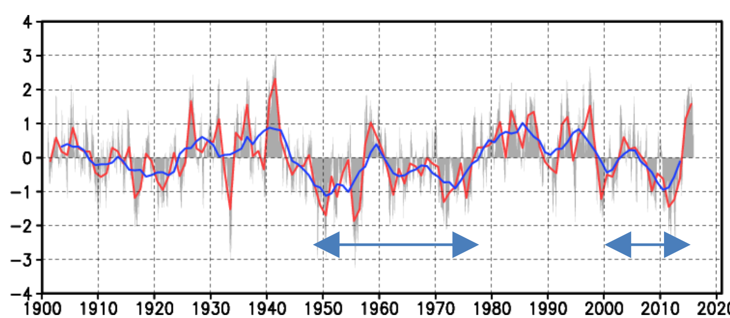

Atlantic Multidecadal Oscillation (AMO)

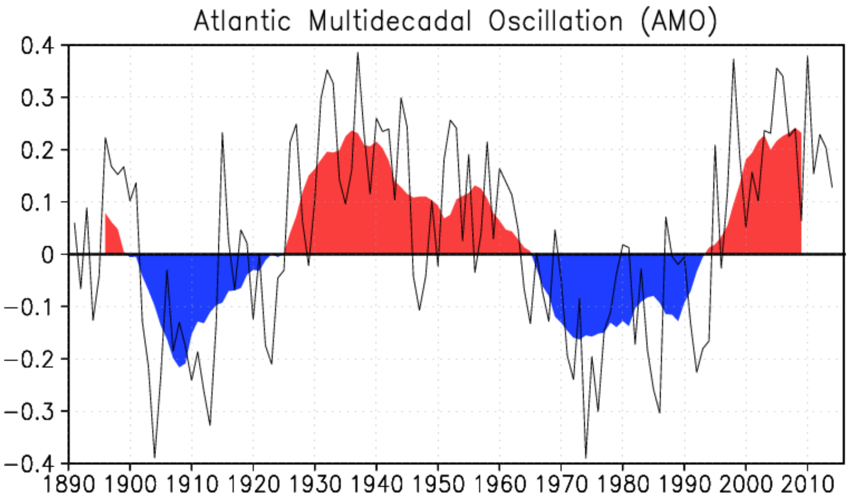

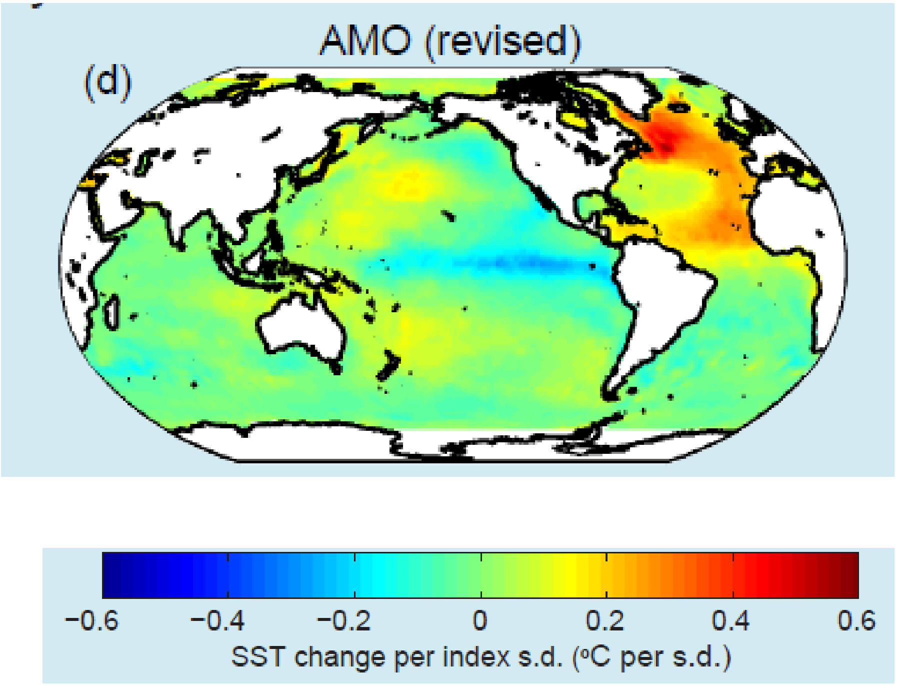

SST anomalies averaged in North Atalntic after removed linear trend. From JMA-HP

Decadal variability of ENSO/ Monsoon and their relationship

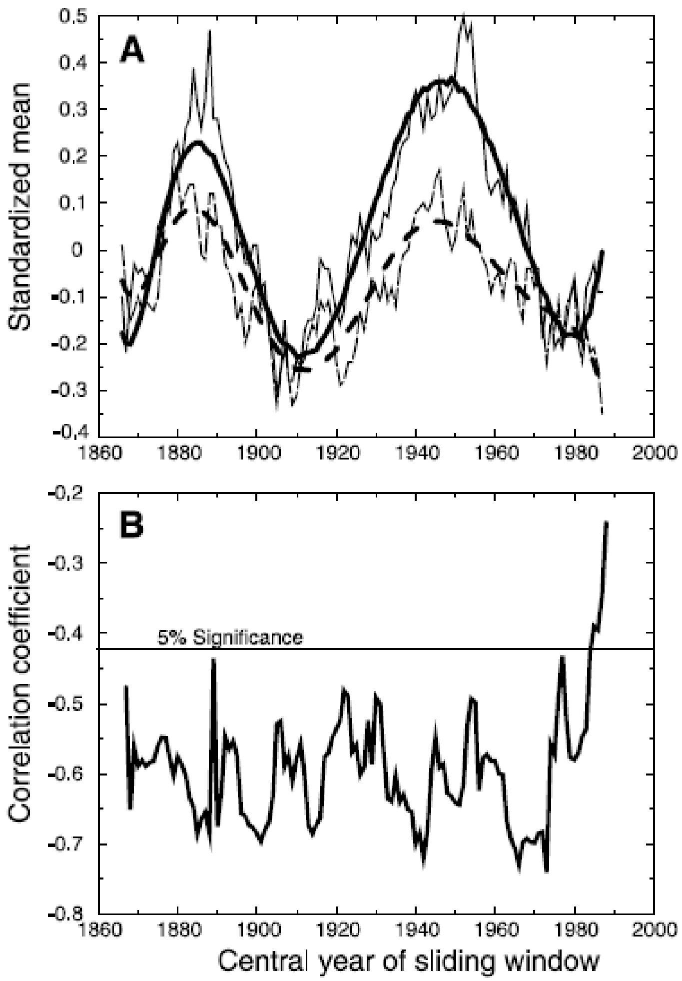

Fig. 1. (**A**) Shown are 21-year sliding standardized means of Indian summer monsoon rainfall (thin line) and June to August (JJA) NINO3 SST anomalies (thin dashed line) during 1856–1997. The corresponding solid lines represent the smoothed values (smoothing is done by fitting a polynomial). The sign of NINO3 SST is reversed to facilitate direct comparison. (**B**) Shown are 21-year sliding correlations between Indian summer monsoon rainfall and NINO3 SST anomalies (JJA) during 1856–1997. The horizontal line shows the 5% significance level.

On the Weakening Relationship Between the Indian Monsoon and ENSO

K. Krishna Kumar,[1*†] Balaji Rajagopalan,[2] Mark A. Cane[2] 1999

Outline of the lecture

1. Climate System (60 min. + α)
   1.1 Introduction
   1.2 Radiative Balance
   1.3 Horizontal Radiative Imbalance and Circulations
   1.4 Seasonal Change
   1.5 Role of Orography on Climate
2. Climate Variability (90 min. + α)
   2.1 Introduction
   2.2 Intraseasonal Variability: Quasi-stationary Rossby wave, MJO and equatorial waves
   2.3 Interannual Variability: ENSO, El Nino Modoki, IOD
   2.4 Decadal Variability: PDO, ENSO-Monsoon relation
3. Climate change due to anthropogenic forcing (30 min. + α)

WORLD METEOROLOGICAL ORGANIZATION
Weather · Climate · Water

English

2017 is set to be in top three hottest years, with record-breaking extreme weather

Tags: Climate

6 Published 6 November 2017

"The past three years have all been in the top three years in terms of temperature records. This is part of a long term warming trend," said WMO Secretary-General Petteri Taalas.

Press Release Number: 06112017

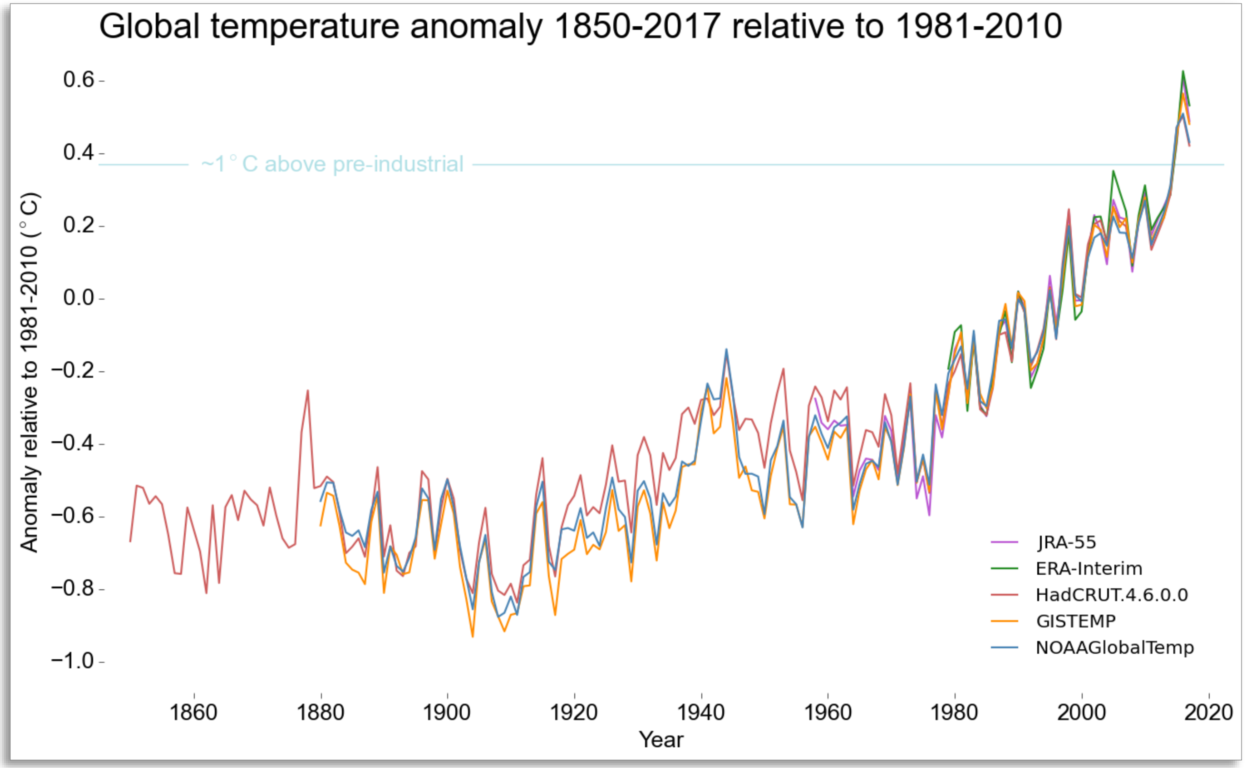

Global mean surface air temperature

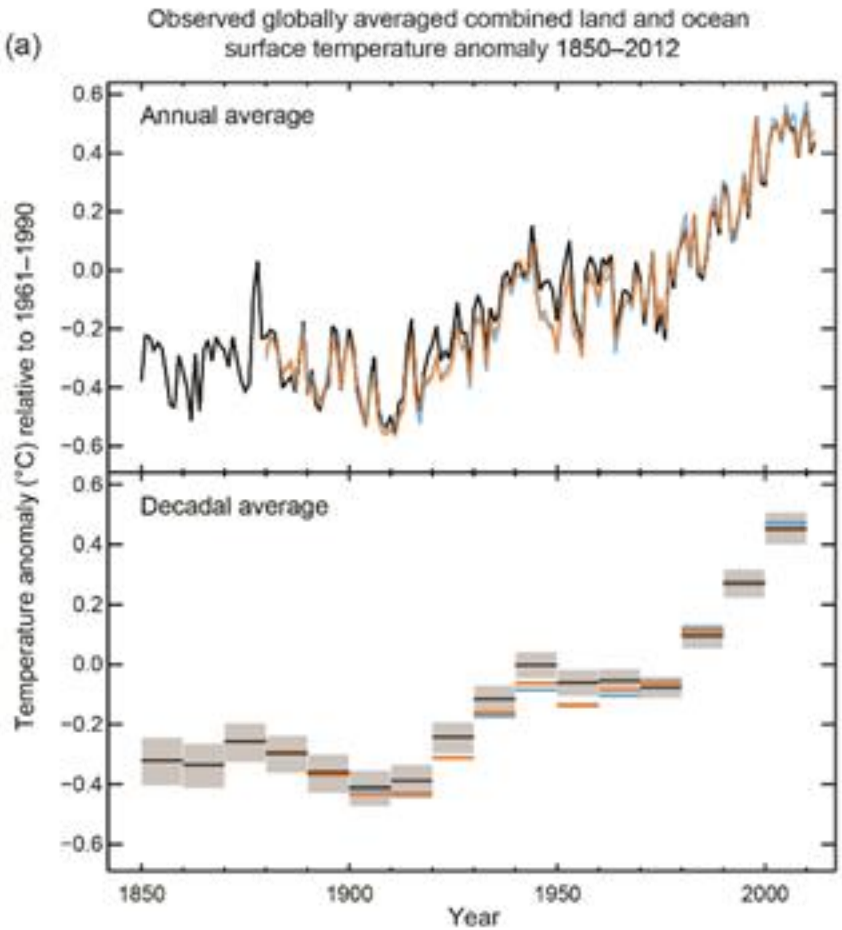

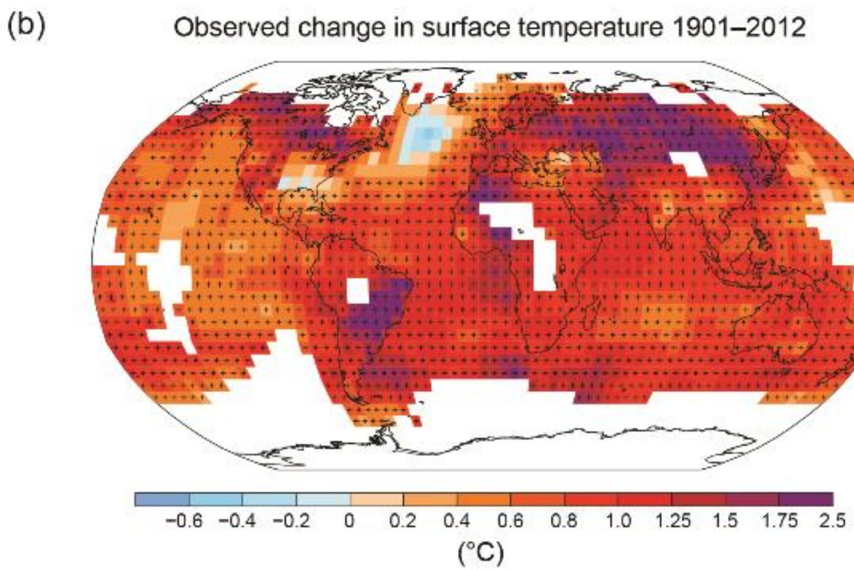

WGI_AR5_FigSPM-1

Annual precipitation over land

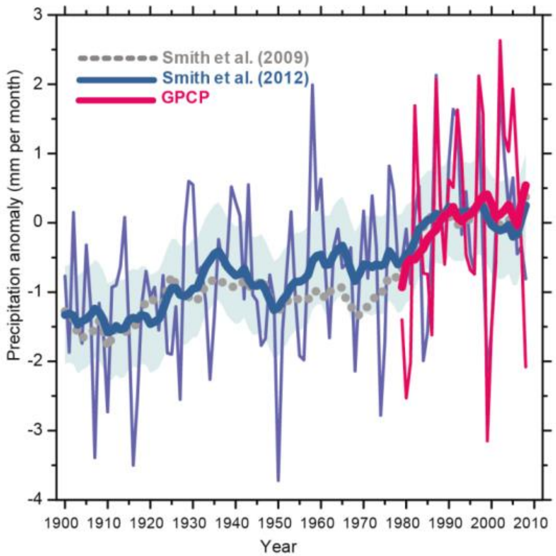

WGI_AR5_Fig3-7

WGI_AR5_FigSPM-2

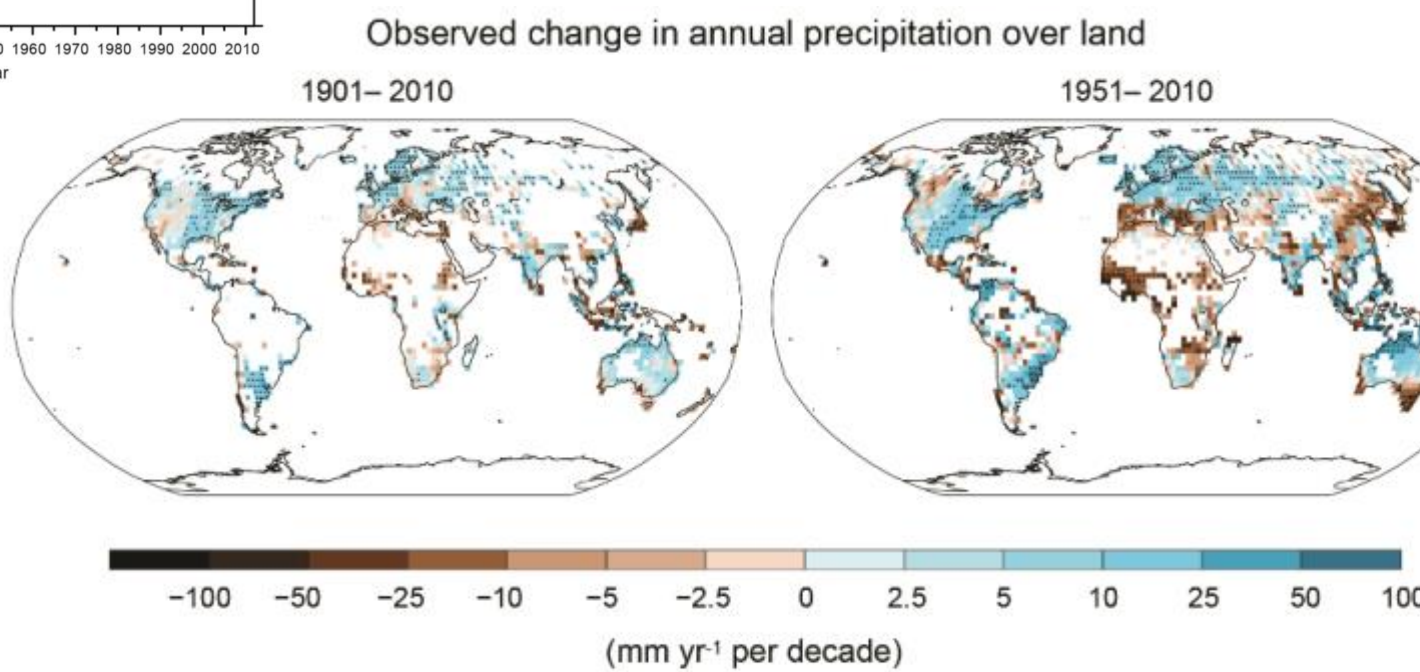

Changes in greenhouse gases

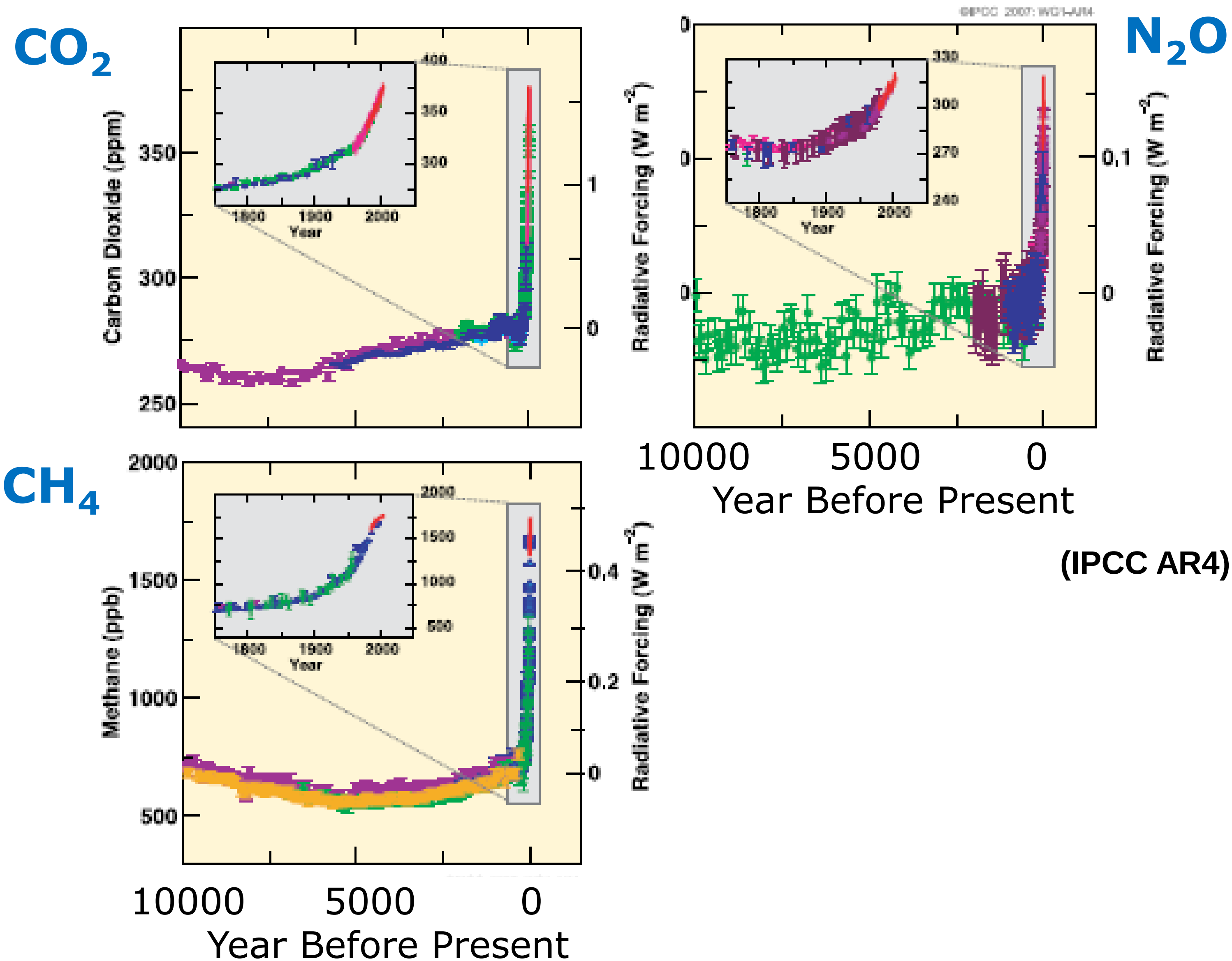

(IPCC AR4)

The climate system is complicated!

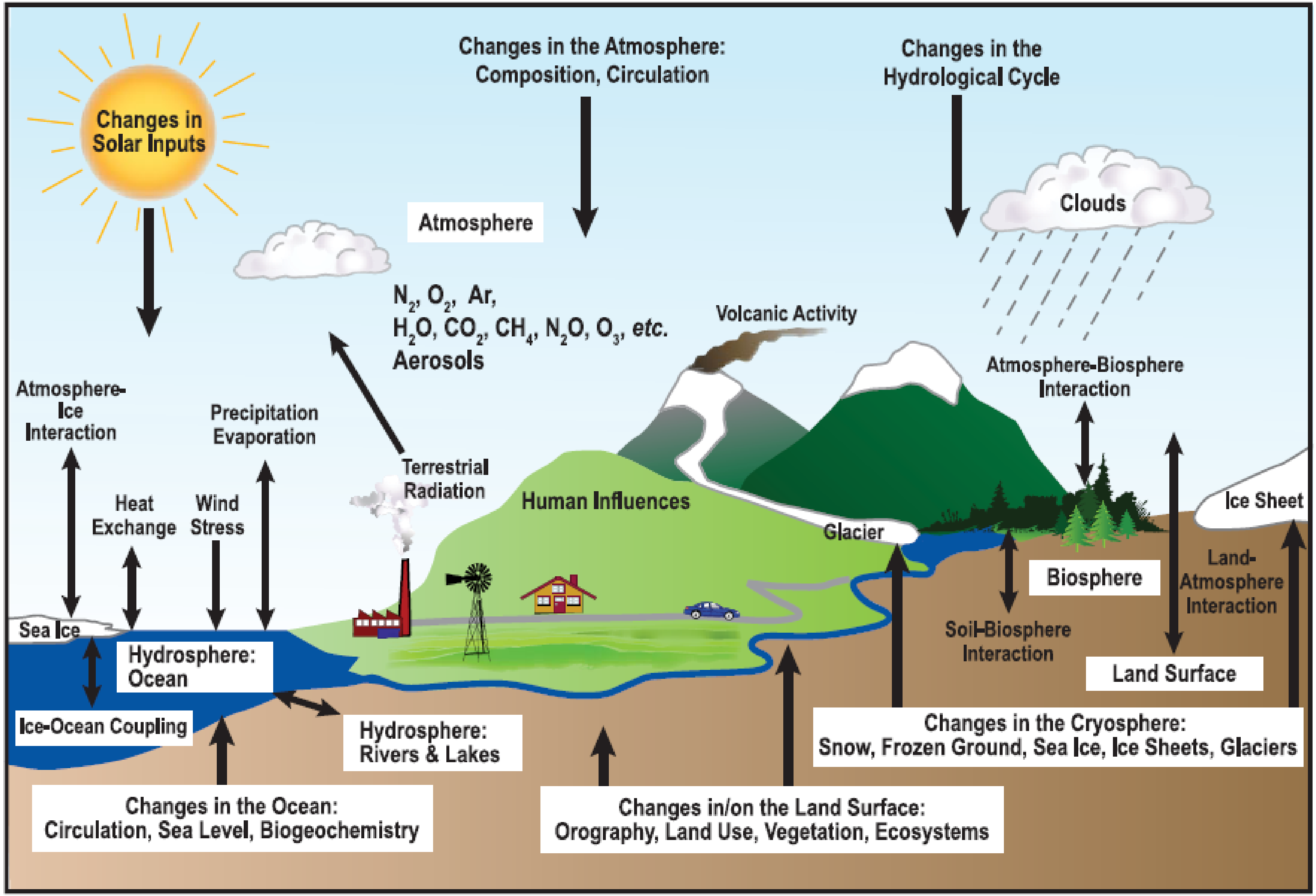

FAQ 1.2, Figure 1. *Schematic view of the components of the climate system, their processes and interactions.*

(IPCC AR4)

Example: MRI Earth System Model

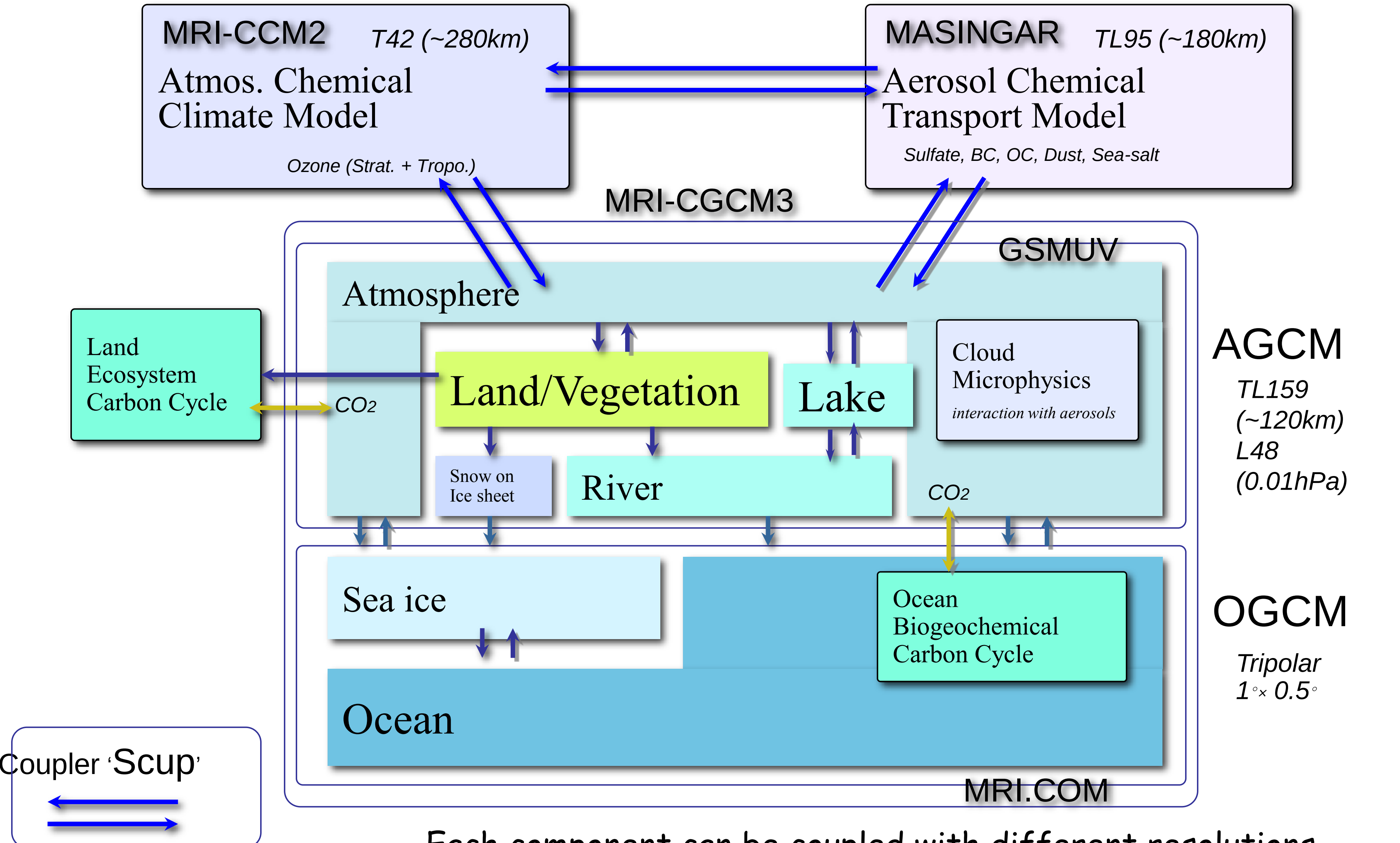

Each component can be coupled with different resolutions

Historical Global Warming Experiments

Model Experiments

WGI_AR5_Fig10-1

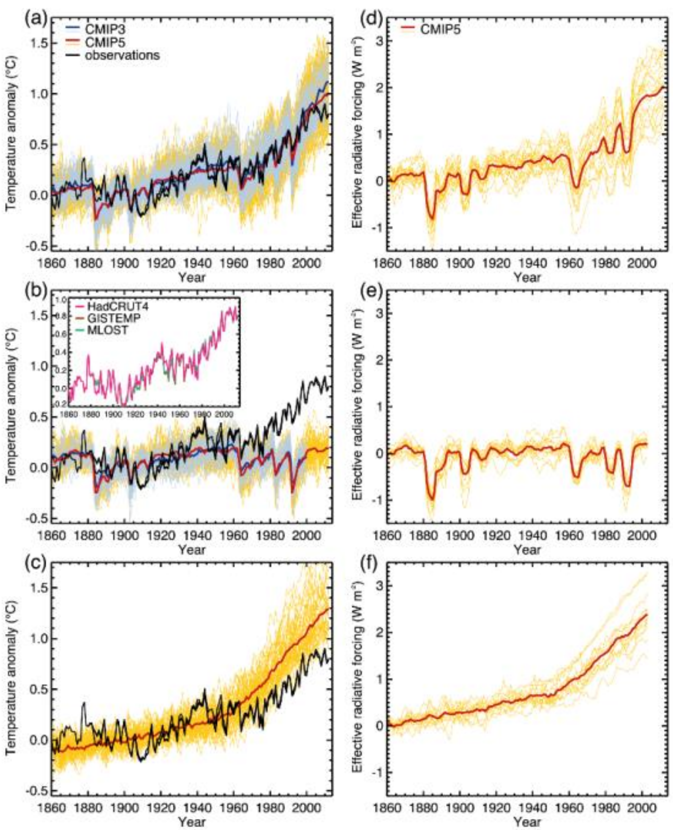

Radiative Forcing

WGI_AR5_FigSPM-5

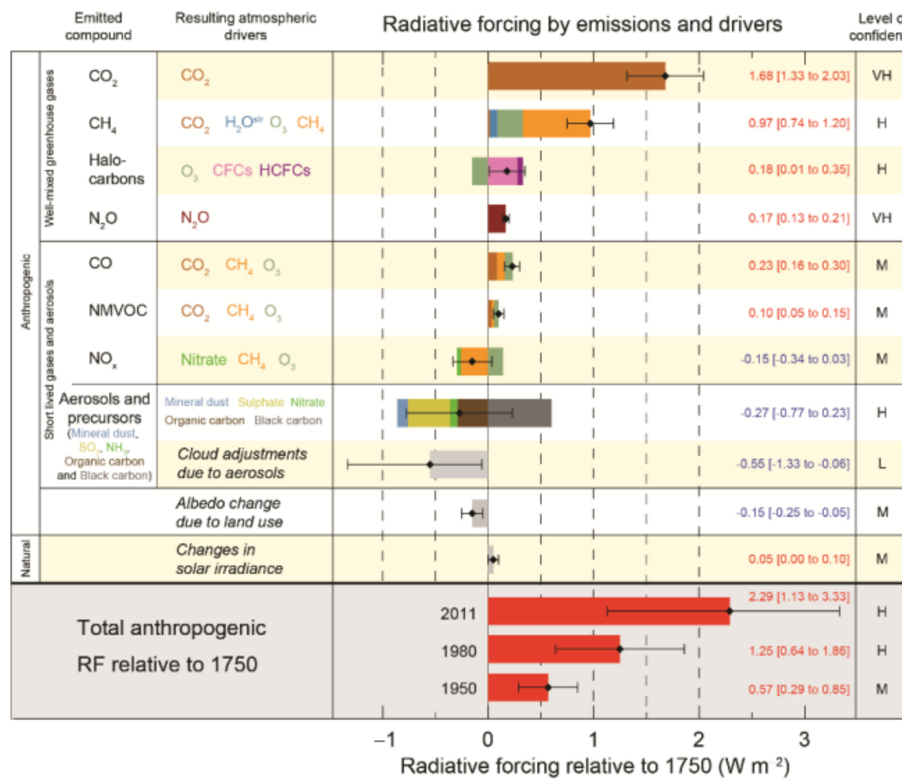

Future Scenarios

Radiative Forcing

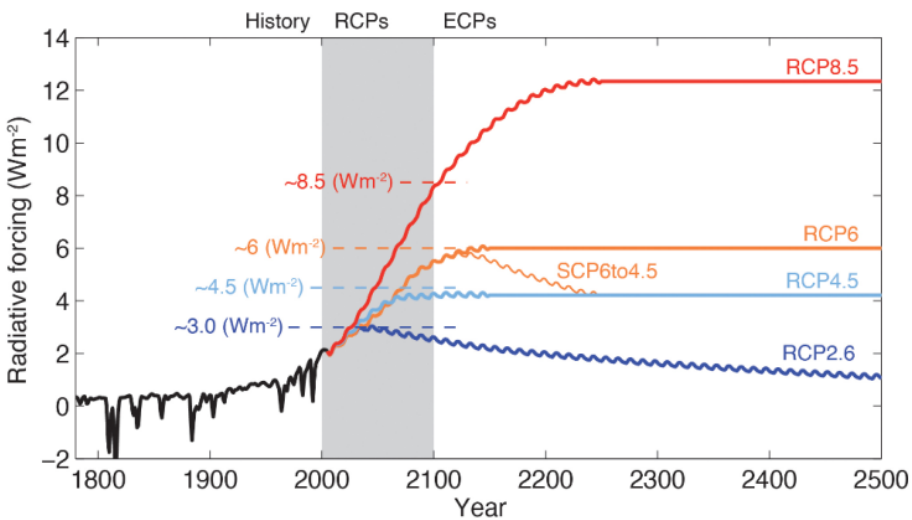

WGI_AR5_FigBox11-1

CO2 and Emisson

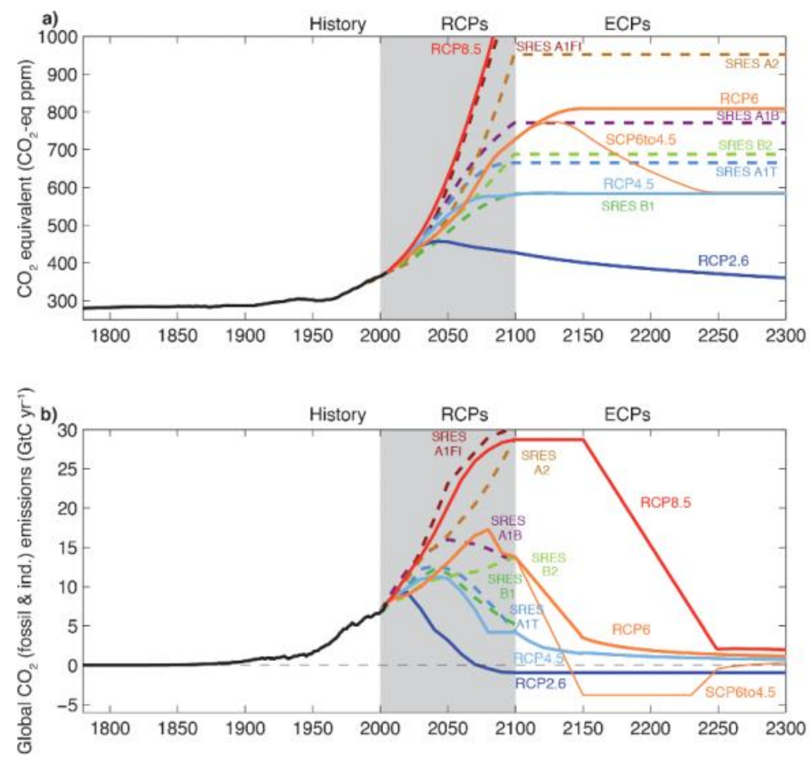

WGI_AR5_FigBox1_1-3

Future Projection

Surface temperature

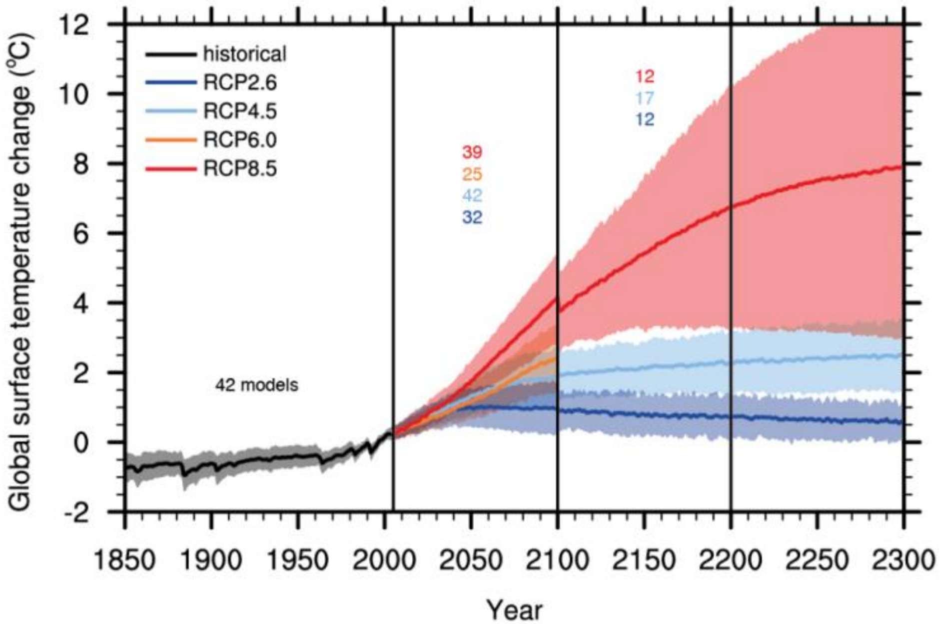

WGI_AR5_Fig12-5

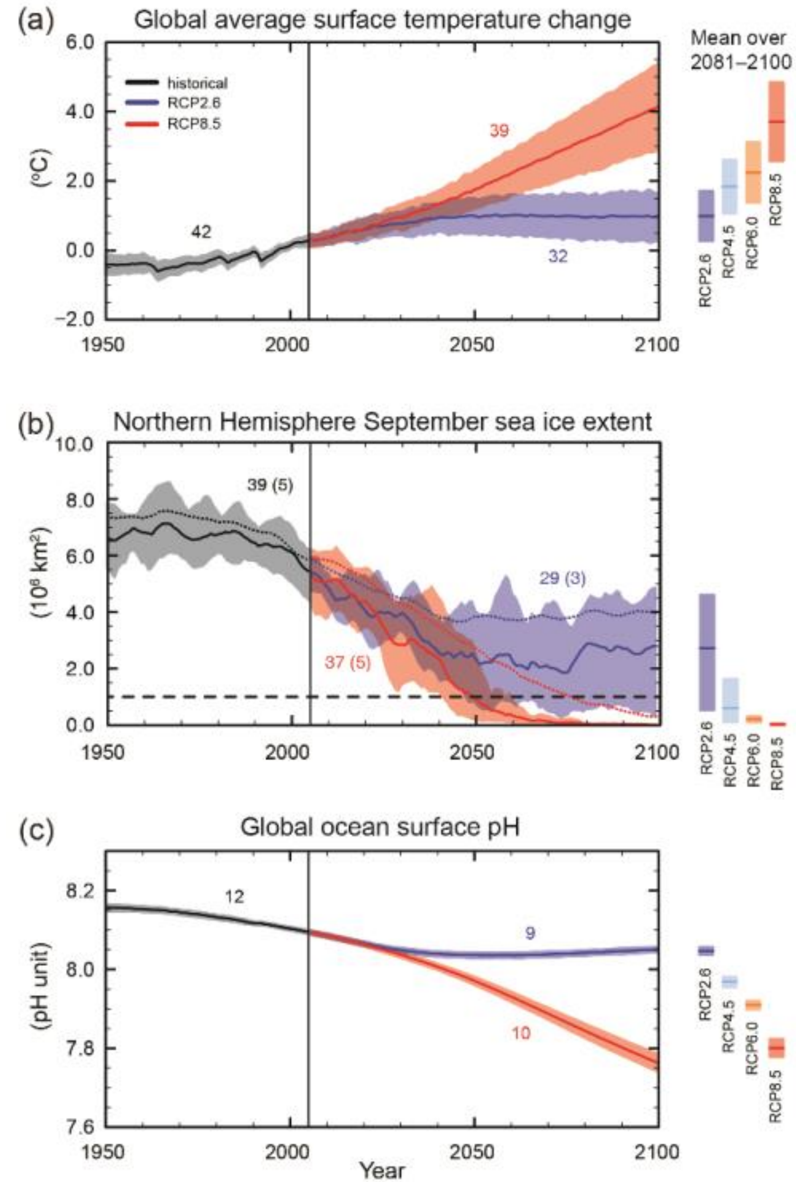

WGI_AR5_FigSPM-7

Map of Warming Projections for Late 21C

- Large difference depending on the regions
- Larger warming over lands and high-latitudes

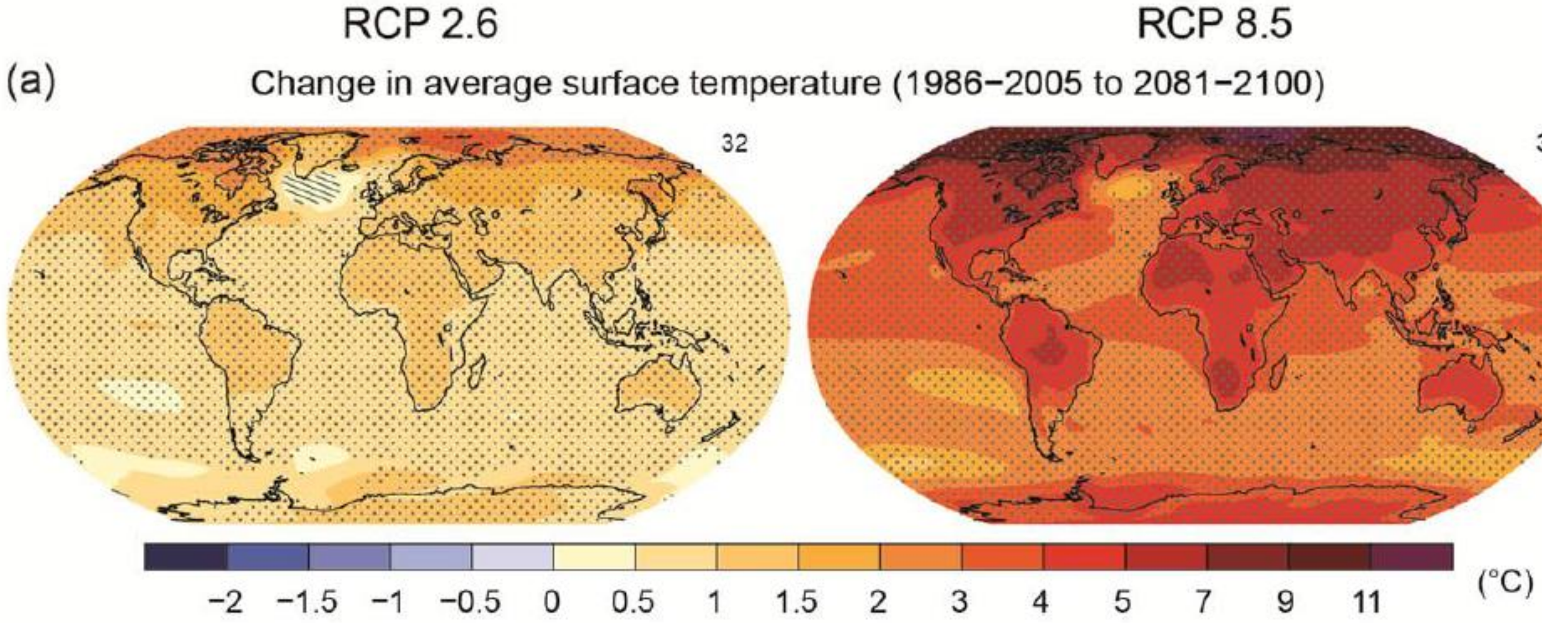

(IPCC AR5)

Precipitation Change

- Increase of precipitation near the currently rainy regions
  ("wet-get-wetter" effect)
- Both flood risk and drought risk should be considered

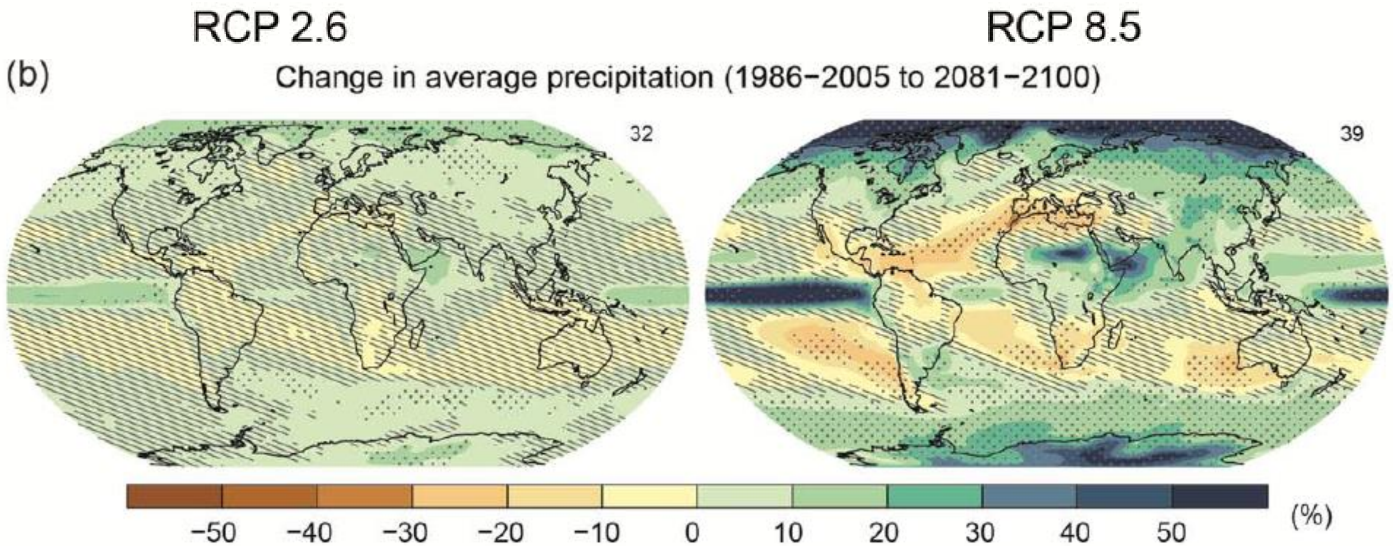

(IPCC AR5)

Temperature Change vs Cumulative CO2 Emission

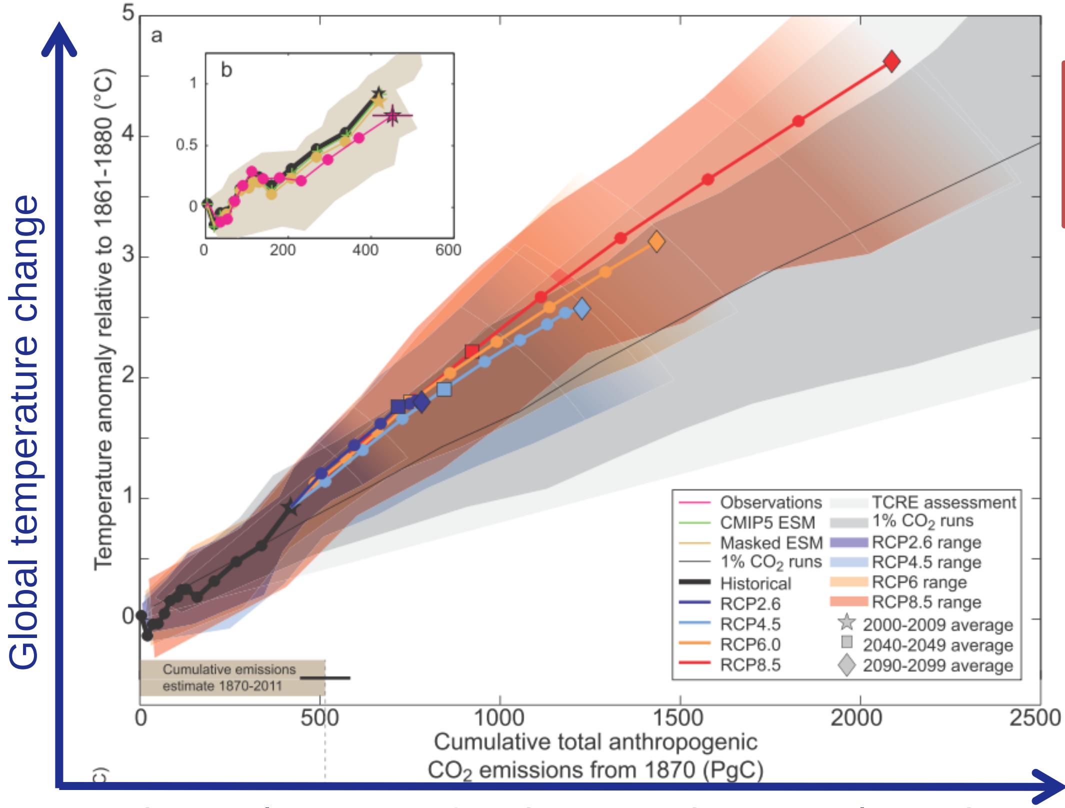

The total amount of anthropogenic CO2 released in the atmosphere since pre-industrial

(IPCC AR5)

Warming is proportional to total cumulative CO2 emissions

Warming continues even if emission is reduced.

Zero emission is not enough to go back.

Sea Level Rise

Sea level rise comes from thermal expansion, as well as retreating glaciers and ice sheet

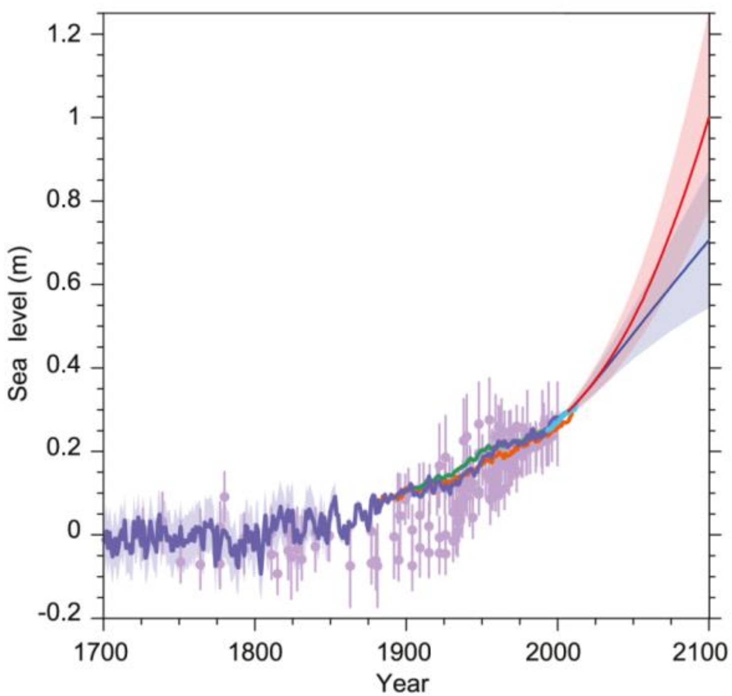

WGI_AR5_Fig13-27

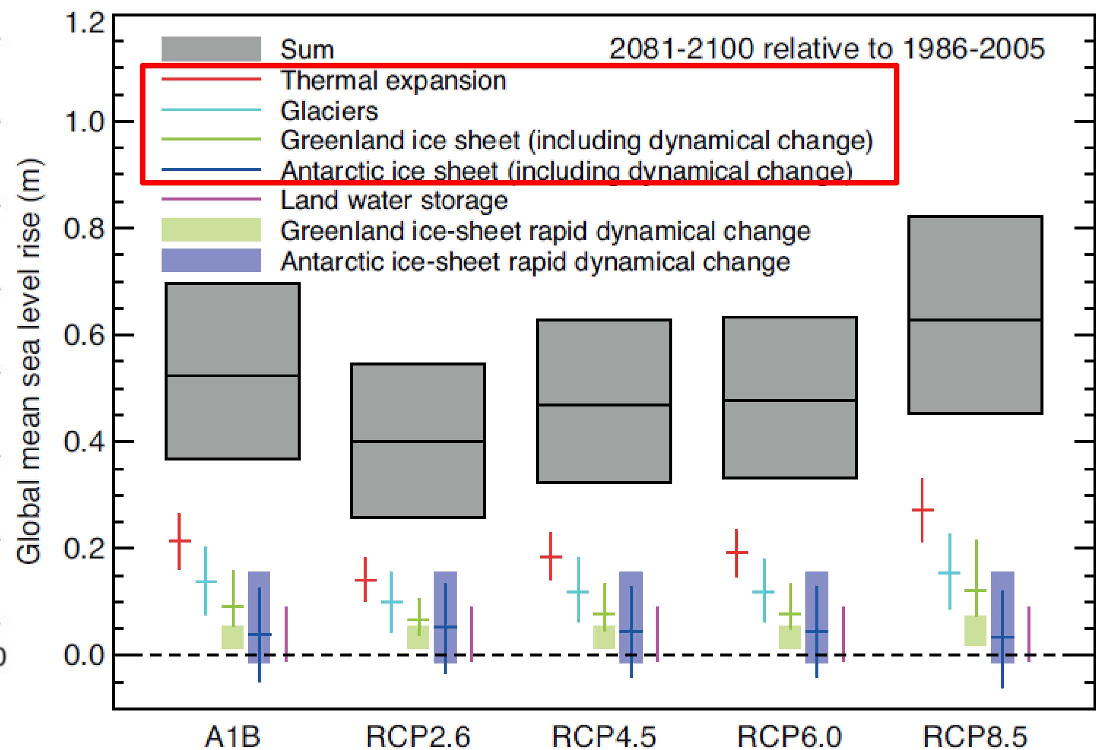

WGI_AR5_Fig13-10

Five-day Precipitation amount and Dry days

WGI_AR5_Fig12-26

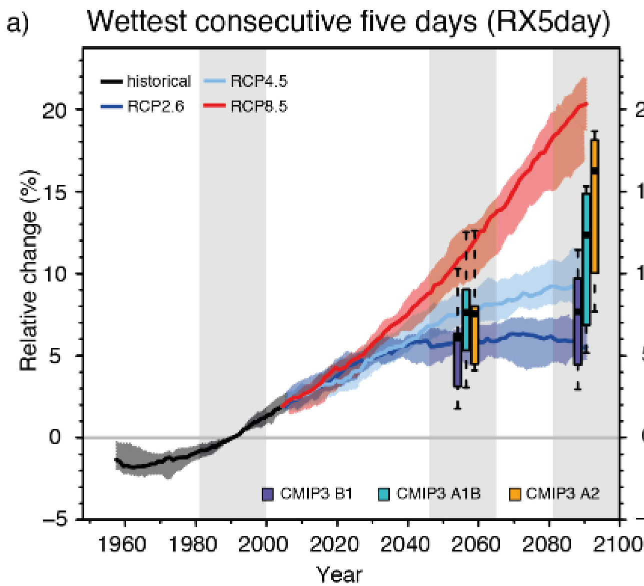

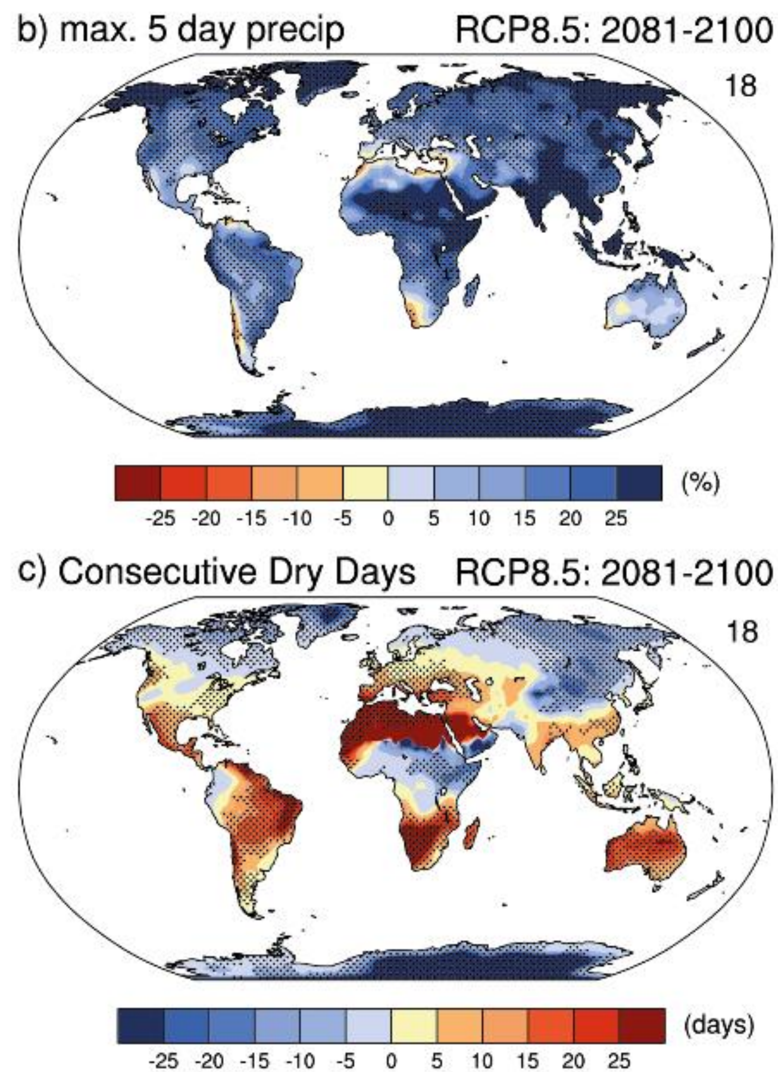

Figure 12.26 | (a, b) Projected percent changes (relative to the 1981–2000 reference period in common with CMIP3) from the CMIP5 models in RX5day, the annual maximum five-day precipitation accumulation. (a) Global average percent change over land regions for the RCP2.6, RCP4.5 and RCP8.5 scenarios. Shading in the time series represents the interquartile ensemble spread (25th and 75th quantiles). The box-and-whisker plots show the interquartile ensemble spread (box) and outliers (whiskers) for 11 CMIP3 model simulations of the SRES scenarios A2 (orange), A1B (cyan) and B1 (purple) globally averaged over the respective future time periods (2046–2065 and 2081–2100) as anomalies from the 1981–2000 reference period. (b) Percent change over the 2081–2100 period in the RCP8.5 scenario. (c) Projected change in annual CDD, the maximum number of consecutive dry days when precipitation is less than 1 mm, over the 2081–2100 period in the RCP8.5 scenario (relative to the 1981–2000 reference period) from the CMIP5 models. Stippling indicates gridpoints with changes that are significant at the 5% level using a Wilcoxon signed-ranked test. (Updated from Sillmann et al. (2013), excluding the FGOALS-s2 model.)

Changes in Regional Climate and Extreme Events

- **Changes in high-impact weather events are the direct risk to people.**
- **However, regional characteristics of the changes cannot be directly simulated by CMIP5 global climate models.**

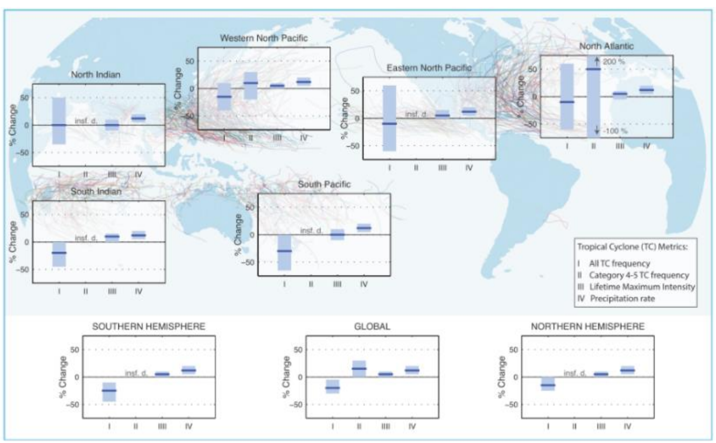

Phenomenon and direction of trend	Likelihood of further changes		
		Late 21st century	
Warmer and/or fewer cold days and nights over most land areas	{11.3}	*Virtually certain*	{12.4}
		Virtually certain *Virtually certain*	
Warmer and/or more frequent hot days and nights over most land areas	{11.3}	*Virtually certain*	{12.4}
		Virtually certain *Virtually certain*	
Warm spells/heat waves. Frequency and/or duration increases over most land areas	{11.3}	*Very likely*	{12.4}
		Very likely *Very likely*	
Heavy precipitation events. Increase in the frequency, intensity, and/or amount of heavy precipitation	{11.3}	***Very likely*** over most of the mid-latitude land masses and over wet tropical regions	{12.4}
		Likely over many areas *Very likely* over most land areas	
Increases in intensity and/or duration of drought	{11.3}	***Likely*** *(medium confidence)* on a regional to global scale[h]	{12.4}
		Medium confidence in some regions *Likely*[e]	
Increases in intense tropical cyclone activity	{11.3}	***More likely than not*** in the Western North Pacific and North Atlantic[l]	{14.6}
		More likely than not in some basins *Likely*	
Increased incidence and/or magnitude of extreme high sea level	{13.7}	***Very likely***[l]	{13.7}
		Very likely[m] *Likely*	

(IPCC AR5)

d4PDF:

database for Policy Decision making for Future climate change

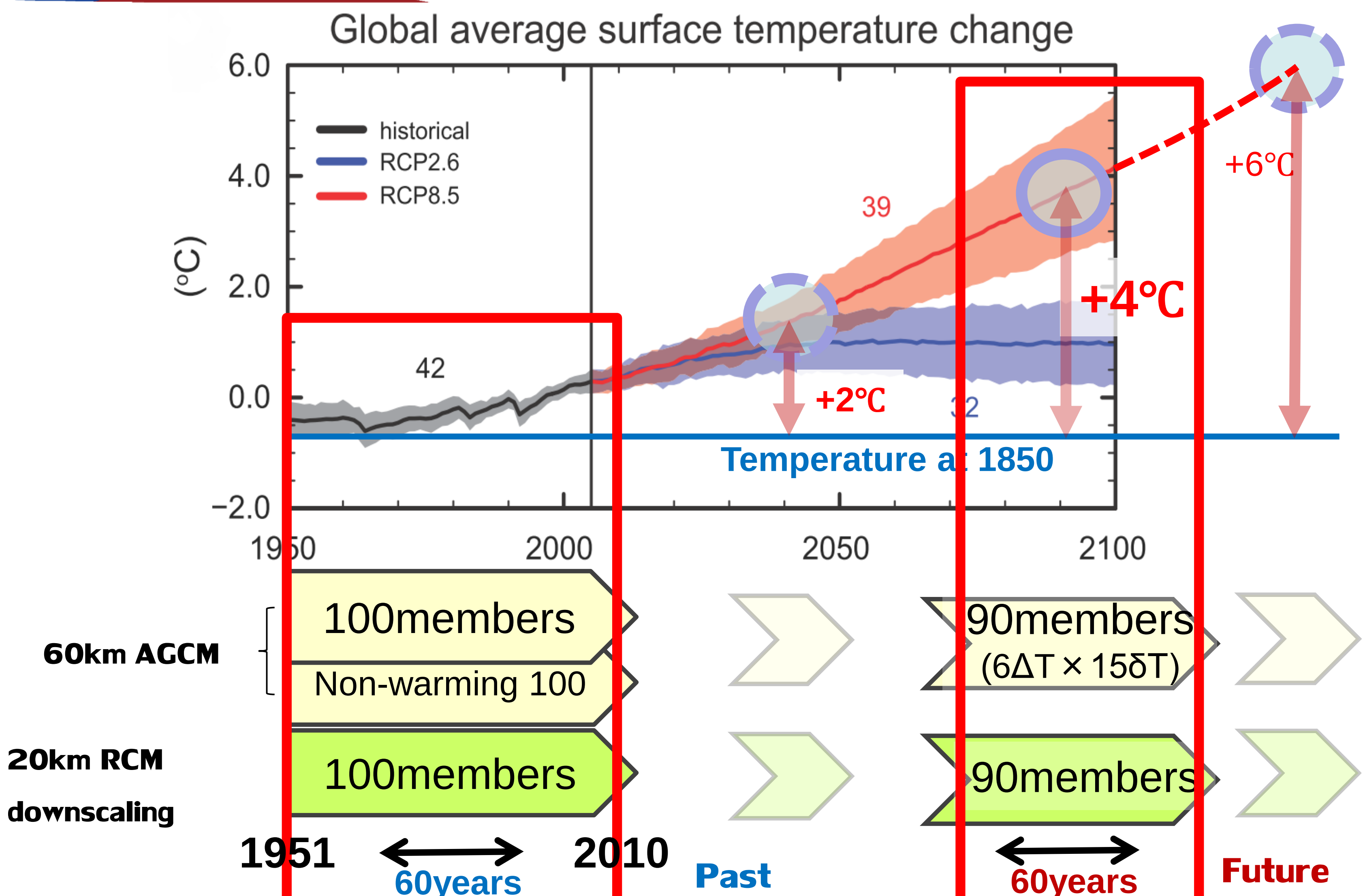

60km AGCM + 20km RCM

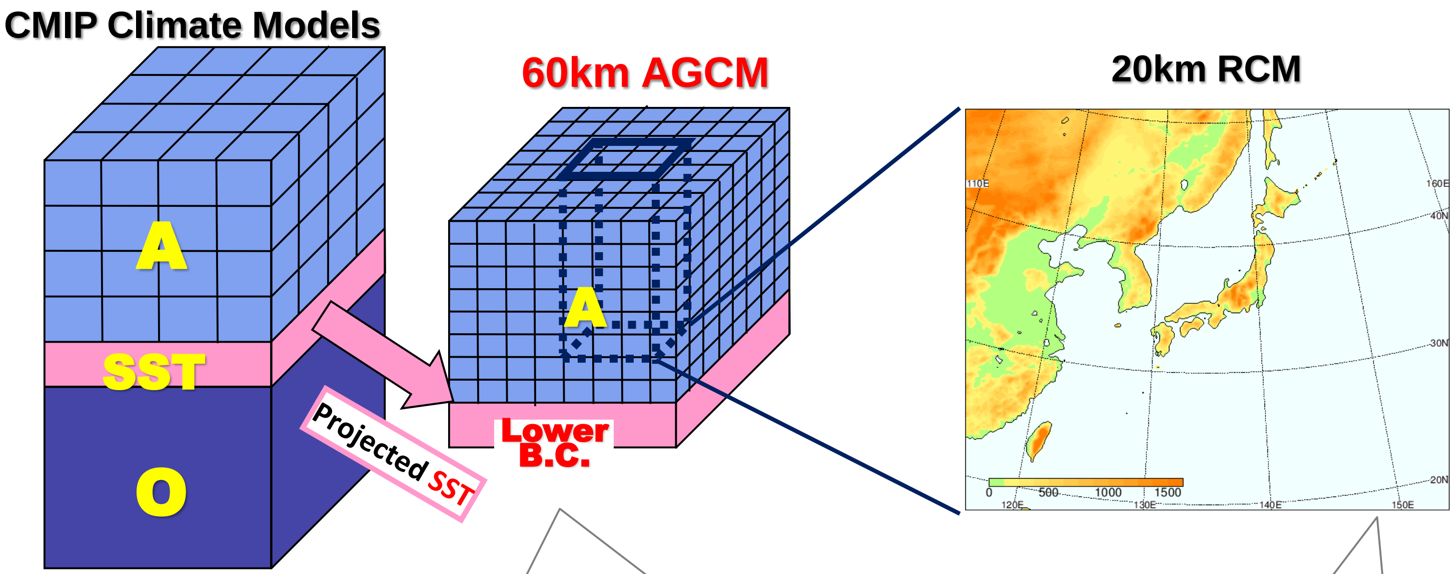

MRI-AGCM3.2 (Mizuta et al. 2012)

NHRCM (Sasaki et al. 2011)

- 60km AGCM is:
  - lowest resolution capable of simulating tropical cyclones
  - highest possible resolution for large ensembles at the latest super computer

Benefits from high-res large ensemble

- Frequency distribution of daily precipitation at Tokyo
  - Ensemble spread between members **(Blue)** is large in rare events
  - Observation **(Black)** is inside the ensemble spread without any bias corrections
  - Results from the total 100 members **(Red)** shows reasonable frequencies of extremes as low as 0.003%(=once in 100 years)
  - Increase is larger in the heavier precipitation rate

Past

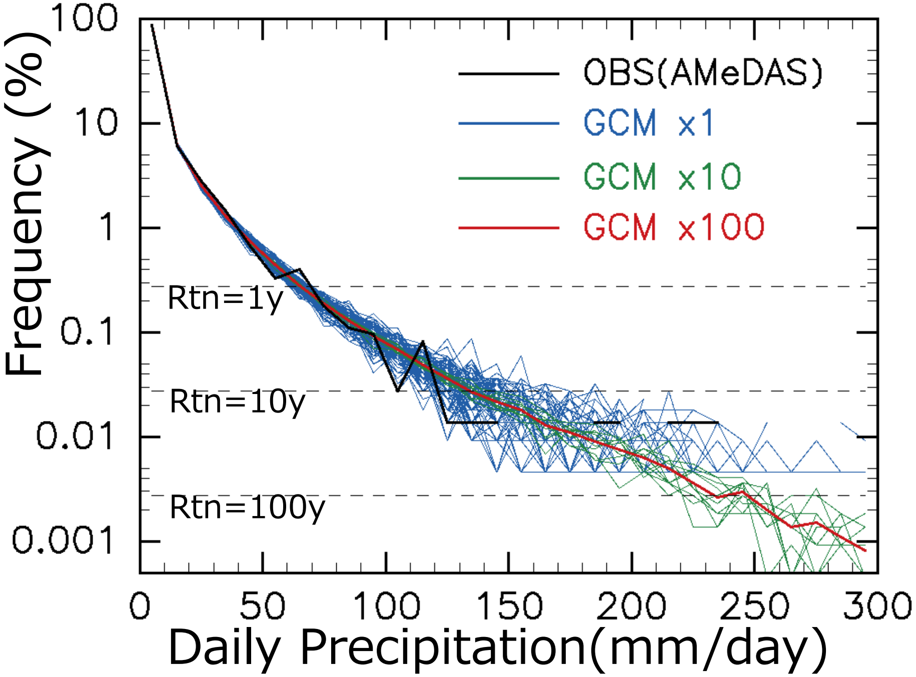

Ratio (+4K / Past)

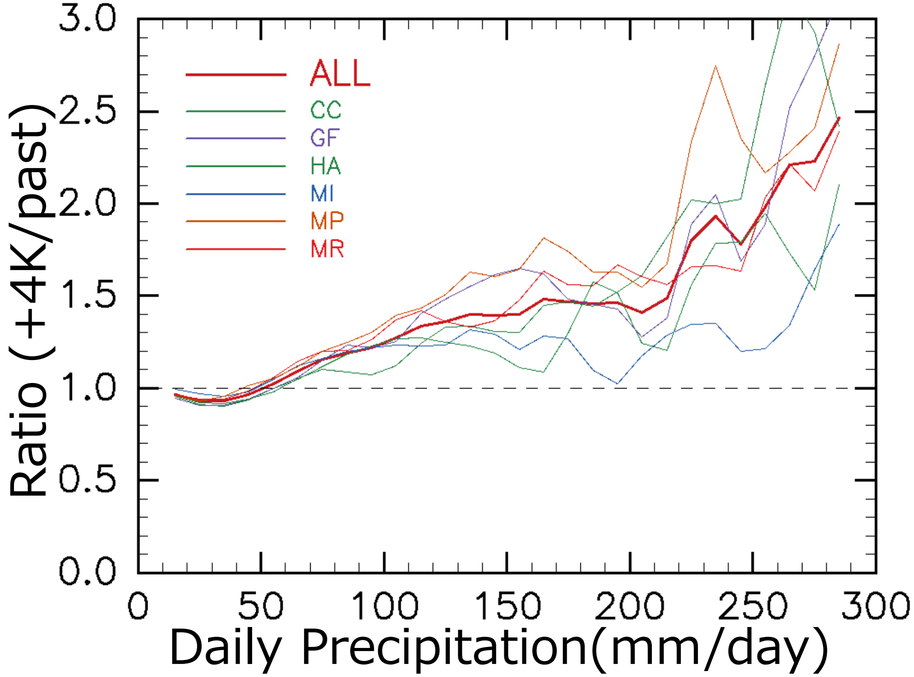

(Mizuta et al. 2017)

10-year return value of daily precipitation

Clear and smooth picture can be obtained by using large ensembles

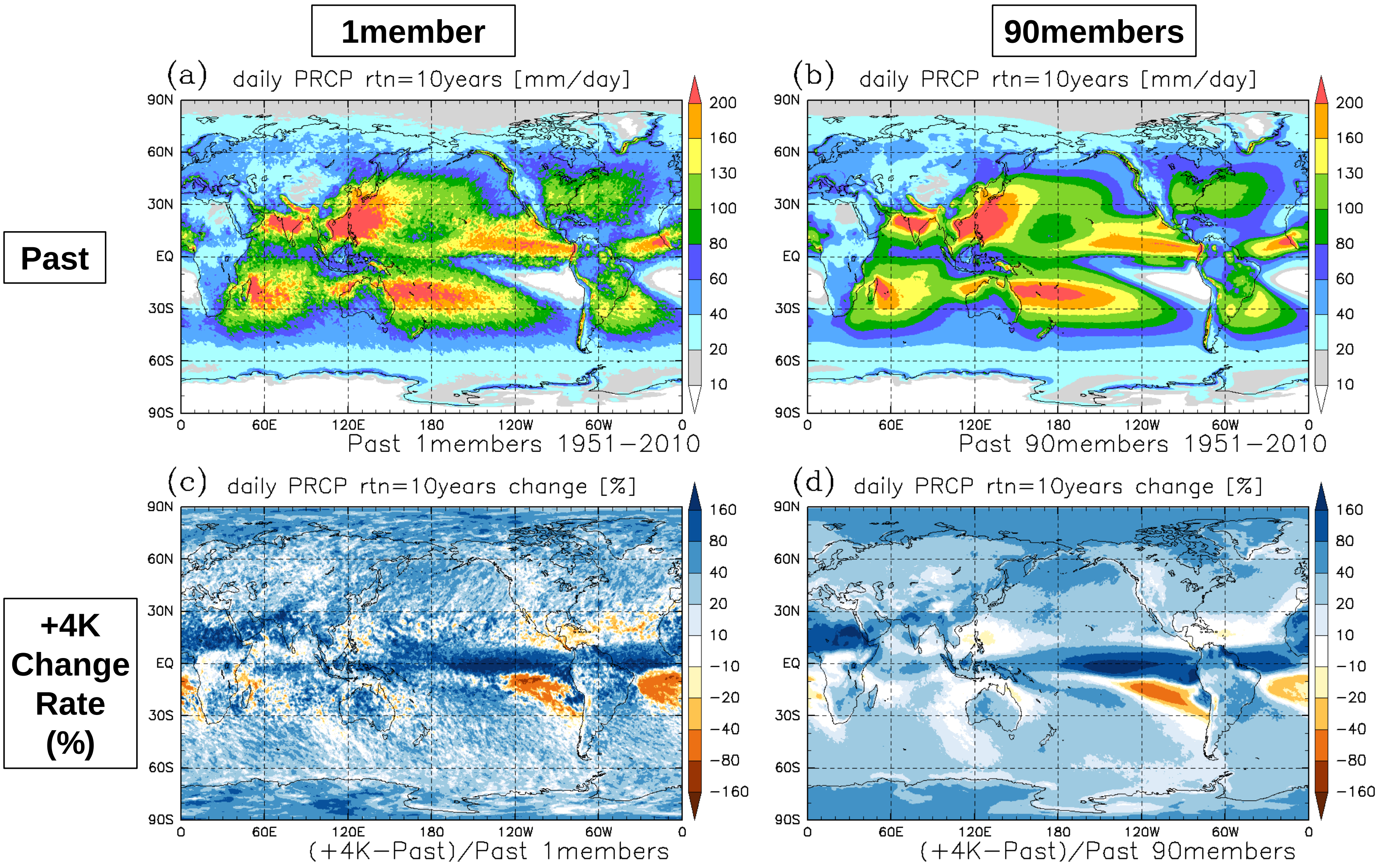

(Mizuta et al. 2017)

Tropical Cyclone Frequencies

- Similar, but smoother distribution compared with the observation
- After the bias correction for the 60km model, Category 4-5 increases on N. W. side of Pacific and Atlantic, as well as eastern side.

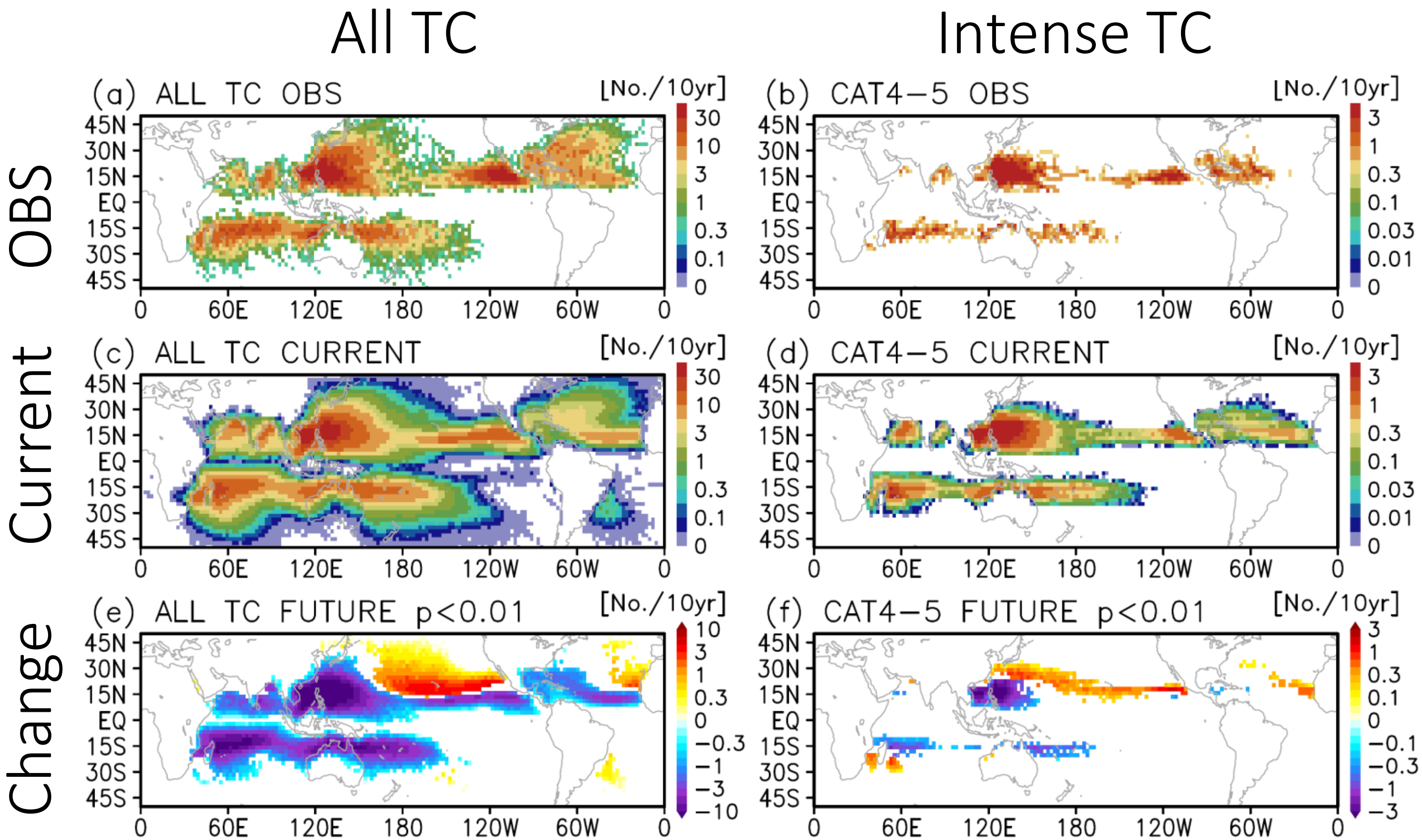

(Yoshida et al. 2017)

Concluding remarks

- The global climate system consists of atmosphere including its composition and circulation, the ocean, hydrosphere, land surface, biosphere, snow and ice, solar and volcanic activities.
- These components interact on various spatial and temporal scales through the exchanges of heat, momentum, radiation, water and other materials.
- Climate variability refers to variations in the mean state and other statistics of the climate on all spatial and temporal scales beyond that of individual weather events.
- Climate variability may be due to natural internal processes within the climate system (internal variability), or to variations in natural or anthropogenic external forcing.
- Experts of climate services must learn climate system, causes, impacts, and predicatbility of climate variability in various spatial and temporal scales.